THE NATIONAL AERONAUTICS AND SPACE ADMINISTRATION RESEARCH GRANT

NGR-05-020-115

"FIELD INFRARED ANALYSIS OF TERRAIN"

SEMI-ANNUAL REPORT

1 November 1966 - 30 April 1967

15 May 1967

REMOTE SENSING LABORATORY

GEOPHYSICS DEPARTMENT

STANFORD UNIVERSITY • STANFORD, CALIFORNIA

TABLE OF CONTENTS

Page No.

This research performed under NASA Grant NGR-05-020-115

copy No. of 200

I. INTRODUCTION

Following requests from NASA/MSC to assist in preparation for accelerated ground support for the P3A aircraft program the Stanford program was increased during the past 6 months from 4.05 to 4.23 man year level,

In detail our allocation of non-project support, exterior to the Stanford program, has been as follows. Previous 12 month levels are indicated.

STANFORD REMOTE SENSING LAB

ALLOCATION OF SUPPORT

	Past 6 mos.	Previous 12 mos.
A, DIRECT SUPPORT FOR NASA		
1. NASA/SAR (Washington, D.C.) Reporting & Publications	21.3%	16.9%
2. NASA/MSC (Houston, Texas) Aircraft & Spaceflight program	6.0% (+ $9600 costs) (over 12 months)	3.1%
B. RESEARCH SUPPORT FOR USDA		
Analysis of Davis Field Data (IR Tape 11)	10.4% (+ $11,025 costs over 12 months)	11.6%

This report covers the third six-month period of the study, for the period November 1, 1966 through April 30, 1967. The original proposal requested a three-year step funding through October 30, 1968. Funding is in hand, however, only for the first two years of this grant but will run out approximately by August 1, 1967. A proposal for the third year extension has been submitted to NASA (SC Control #05-020-115-(233) February 24, 1967. Another proposal, prepared to assist the P3A aircraft and titled "Accelerated Ground Data Acquisition in Support of P3A Airborne Infrared Operations" (SC Control #05-020-115-(225)) was turned down by NASA/SC on April 6, 1967.

Accordingly we are greatly concerned about funding and the costs of reducing the spectrometer data in those forthcoming P3A aircraft missions which were specifically requested by Stanford. No money is allotted to those flights requested by the User Agencies. We have identified clearly defined ways of cutting these costs and the matter is discussed in greater detail in Sections IIC and IIID.5.

The modified SG-4 spectrometer system is now functioning well with the new detector and relay optics systems. The analog data outputs must be converted to digital readouts and digital recording to reduce the data reduction costs.

11. RATE OF EFFORT

A. ANALYSIS OF RATE

The rate of research performed under this grant was increased initially when Dr. R.S. Vickers joined the staff of the Remote Sensing Laboratory in July 1966. The field-work side of the project which has been lagging,picked up appreciably and several data tapes were acquired in field operation at Sonora Pass. At the conclusion of the first year of the project we were precisely on schedule with respect to funding of efforts.

In the late months of 1966 discussion with MSC personnel resulted in our sbmitting a proposal on January 5, 1967 to them for "Accelerated Ground Data Acquisition in Support of P3A Airborne Infrared Operations". This proposal contained three phases:

Phase I	-	Hardware construction (a new portable field spectrometer with digital data output)
Phases II & III	-	Ground Data Acquisition (support of an accelerated program of field data gathering when the IR spectrometer was installed in the P3A aircraft - June-September 1967). The phases were split across the fiscal year at July 1 at MSC request.

In March 1967 we were informed that NASA/SAR were probably not funding a third year extension of our research grant as requested by our "third year" proposal. At that point we were proceding at a slightly increased research level, in expectation of the "Accelerated" proposal being funded. (See Figure 1).

This particular proposal was turned down on April 6, 1967 leaving us without any funds to support the IR spectrometer in air and ground testing, effectively leaving the spacecraft prototype instrument without PI to test its feasibility or to reduce its data to meaningful results.

To this date we have funds in hand which will last until about July 31, 1967, without any field studies at all. Some funds are possibly forthcoming from NASA/MSC but have not been received by this reporting date.

FIGURE 1

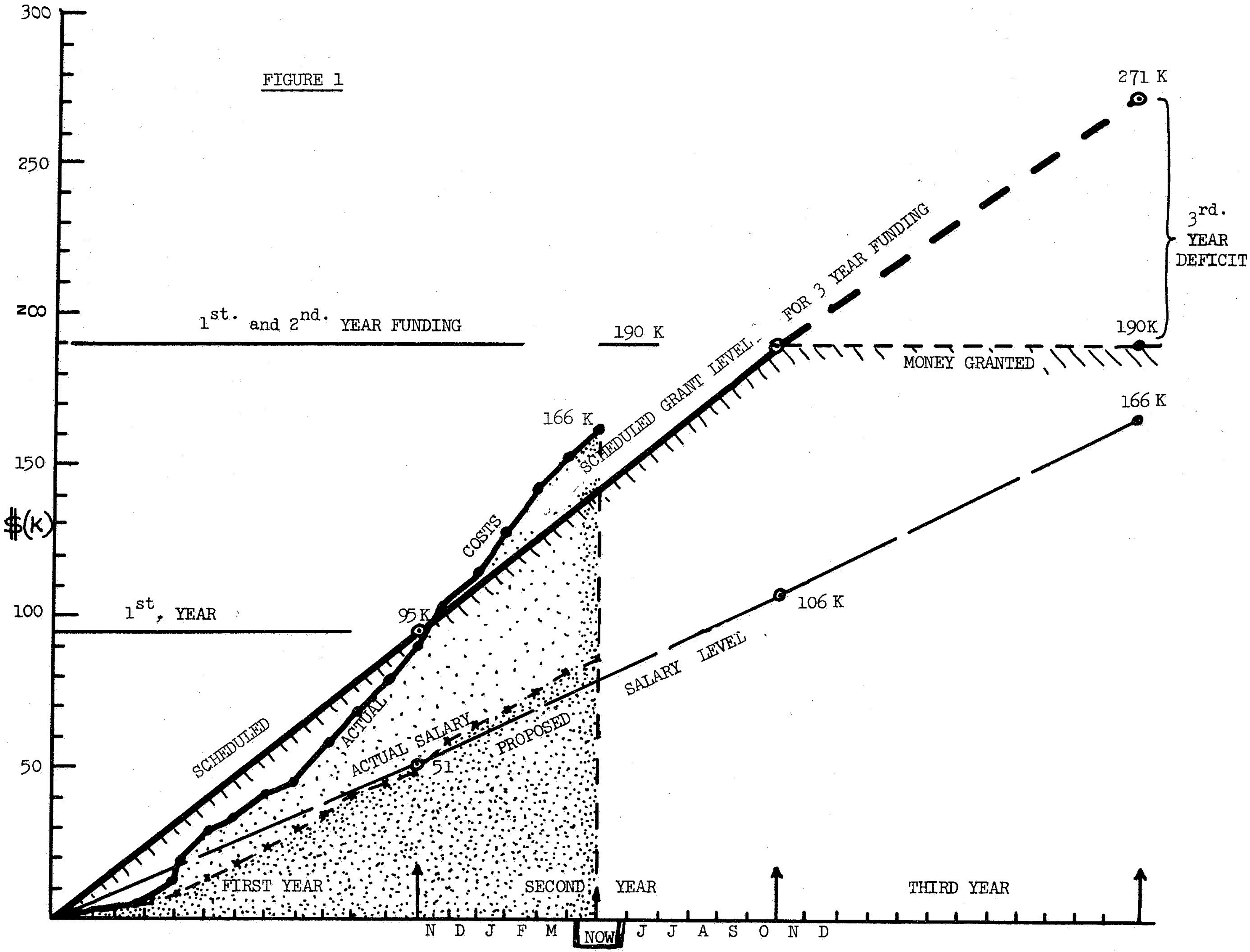

300
250
200
150
100
50
$(K)
1st. and 2nd. YEAR FUNDING
190 K
1st, YEAR
95K
166 K
COSTS
SCHEDULED
ACTUAL
ACTUAL SALARY
51
PROPOSED
SALARY LEVEL
106 K
SCHEDULED GRANT LEVEL FOR 3 YEAR FUNDING
MONEY GRANTED
271 K
190K
166 K
3rd. YEAR DEFICIT
FIRST YEAR
SECOND YEAR
THIRD YEAR
N D J F M NOW J J A S O N D

B. COST OF DATA ANALYSIS

One of the principal expenditures of this research project is the cost of reducing the tape-recorded spectral data. We have devoted considerable time and effort to devising ways to decrease these costs. Most of these costs have been traced to the following trouble points:

1. Analog-digital conversion costs.
2. Telling the computer where each spectrum starts and stops. Mutually-generated times must be encoded from range-coded time in the digital tapes.
3. Setting-up costs for personnel to enter the cards and tapes into the computer.
4. Actual program running times.

DATA REDUCTION COSTS

	Past 6 Mos.	1st Year	Total 18 Mos.
Computer costs	$ 2.37 K	$ 4.34 K	$ 6.71 K
Programmer Support	3.13	3.50	6.63
	5.70	7.84	13.34
+ Personnel time involved (Including overhead) (18.2 man months)	9.95	11.17	21.12
	$ 15.45 K	$ 19.01 K	$ 34.46 K

1. Reducing the cost/spectrum

a. The Problem

The main expense in reducing spectra in an analog form is that after digitizing they are:

(1) of unknown length (i.e. no. of digits)

(2) have no label or I.D. information attached to them.

The computer therefore cycles back and forth looking for a particular spectrum before it can begin to process the data. Identification is presently achieved by noting the sequence in which the spectra were

TABLE I

RELATIVE COSTS FOR STANFORD SPECTRAL MATCHING PROGRAMS

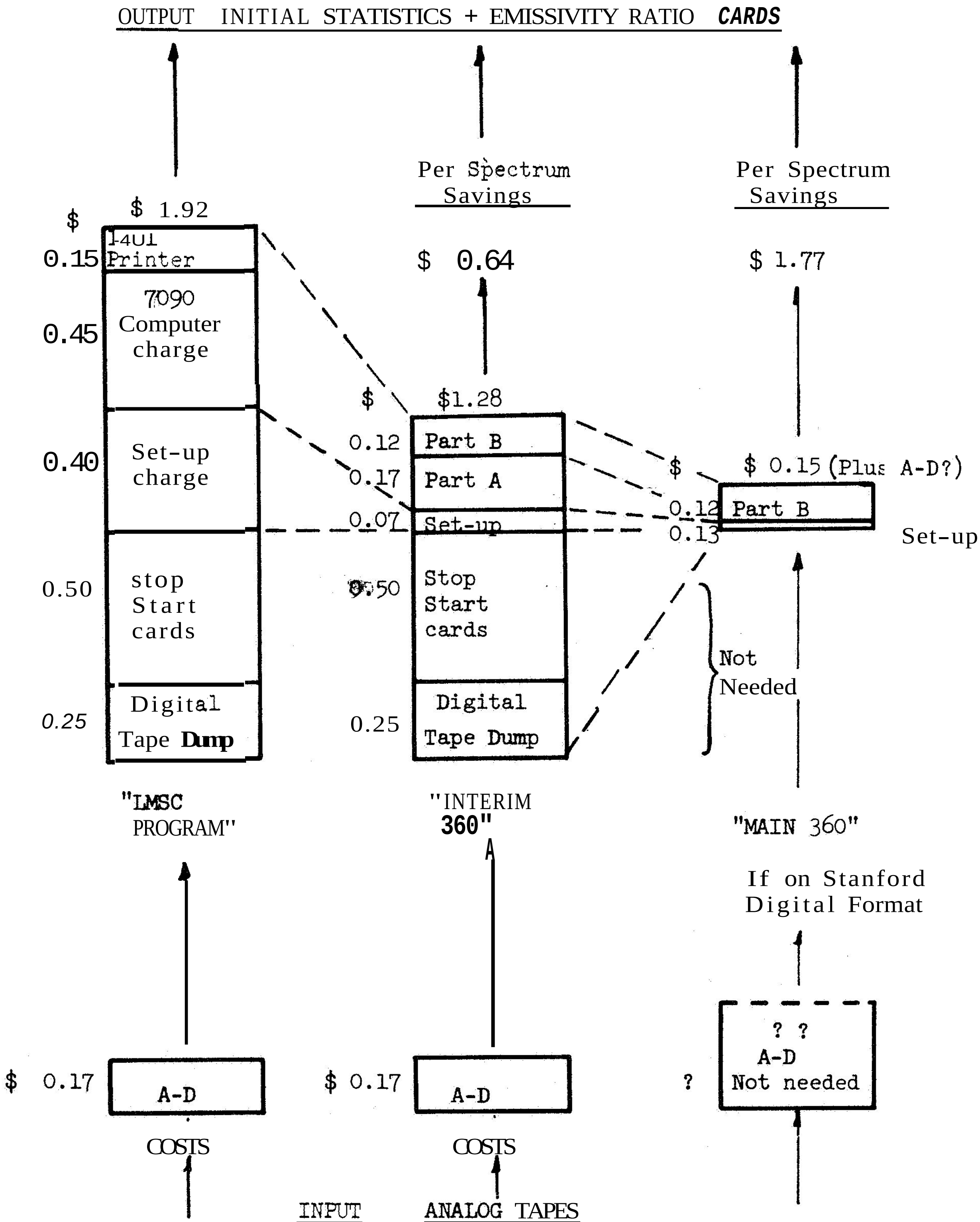

originally taken and manually transferring the sequence to a "dump" of the digital tape. Computer recognition is achieved by putting an artificial time coding (Range-coded time) on each sample during digitizing and providing subsequent manual instructions (punched cards) to the computer as to which time corresponds to which spectrum. Many hours of work are involved in providing these manual instructions, and compiling the input decks of cards to the computer. This is clearly reflected in the cost analysis where 64% of the present system cost ($1.28/spectrum) is due to these steps.

b. The Solution

If each spectrum were always the same number of digital samples in length, and had an easily recognized character at the beginning to denote its first sample, then the start/stop time problem would be removed, The computer could then scan the data for the start of the "n^{th}" spectrum, and with the advance knowledge that the spectrum was going to be (say) 200 samples in length, could start processing immediately. This in itself would save the hours of manual work plus about 50% of the computer time.

If, in addition, each spectrum was accompanied by some identification characters, then at last the computation could be performed automatically without the time consuming intervention of human peripheral equipment. Sounds easy? Let us examine what it means in terms of hardware modifications.

No present-day spectrometer can be relied upon to give spectra which are exactly equal in time, and therefore normal analog to digital (A-D) procedures would not give the equal length records that are so desirable to the computer. The digitizing process therefore has to be controlled by the spectrometer rather than by a master clock as is conventional practice. It is our suggestion that a digital encoder be driven by (i.e. directly coupled to) the grating or filter wheel itself in the spectrometer, and the output pulse-coded so as to provide digitizing instructions for the A-D converter, say every 1/50 micron. Since the wavelength scanned should always be the same no matter what the scanning speed, this procedure results in a constant, predictable, number of samples per spectrum taken in the same wavelength sequence. Again for maximum success some identification data has to be scanned automatically at the beginning of each spectrum. In the case of the P3A aircraft where flight line locations are definable this data may simply be a sequencing count of the number of the spectrum taken to that time for a ground instrument however a more complete identification of the sample could be present on a number of hand switches, which would be scanned before each spectrum.

The nature of the digitizing technique demands the use of incremental (stepping) digital recorders such as the Kennedy 1400 or Digi-Data 1450 although a higher stepping rate (600/sec) would be desirable. The total capital investment indicated for this major step in cost reduction is only $10,000 per complete unit, When one figures the savings on

a. airborne system--$1.15/spectrum for 10^4 spectra/site or $11,500 per site and

b. ground system $1.15/spectrum for 4×10^2 spectra/day or $460 per day

The answer is clear.

TABLE II

DATA REDUCTION OPTIONS - SUMMARY

GROUND DATA

PER SPECTRUM CQST

1. IF USING OUIDATED SG-4 ANALOG SYSTM

OPTION 1A = (A - D) + (CARDS) + (LMSC Program)	=	$	1.92
OPTION 1B = (A - D) + (CARDS) + (Interim 360 program)	=		1.28

2. IF USING MODIFIED ANALOG-DIGITAL SG-4 UNIT

CAPITAL OUTLAY $10,000

OPTION 2 = (PART B - Interim 360 Program)	=		0.15

P3A AIRBORNE DATA

3. IF STANFORD RECEIVES EDITED & BLOCKED DIGITAL TAPES

A1. If identifications appear before every spectrum i.e. 6 per second

OPTION 3A1 = (Main 360 Program)	=	$	0.13

A2. If no identification is placed on the tapes. Range coded times must be used and cards generated to find spectra.

OPTION 3A2 = (CARDS) + (Interim 360 Program)	=		1.11

4. IF STANFORD RECEIVES RAW ANALOG TAPES

OPTION 4 = (1B APPLIES) = (A - D) + (CARDS) + (Interim 360 Program)	=		1.28

TABLE III

DETAILED ANALYSIS DATA REDUCTION COSTS

UNIT COSTS BASED ON 300 SPECTRA/GROUND TAPE

1. GROUND OPERATIONS USING OUTDATED SG-4 (ANALOG) UNIT

				Unit Costs
ANALOG	1.	A-D Conversion $50.00 per tape		.17
DIGITAL	2.	Tape Dump $75.00	.25	
DIGITAL	3.	Manual stop-start times location and card-coding $150.00	.50	
			.75	.75
			Initial Costs	.92

A. LMSC Program

Set up costs (Kooyers)	0.40	
7090 running costs	0.45	
1401 excess printer costs	0.15	
	1.00	

B. Interim 360 Program

Set up costs (2 hrs.)	0.07	.07
Part A load & Compile	0.02 (70 secs)	
Part A execute	0.15	.17
Part B load	0.04 (45 secs)	
Part B execute	0.08	.12
	0.36	0.36

OPTION 1A = (A-D) + (CARDS) + (LMSC program) = 1.92/spectrum

OPTION 1B = (A-D) + (CARDS) + (Interim 360 program) = 1.28/spectrum

2. GROUND OPERATION USING MODIFIED ANALOG-DIGITAL SG-4 UNIT

Digital encoder	$ 1000
A-D converter (x channels)	4000*
Direct digital recording	5000

Total CAPITAL OUTLAY $10,000
(This can be reduced to $6,000 if MSC gets A-D unit* for Stanford.)

Program Costs

A-D costs	NIL
Tape Dump	NIL
Start-Stop cards	NIL

Computer uses main 360 program

Set up costs	0.03/spectrum
260 Part B costs	0.12/spectrum

OPTION 2 (Part B - 360 Program) 0.15 per spectrum based on 300 spectra per ground tape.

DETAILED ANALYSIS DATA REDUCTION COSTS (Continued)

3. AIRCRAFT OPERATION

A. IF STANFORD RECEIVES EDITED & BLOCKED DIGITAL TAPE

A1. IF IDENTIFICATIONS APPEAR BEFORE EVERY SPECTRUM i.e. 6 PER SECOND

Computer uses main 360 program

Set up costs (1 hr.)	10.00
Part B Load (60 secs.)	3.75
Part B Execute (1.3 secs/spectrum)	24.60
	38.35

OPTION 3A1 - Based upon 300 spectra/aircraft tape = 0.13/spectrum

A2. IF NO IDENTIFICATION IS PLACED ON THE INDIVIDUAL SPECTRAL RECORD (either when recorded or in subsequent A-D steps)

Marker ID's are needed to be placed on the digital tape,

OR the LMSC "Range-coded time" system or its equivalent must be on the tape. Stop-start times must be manually extracted and option 1B costs apply.

OPTION 3A2 - (CARDS) + (interim 360 program) = $1.11/Spectrum

4. IF STANFORD RECEIVES RAW ANALOG TAPES
Option 1B applies

OPTION 4 = (A-D) + (CARDS) + Interim 360 program = $1.28/Spectrum

III. ACHIEVEMENTS IN PAST SIX MONTHS

A. PATTERNS OF WORK ALLOCATION

Reasonably detailed records have been kept from which it is possible to examine the pattern of research and support functions performed for NASA/SAR, NASA/MSC, and the User Agencies.

1. Direct support for NASA/SAR - Reporting & Publications (21% of effort)

This six-month period we have produced two technical publications and three Technical Reports (SRSL 67-1, 67-2 and 67-3). The publications have been photo-copied and appear in Appendices B & C of this report. The Technical Reports represent our plan to place the data handling and spectral matching techniques in the hands of as many users as possible. These reports on spectral matching have been given a much more reduced circulation (50 copies) than the semi-annual and annual reports which have 200-300 copy distributions. In all cases at least 5 reports have been sent to the Technical Reports office, Washington, D.C. and 10-25 copies to the Data Facility at NASA/MSC Houston, Texas,

2. Direct support for NASA/MSC - aircraft and spaceflight programs (6% of effort).

With the identification of MSC as head center for the aircraft program and for the possible Apollo Applications B & D spaceflights we have found more of our support efforts needed to be directed towards Houston. We have made 7 man-trips in the past 6-month period alone which have cost us $2000 in time and airfares. On the credit-side however we feel that we have a greater rapport with MSC personnel and that our aircraft experiment is progressing well, Table IV details these costs.

3. User Agency Support (USDA - 10% of effort)

Most of the research and support effort this six month period has been devoted to the USDA rather than to the USGS. Our continuing analysis of the Davis Field spectra (Tape 11) has occupied a further 10.4% of our effort. Research costs for this support (See Table IV) have now risen over $11,000. Some preliminary data from these tapes was shown in the Annual Report (p. 15-19) and additional results are recorded here in Section IIID.2.

4. Main Stanford Research Effort

Table XIV at the rear of the report shows in detail the allocation of research effort by level for the past six months. Significantly the rate of gathering of new spectral data has slowed up, due mainly because of the data reduction problems. It is unwise to collect more data at our present rate (300-500 per day) if the reduction costs are so high. Our suggested modifications, which will save us over $1.00 per spectrum in costs, must be made before we go into the field again for an active season.

TABLE IV

SUPPORT FOR NASA/MSC

Aircraft Operational Scheduling and Spaceflight Experiment Specifications

Six Month Period (Nov. 1, 1966 – May 1, 1967)

	Year ending Nov. 1, 1966 Man Months	$ (Actual)	Past 6 months Man Months	(Actual)
Personnel Time				
R.J.P. Lyon	1.25	-	0.62	-
R.S. Vickers	0.25	-	0.90	-
	1.50 mm	$2,900	1.52 mm	$2,960
Travel Costs				
6 round trips		1,800	7 round trips	2,002
		$4,700		$4,962

TOTAL EFFORT FOR MSC 3.02 man months

TOTAL COSTS OF MSC SUPPORT $9,662.

TABLE V

SUPPORT FOR U.S. DEPT. OF AGRICULTURE

DAVIS TEST SITE (FIELD DATA TAPE 11)

Spectral Study of Crops, Vegetables and Fruit Trees and Vines

RESEARCH EFFORT	Year ending Nov. 1, 1966 Man Months	$ (Actual)	Past 6 months Nov. 1 – May 1, 1967 Man t>s	(Actual)
A. Personnel Time				
1. Field Operation	0.60	630	-	-
2. Preparing SG-4 instrument	1.80	2,080		
3. Data Reduction Time	0.60	630	.08	1,569
LABOR INC. OVERHEAD COSTS	3.02 mm	$ 5,245	.08	$2,460
B. Data Reduction				
1. 7090 computer oosts (incl 1401 printer)	(0.25 >r)	57	(0.81 hr.)	258
2. Field Engineering Support	-	240	-	-
3. Programmer Assistance charges	1.16	1,855	0.57	910
	4.16 mm	$ 7,397	2.65 mm	$3,628

TOTAL RESEARCH EFFORT FOR U.S.D.A. 6.81 man months

TOTAL RESEARCH COSTS FOR U.S.D.A. SUPPORT $11,025.

B. PUBLICATIONS

During this 6-month period a number of reports and publications were issued from this laboratory. The first of these was a general article in a University publication, Stanford Today, and it described in terms understandable to the scientific layman the purpose and progress of the research being carried out under the grant, as well as commenting on the other techniques being used in remote sensing. In April a paper entitled "Infrared Sensing from Spacecraft - A Geological Interpretation" was presented at a plenary session of the Thermo-Physicist' Conference (A.I.A.A.) in New Orleans. The paper concerned itself primarily with the potential value to a geologist of IR emission spectral analysis. Copies of both these papers are appended to this report.

In addition to the publication mentioned, the Remote Sensing Laboratory is issuing a series of technical letters. A brief summary of their content is given below.

SRSL Tech, Report #67-1

This report describes the original Lockheed program, which provides correlation analysis between test spectra and a library of fifty spectra taken from rocks of known composition. This basic program was used to produce the data from the first series of field trips on this project.

SRSL Tech Report #67-2 and 67-3

Part II describes the modifications to the basic program that were made by the Stanford group to a) enable the program to run on the Stanford 7090 and b) to compensate for a number of instrumental effects present in the data. In particular the voltage drift procedures are described in 67-3.

Further technical memos will be issued in the next reporting period describing new developments in the data reduction program.

C. FIELD EFFORTS

Reno - January 1967

The Sonora Pass field operation in the Fall, 1966, was conducted with a thermistor detector system installed in the Stanford SG-4 spectrometer. The resulting spectra taken with this equipment were of poor quality, thus it was decided to take spectra of Sonora Pass rock samples at a later date when the SG-4 could be operated with suitable detection equipment.

Approximately 60 representative rock samples were collected from 7 test sites along the major flight line at the Sonora Pass test site by the University of Nevada-NASA group. These samples were held in storage at the University of Nevada and were made available to the Stanford Remote Sensing group for infrared analysis during the latter part of January, 1967.

The Stanford SG-4 spectrometer equipped with a Cu-Ge detector; data recording equipment; Digitec thermometers; humidity, wind velocity and solar radiation monitors; and ancillary equipment were transported to Reno, Nevada, January 26, 1967, via Stanford Remote Sensing vehicle. In order to duplicate the meteorological conditions of the Sonora Pass test site as closely as possible, a test area at 6000 feet altitude (the ranch-home of Mr. Jack Quade, NASA-Nevada Project Co-ordinator) was chosen.

The rock samples were brought from storage and set up for analysis on the porch surface adjacent to the Quade ranch house. The spectrometer was set up on the porch surface and was connected electronically to the data recording equipment mounted in the truck. Rock samples were left in the storage trays and allowed to come to thermal equilibrium in sunlit condition before being placed beneath the spectrometer for analysis. Surface temperatures of each test rock sample, a blackbody, a reference rock, and air temperatures were monitored throughout the test procedure. Humidity, solar radiation, and wind velocity measurements were taken continuously. Stereo-color photos were taken of each test sample just prior to recording the spectra of the sample.

Spectra were taken of representative igneous rocks, natural rock surfaces (including lichen and plant covered surfaces), volcanic and meta-sedimentary rocks from the Sonora Pass test site. In addition to these samples, about 20 representative rock samples from the Mesquite Sedimentary test site were also included in the field analysis. In order to provide an extra check on the behavior of the SG-4 during this operation, polystyrene absorption spectra were included at regular intervals during the data recording periods. This form of wavelength calibration is now standard practice with the SG-4. The entire test operation was conducted over a period of 5 days, no field work was done on two of these days owing to rainy and high-humidity conditions. It was also noticed that little spectral contrast between samples was obtainable when the rock temperatures fell to a few degrees above 0°C. This effect has been ascribed to the high cavity signal of the SG-4 Cassegrain system swamping out the smaller contribution from the cold rock.

The data from this field operation (& Tables VI ABC) is presently being analyzed by appropriate statisticalmethods. A delay in analysis was caused by having to obtain permission from the Air Force to use their Analog to Digital converter facility at Lockheed Missiles and Space Co. Computer Facility in Sunnyvale, California. Analysis of data interlock between spectral and meteorological variables, computing modal compositions from spectra, and discrimination between rock types (viz. granites vs. quartz diorites, granite vs. basalt, igneous vs. sedimentary) are planned in the continuing statistical analysis of 'the Sonora Pass data.

Mesquite and Pisgah Crater March 1967

Dr. R.J.P. Lyon and M.A. Kuntz of the Remote Sensing Laboratory, Stanford University, took part in field operations associated with overflights by NASA 926 at Mesquite and Pisgah Crater test sites during the period March 21-23, 1967. The purpose of the field operations was to collect ground truth data to be used in the interpretation of imagery of the test sites taken from the aircraft.

KEY FOR TABLES VI A,B & C

Weather and temperature data and instrument location and operating parameters collected in the Reno field study area is displayed in computer output format in Tables A,B &C. This is a direct readout from input cards, which are themselves rapidly generated from the field data sheets (See Pisgah data in next section). These are actually IBM coding forms with added basic notations.

On these 3 tables any horizontal line may be read as follows:

COLUMN		CODE	EXAMPLES	CODE
1.	Value	(VAL)	Not used	(S for sampled N for none taken)
2.	Target	(TARGET)	CNKO6D	Cinko Lake granodiorite
3.	Location	(LOCN)	ST1SP2	
4.	Tape No.	(TAPE)	1704 (A-K)	170 (letter not printed)
5.	Day No.	(DAY)	Jan, 27	27
6.	Time now	(TIME)	11:09 A.M.	1109
7.	Lapsed time since start of cooling	(LAPSE)	69 mins. since coolant added	69
8.	Blackbody Temp.	(BB)	17°C	17
9,10.	Rock, Reference Rock	(ROCK,RFRK)	19°,15°C (2 rocks	19,15
11.	Barnes Radiometer . rdg.	(BRMS)	17°C (IT3)	17
12.	Air Temp	(AIR)	8°C	8
13.	Relative Humidity	(RH)	60% RH	60
14.	Wind velocity	(WND)	1 mile/hr.	1
15.	View angle of spectrometer	(VIEW)	24°	24
16.	Tilt angle of dewar	(TILT)	25°	25
17.	Dip of rock surface	(DIP)	(not used)	0
18.	Spectrometer period	((PRD)	10 seconds	10
19.	Spectrometer gain	(GN)	Gain setting 8.1	81
20.	Spectrometer Bandpass	(BP)	Bandpass 6 cps	6
21.	Radiometer offset	(QSET)	offset at .99	99
22.	Radiometer gain	(GNR)	Gain at 5.00	500
23.	Radiomter reading	(RDG)	reading 39	39
24.	Range to target	(RANGE)	range 6 feet	6
25.	Solarimeter reading	(SOL)	reading in millivolts	3.52

P1A3

IR AND WEATHER DATA 19[illegible] FIELD SEASON
RENO,QUADE RANCH SITE-SONORA PASS SAMPLES
LAT 39.[illegible]4DEG LONG 11[illegible].80DEG ALT 5000 STANFORD GRATING 16.4 MIN 29.3 DEG MAX SBRC GE-CU FILTER 7.46*4

VAL	TARGET	LOCN	TAPE	DAY	TIME	LAPSE	BB	ROCK	AFAK	EANS	AIR	RH	WND	VIEW	TLT	DIP	PAD	GN	BP	OSET	GNR	ROG	RANGE	SOL
	NEW	DAY	0	0	0	0	0	0	0	0	0	0	0	0	0	0	0	0	0	0	0	0	0	0
	BB	SRQR01	1701	27	1051	51	22	0	16	20	10	61	0	24	25	0	10	81	6	50	500	4	6	310
	BBPOLY	SRQR01	1702	27	1056	56	19	0	16	22	9	46	0	24	25	0	10	81	6	99	500	46	0	363
	CNKOGD	ST1SP1	1703	27	1104	64	16	0	15	18	8	62	0	24	25	0	10	81	6	99	500	36	6	358
	CNKOGD	ST1SP2	1704	27	1109	69	17	19	15	17	8	60	1	24	25	0	10	81	6	99	500	39	9	352
	BBPBST	ST8SP1	1705	27	1115	75	15	16	14	18	8	60	3	24	25	0	10	81	6	99	500	40	6	358
	CNKOGD	ST1SP3	1706	27	1119	79	16	14	14	17	7	64	0	24	25	0	10	81	6	99	500	34	6	342
	CNKOGD	ST1SP4	1707	27	1123	83	17	16	14	18	9	62	0	24	25	0	10	81	6	99	500	35	6	378
	BBPOLY	SRQR01	1708	27	1127	87	18	0	15	24	9	61	0	24	25	0	10	81	6	99	500	39	6	420
	BBPBST	ST8SP2	1709	27	1131	91	19	20	15	21	10	51	4	24	25	0	10	81	6	99	500	33	6	428
	CNKOGD	ST1SP5	1710	27	1136	96	14	9	14	22	8	61	8	24	25	0	10	81	6	99	500	30	9	382
	CNKOGD	ST1SP6	1711	27	1140	100	13	17	14	23	9	55	0	24	25	0	10	81	6	99	500	28	6	350
	STDBST	SRQR01	1712	27	1144	104	13	22	13	25	7	58	0	24	25	0	10	81	6	99	500	35	6	455
	GNKOGD	ST1SP7	1713	27	1149	109	18	18	14	22	10	51	0	24	25	0	10	81	6	99	500	15	6	422
	DLFRAL	ST2SP1	1714	27	1153	113	17	17	14	19	10	59	3	24	25	0	10	81	6	99	500	3	6	320
	BB	SRQR01	1715	27	1158	118	15	0	13	17	11	50	2	24	25	0	10	81	6	99	500	10	6	220
	BBPOLY	SRQR01	1716	27	1201	121	16	0	13	18	11	41	3	24	25	0	10	81	6	99	500	4	6	225
	BBPBST	ST8SP3	1717	27	1206	126	15	18	13	20	11	47	0	24	25	0	10	81	6	99	500	1	9	240
	DLALTR	ST2SP2	1718	27	1211	131	15	18	13	17	11	45	5	24	25	0	10	81	6	99	500	0	9	400
	DLALFR	ST2SP3	1719	27	1217	137	21	18	14	20	12	36	0	24	25	0	10	81	6	99	500	70	6	364
	TPOPO1	SRQR01	1720	27	1222	142	24	20	14	20	13	34	2	24	25	0	10	81	6	99	500	68	6	320
	BBPBST	ST8SP4	1721	27	1226	146	21	14	14	22	11	32	2	24	25	0	10	81	6	50	500	70	6	300
	DLALLM	ST2SP4	1722	27	1233	153	16	16	13	19	11	34	6	24	25	0	10	81	6	50	500	67	6	300
	BBPOLY	SRQR01	1723	27	1237	157	15	0	13	17	10	35	7	24	25	0	10	81	6	50	500	64	6	290
	CNKOGD	ST2SP5	1724	27	1243	163	13	17	13	19	10	32	10	24	25	0	10	81	6	50	500	76	9	270
	BBPOLY	SRQR01	1725	27	1328	208	16	0	12	17	13	35	0	24	25	0	10	81	6	50	500	74	6	200
	BBPBST	ST8SP5	1726	27	1333	213	15	16	12	17	13	35	0	24	25	0	10	81	6	50	500	62	9	290
	DLALGP	ST2SP6	1727	27	1341	221	17	14	12	16	12	38	0	24	25	0	10	81	6	50	500	63	6	280
	METAGP	ST3SP1	1728	27	1346	226	14	16	12	17	13	38	0	24	25	0	10	81	6	50	500	65	6	190
	BBPBOO	ST8SP6	1729	27	1353	233	15	17	12	19	13	33	0	24	25	0	10	81	6	50	500	68	6	190
	METADP	ST3SP2	1730	27	1358	238	15	16	12	17	12	31	4	24	25	0	10	81	6	50	500	67	6	190
	KTLFMO	ST7SP1	1731	27	1403	243	15	12	12	15	12	33	3	24	25	0	10	81	6	50	500	67	6	170
	MSSHPN	ST3SP3	1732	27	1410	250	14	11	12	14	12	33	0	24	25	0	10	81	6	50	500	68	6	170
	BBPOLY	SRQR01	1733	27	1416	256	15	11	12	16	12	34	2	24	25	0	10	81	6	50	500	70	6	142
	FRMONZ	ST7SP2	1734	27	1421	301	12	12	12	17	11	32	5	24	25	0	10	81	6	50	500	69	6	125
	METASD	ST3SP4	1735	27	1426	306	11	11	11	16	9	35	8	24	25	0	10	81	6	50	500	68	6	125
	KTLLMS	ST7SP3	1736	27	1430	310	11	11	11	11	10	29	12	24	25	0	10	81	6	50	500	68	6	120
	METADP	ST3SP5	1737	27	1436	316	11	11	10	13	10	31	7	24	25	0	10	81	6	50	500	69	9	127
	MONOSB	SRQR01	1738	27	1441	321	11	10	10	11	9	33	6	24	25	0	10	81	6	50	500	69	6	125
	KTLFMO	ST7SP4	1739	27	1446	326	11	11	10	11	10	32	6	24	25	0	10	81	6	50	500	70	6	122
	MSGPHZ	ST3SP6	1740	27	1451	331	11	10	10	10	10	32	0	24	25	0	10	81	6	50	500	70	6	118
	KTLFMG	ST7SP3	1741	27	1455	335	11	9	10	10	10	31	0	24	25	0	10	81	6	50	500	70	6	110
	BBPOLY	SRQR01	1742	27	1459	339	12	10	10	12	10	31	0	24	25	0	10	81	6	50	500	71	a	98
	MSGPVT	ST3SP7	1744	27	1505	345	11	9	9	9	9	36	0	24	25	0	10	81	6	50	500	70	6	60
	KTLGPL	ST7SP6	1745	27	1509	349	10	90	99	11	9	35	0	24	25	0	10	81	6	50	500	68	6	110
	MSPPOO	ST3SP8	1747	27	1520	360	12	10	9	11	10	37	0	24	25	0	10	81	6	50	500	71	9	170
	BBPOLY	SRQR01	1748	27	1523	363	14	9	9	15	11	35	3	24	25	0	10	81	6	50	500	73	6	150
	NEW	TAPE	0	0	0	0	0	0	0	0	0	0	0	0	0	0	0	0	0	0	0	0	0	0
	BB	SRQR01	1801	27	1544	384	14	10	9	14	10	43	0	24	25	0	10	81	6	50	500	74	6	80

IR AND WEATHER DATA 1967 FIELD SEASON

RENO, QUADE RANCH SITE-SONOMA PASS SAMPLES

LAT 39.44DEG LONG 119.80DEG ALT 5000 STANFORD GRATING 16.4 MIN Z9.3 DEG MAX OBRC GE-CU FILTER 7.46*4

VOL TARGET	LOCN	NAME	DAY	TIME	LAPSE	BB	ROCK	RFRK	BRNS	AIR	RH	WND	VIEW	TLT	DIA	PRD	GN	BP	OSET	GNR	RDA	RANGE	SOL
NEW	DAY	0	0	0	0	0	0	0	0	0	0	0	0	0	0	0	0	0	0	0	0	0	0
BB	SRQR01	1901	32	1004	34	3	0	4	1	2	80	0	17	20	0	10	81	6	6	300	18	4	137
BBPOLY	SRQR01	1902	32	1007	37	3	0	4	2	2	80	0	17	20	0	10	81	6	6	300	16	7	142
KTLMZL	ST7SP7	1903	32	1014	44	4	5	4	5	2	80	0	17	20	0	10	81	12	6	300	15	7	195
ANAUTF	ST6SP1	1904	32	1020	50	4	7	3	6	2	80	0	17	20	0	10	81	12	6	300	13	7	200
KFLWMZ	ST4SP1	1905	32	1024	54	4	3	3	4	0	80	3	17	20	0	10	81	12	6	300	12	7	210
ANAUTW	ST6SP2	1906	32	1030	60	4	1	2	4	0	80	2	17	20	0	10	81	12	6	300	14	7	222
KFLFMZ	ST4SP3	1907	32	1034	64	4	2	3	2	0	80	2	17	20	0	10	81	12	6	300	14	7	230
BB	SRQR01	1908	32	1038	68	4	0	3	4	1	80	0	17	20	0	10	81	12	6	300	50	7	310
BBPOLY	SRQR01	1909	32	1042	72	5	0	3	4	4	80	0	17	20	0	10	81	12	6	300	50	7	370
ANATWC	ST6SP3	1910	32	1047	77	6	5	4	4	5	80	0	17	20	0	10	81	12	6	300	45	7	350
KFLIRN	ST4SP4	1911	32	1050	80	6	3	4	4	3	80	0	17	20	0	10	81	12	6	300	57	7	350
ANDWAU	ST6SP4	1912	32	1054	84	9	4	4	4	5	80	0	17	20	0	10	81	12	6	300	50	7	355
APLDIK	ST4SP5	1913	32	1058	88	10	2	4	3	2	80	0	17	20	0	10	81	12	6	300	52	7	330
MONOBS	SRQR01	1914	32	1104	94	10	3	4	4	3	80	0	17	20	0	10	81	12	6	300	50	7	280
QRSKYO	SRQR01	1915	32	1108	98	10	0	4	4	5	80	0	0	20	0	10	81	12	6	300	0	0	270
ANDFCU	ST6SP5	1916	32	1112	102	10	2	4	5	2	80	0	17	20	0	10	81	12	6	300	50	7	300
KFLFPM	ST4SP6	1917	32	1116	106	10	4	4	4	2	80	0	17	20	0	10	81	12	6	300	49	7	315
BB	SRQR01	1918	32	1119	109	8	0	4	8	2	80	0	17	20	0	10	81	12	6	300	50	7	330
BBPOLY	SRQR01	1919	32	1123	113	7	0	4	8	2	80	0	17	20	0	10	81	12	6	300	50	7	340
KFLGPL	ST4SP2	1920	32	1127	117	9	6	4	4	3	80	0	17	20	0	10	81	12	6	300	50	7	340
DNFBLS	LS6CLN	1921	32	1132	122	11	5	4	5	4	80	0	17	20	0	10	81	12	6	300	50	7	335
KFLAIR	STASPL	1922	32	1136	126	11	4	5	5	3	80	0	17	20	0	10	81	12	6	300	50	7	337
PCSRSS	N6171	1923	32	1140	130	12	5	6	5	5	80	0	17	20	0	10	81	12	6	300	51	7	330
KFLAFG	SP3	1924	32	1145	135	13	5	5	4	7	70	0	17	20	0	10	81	12	6	300	51	7	342
PKFWLS	N6206	1925	32	1150	140	14	5	5	4	5	70	0	17	20	0	10	81	12	6	300	50	7	305
BB	SRQR01	1926	32	1154	144	12	0	5	11	6	70	0	17	20	0	10	81	12	6	300	51	7	250
BBPOLY	SRQR01	1927	32	1157	147	10	0	5	10	4	70	0	17	20	0	10	81	12	6	300	50	7	230
KFLAWT	SP4	1928	32	1202	152	9	3	5	5	3	70	0	17	20	0	10	81	12	6	300	50	7	250
TVOBSF	N6191	1929	32	1206	156	8	3	4	5	3	70	0	17	20	0	10	81	12	6	300	51	7	258
KFLAXN	SP5	1930	32	1211	161	8	4	4	5	3	70	0	17	20	0	10	81	12	6	300	50	7	240
BBPOLY	SRQR01	1931	32	1214	164	7	0	4	7	2	70	0	17	20	0	10	81	12	6	300	50	7	240
BB	SRQR01	1932	32	1217	167	7	0	4	6	3	70	0	17	20	0	10	81	12	6	300	50	7	270
NEW	TAPE	0	0	0	0	0	0	0	0	0	0	0	0	0	0	0	0	0	0	0	0	0	0
BB	SRQR01	2001	32	1247	197	16	0	6	16	4	62	0	17	20	0	10	81	12	6	300	57	7	430
BBPOLY	SR	2002	32	1250	200	14	0	6	15	4	62	0	17	20	0	10	81	12	6	300	57	7	270
KFLAFP	SP8	2003	32	1346	6	21	11	8	12	6	64	0	17	20	0	10	81	12	6	300	58	7	630
KFLAFM	SP6	2004	32	1350	10	22	7	7	10	7	58	0	17	20	0	10	81	12	6	300	58	7	770
PCFSCH	N6175	2005	32	1355	15	22	7	7	9	6	57	0	17	20	0	10	81	12	6	300	58	7	322
KFLWMZ	ST5SP1	2006	32	1358	18	17	11	7	16	5	57	0	17	20	0	10	81	12	6	300	58	7	280
MONOBS	SRQR01	2007	32	1404	24	14	7	7	16	5	58	0	17	20	0	10	81	12	6	300	58	7	400
KFLAAD	SP7	2008	32	1407	27	13	6	7	6	4	58	0	17	20	0	10	81	12	6	300	57	7	345
PKLWLS	N6238	2009	32	1411	31	13	5	7	6	5	60	0	17	20	0	10	81	12	6	300	58	7	320
BB	SRQR01	2010	32	1414	34	10	0	6	11	4	61	2	17	20	0	10	81	12	6	300	58	7	275
BBPOLY	SRQR01	2011	32	1417	37	10	0	7	10	5	60	0	17	20	0	10	81	12	6	300	57	7	275
KFLWIR	ST5SP3	2012	32	1421	41	11	9	7	12	4	55	0	17	20	0	10	81	12	6	300	58	7	290
PSFRSI	N6209	2013	32	1425	45	15	5	7	7	5	53	0	17	20	0	10	81	12	6	300	58	7	420
KFLGIR	ST5SP4	2014	32	1427	47	16	9	7	12	7	52	0	17	20	0	10	81	12	6	300	58	7	340
PCFPSS	N6164	2015	32	1431	51	16	7	7	8	7	48	0	17	20	0	10	81	12	6	300	58	7	410

P. 3 of 3

IR AND WEATHER DATA 1967 FIELD SEASON
RENO, QUADE RANCH SITE-SONORA PASS SAMPLES
LAT 39.44DEG LONG 119.80DEG ALT 5000 STANFORD GRATING 16.4 MIN 29.3 DEG MAX RC GE-CU FILTER 7.46*4

VOL TARGET	LOCN	TAPE	DA	*TIME	LAPSE	BB	ROCK	RFRK	BRNS	AIR	RH	WNO	VIEW	TLT	DIP	PAD	GN	BP	OSET	GNA	RDG	RANGE	SOL
PNFCCP	LS6	2016	32	1434	54	16	9	7	8	7	41	0	17	Z0	0	10	81	12	6	300	59	7	410
KFLFPK	ST5SP6	2017	32	1437	57	15	11	7	12	9	40	0	17	Z0	0	10	81	12	6	300	60	7	330
WATERC	SRQR01	2018	32	1442	62	13	15	8	11	9	44	0	17	Z0	0	10	81	12	6	300	0	7	360
BB	SRQR01	2019	32	1445	65	9	0	8	9	6	45	3	17	Z0	0	10	81	12	6	300	58	7	360
BBPOLY	SRQR01	2020	32	1447	67	9	0	8	8	5	48	4	17	Z0	0	10	81	12	6	300	57	7	350
KFLAA	SP1	2021	32	1449	69	9	7	7	9	5	48	2	17	Z0	0	10	81	12	6	300	57	7	275
APLDIK	ST5SP5	2022	32	1452	72	9	10	7	11	5	48	0	17	Z0	0	10	81	12	6	300	36	7	270
KTLAFM	SP2	2023	32	1455	75	8	8	7	12	5	48	0	17	Z0	0	10	81	12	6	700	37	7	210
KTLADM	SP3	2024	32	1458	78	8	7	7	11	6	47	0	17	Z0	0	10	81	12	6	700	37	7	150
KTLAOW	SP4	2025	32	1500	80	6	8	7	10	5	47	0	17	Z0	0	10	81	12	6	700	36	7	225
KFLAFR	SP5	2026	32	1502	82	6	9	7	12	5	46	0	17	Z0	0	10	81	12	6	700	36	7	245
BB	SRQR01	2027	32	1505	85	9	0	7	9	5	44	0	17	Z0	0	10	81	12	6	700	36	7	240
BBPOLY	SRQR01	2028	32	1508	88	11	0	7	11	5	44	0	17	Z0	0	10	81	12	6	700	36	7	200
VIEWOF	SRQR01	2029	32	1512	92	16	0	6	0	5	48	0	17	Z0	0	10	81	12	6	700	0	9999	225
SKYNCL	SRQR01	2030	32	1514	94	18	0	6	0	5	46	0	17	Z0	0	10	81	12	6	700	0	9999	210

Lyon and Kuntz left Menlo Park on March 19 at 5:30 P.M. and flew from San Francisco to Las Vegas via Western Airlines. At the Las Vegas airport they were met by Jack Quade, Peter Chapman and Peter Brennan of the NASA-Nevada Remote Sensing group. After dinner in Las Vegas, the group traveled via University of Nevada's field vehicle to Mesquite, Nevada, the base for the field operations at the Mesquite test site. The day of March 20 was spent traveling by very rough road to the test site, approximately 20 miles southeast of Mesquite, Nevada, and planning the field operations for the first set of overflights. Field stations were set up at three locations along the flight line, one at each end and one near the center of the flight line. Meteorological equipment and radiometers were monitored and checked out during the day. The first 2 overflights were to take place at 0400-0430 hours on March 21. The field parties left Mesquite at 0200 hours and drove to each of the test stations and began monitoring each of the test sites approximately one hour before the flights. Communications between field stations were conducted with walkie-talkies and Bayside radios. Excellent communications between the aircraft and each field station was maintained with Bayside radios throughout the overflight. The location of each field station for the night flights was marked by headlights and spotlights powered from portable generators. Most of the field crew returned to Mesquite for food and rest prior to the next series of flights. The second series of overflights of the Mesquite site took place at 1400-1430 hours, March 21. Again, three field stations were occupied and ground truth data was monitored at each of them. Locations of the field stations were marked by "home-made" smoke bombs provided by the pyrotechnic division of the NASA-Nevada group. Personnel at each of the test sites were:

Site 1 (South)	Site 2 (Central)	Site 3 (North)
Bill Tafuri	R.J.P. Lyon	J. Quade
Frank Fierce	M.A. Kuntz	P. Chapman
	Peter Brennan	

After completing ground truth work at Mesquite, the crew traveled to Las Vegas and later drove on to Barstow, California, arriving there at approximately 0100 hours, March 22. The crew made a concerted effort to set up ground stations prior to 1000 hours, March 22, the time set for the first series of overflights at the Pisgah test site. Luckily the NASA plane did not arrive at the test site until 1030 hours and the crews were in position at ground stations at that time. One station was set up at the north end of Pisgah Crater on the access road leading to the cinder quarry on the northwest flank of the Crater. It was originally planned to set up a ground station on the crater at the former test site, but the gate on the access road was locked. Another ground station was set up at the south end of the test site at the junction of the basalt flows and the lake bed sediments of Lavic lake. Meteorological and surface temperature data were recorded at both ground stations during the series of daylight overflights. Three passes were made by NASA 926 along flight line number 1 in addition to passes made on various other flight lines. Smoke bombs were again used and more clearly visible to the aircraft. After completion of the daylight overflight, both crews returned to Barstow to catch up on some needed rest in preparation for the pre-dawn overflight of the Pisgah test site. On March 23, both crews awoke at 0200 hours and proceeded to the test site ground stations in preparation for the night overflight. The location of each of the ground stations was again marked by auto headlights and flood lights, and NASA 926 reported that these lights were easily, visible from the air. Meteorological and surface temperature data were monitored for the entire period of the night overflights. Personnel at each of the test sites were:

Site 1 (North)	Site 2 (South)
J. Quade	R.J.P. Lyon
P. Chapman	M. Kuntz
P. Brennan	

At the completion of the night overflight, the NASA-Nevada crew returned to Reno via truck and Lyon and Kuntz returned to Las Vegas via rental car. They traveled from Las Vegas to SFO via Western Airlines and arrived at 1400 hours.

Ground truth data was monitored at Mesquite and Pisgah test sites- Pisgah data are given below.

KEY
* NO. OF SPECTRA IN GROUP
** BARNES RADIOMETER Use Column

Balqol Coding Form
FIELD DATA

Page A

MAR 1 5 1967

Version

GRATING ANGLE ____ ° Min ____ ° Max

Coder: M.A. Kuntz LOCATION: Pisgah - Lavic PCLL00 Date: 3/22/67 DAY: 81 Charge No: Ext No 4142/3

HELIUM FILL TIME: HRS ALTITUDE: SL. LAT: N LONG: W

DIP SLOPE, +E 180° -D VIEW ANGLE, DEWAR TILT

ADDITIONAL DESCRIPTION	SAMPLE DESCRIPTION: TGT TYP	LOCATION	TAPE NO.	TGT NO.	*	DAY	TIME NOW	LAPSE	TEMPS °C: BB	RK	SND	**	WEATHER: AIR	RH	WND	SPECTROMETER: BSLT	R AV	DIP SLOPE	SPEC PRD	GAIN	BP	RADIOMETER: OFFSET	GAIN	READ	RANGE FT	SOLAR METER mv	VAL	SKY	SEQ. NO.	CLOUDS
		PCLL03				081	1028	10.0	47	42	36		32	10	00	64	60									7.4		-40		
		PCLL03				081	1033	10.5	50	43	36		32	09	00	52	40									7.6		-40		
		PCLL03				081	1052	11.4	44	38	34		31	09	01	42	38									7.9		-40		
		PCLL03				081	1104	13.6	45	41	36		32	08	06	48	39									8.1		-40		
		PCLL03				081	1123	15.5	48	41	38		35	00	04	52	41									8.1		-40		
		PCLL03				081	1148	17.5	48	42	39		34	07	04	54	43									8.0		-40		
		PCLL03				081	1212	10.4	52	42	42		38	07	06	58	44									7.9		-40		
		PCLL03				081	1230	12.2	51	41	43		39	05	04	57	46									8.0		-40		
	1	7	13	15	17	19	22	26	29	31	33	35	37	39	41	43	46	48	50	53	55	57	60	63	66	70	73		80	

D. LABORATORY AND DATA REDUCTION

1. Laboratory Studies

The present set of library spectra* used in the Stanford correlation program were taken under laboratory conditions with a Perkin-Elmer Mod. 12 spectrometer. The samples had to be heated to over 600°K to raise the emitted energy to a suitable level. By the early part of this year the SG-4 system was operating in a fairly reliable manner and it was decided to compile a new library, using spectra taken outside the laboratory (although under fairly controlled conditions) with the SG-4. In this manner the sample and reference spectra from future field work would be derived from the same instrument. The spectra of some twenty rocks were taken for this purpose, and the data is presently being reduced.

The recent completion of a test console for I.R. radiometers detectors led to a brief but interesting study of the response times of a number of radiometers. Such a measurement is important if one wishes to use a radiometer in a mobile mode (e.g. the PRT-5 radiometer on board NASA 927). At this time we have measured only three radiometers all by the same manufacturer. When more data has been collected, the results of these tests will be published in a Technical Report.

---

* See Lyon (1964), NASA CR-100.

2. Analysis of the Field IR Spectra from the Davis Agricultural Test Site

In the Annual Report (p 15-19) we discussed the methods used in taking the field spectra May 23-25 last year. The SG-4 (short wavelength) unit (Fig. 2) on loan to Stanford from NASA/MSFC was mounted in a "cherry picker", a high-rise unit provided by the University of California (See Fig. 3) By this method the spectrometer, an operator, and a battery of cameras was raised 60 to 80 feet above the various crops, trees, vines and cereal plantings of the UC-Davis test farm. A standardized white reflectance card was viewed spectrally before each plant spectrum (Fig, 4). Close up black and white prints from vegetation color photos using both Kodachrome II and CD false color film are shown in Figs. 5 A & B.

The Stanford data truck was driven as close nearby as possible and the 100 foot cables connected between the truck recording system and the spectrometer (See Fig. 6). A total of 437 spectra from 58 groups of vegetation types was collected in the 3-day period and recorded on magnetic tape (Stanford Tape 11).

A total research effort of 6.81 man months and $11,025 in expenditures has been made on behalf of the USDA and Weslaco in setting up the spectrometer, gathering the data and in reducing the tapes.

a. Effect of Various Libraries in the Computer Program

Considerable delays in the data reduction have been caused by the absence of suitable library of plant spectra of an equivalent type for comparison in the computer program (See SRSL Tech Report #67-1 and 67-2). Initially, we collected spectra out of the literature for this purpose. We quickly found two problems.

i) very few published spectra were of the same materials as our field crops, trees and vines,

and ii) of the few we found of the right type, none extended over the wavelength spread of our field data ($0.75 - 2.1\mu$).

We then prepared a library from other laboratory measurements taken on similar plant leaves collected in the field by Weslaco personnel.

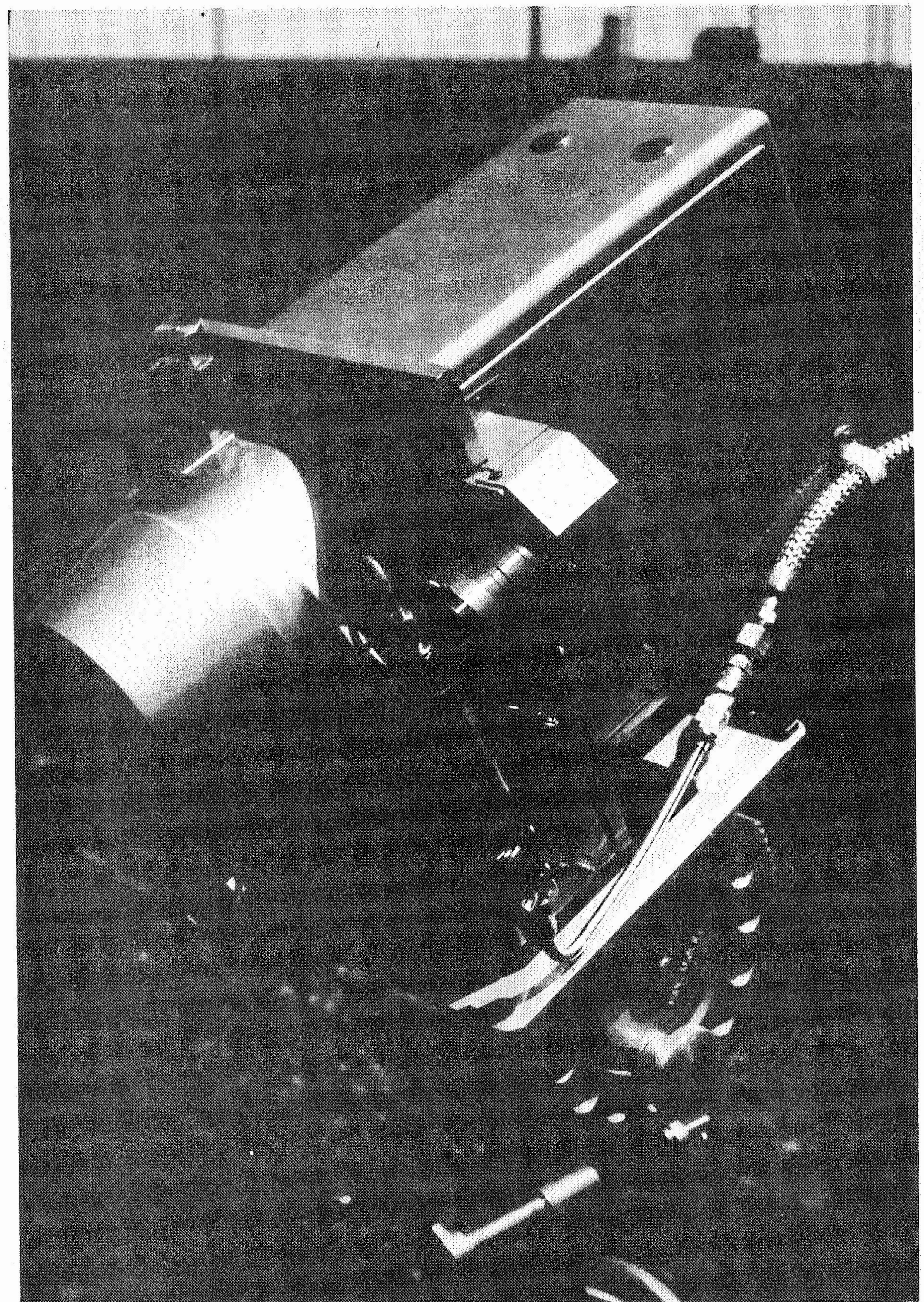

FIG. 2--SG-4 Shortwavelength Spectrometer on loan to Stanford from NASA/MSFC. Note 1/2" flexible line bringing high pressure gaseous nitrogen to cool the detector.

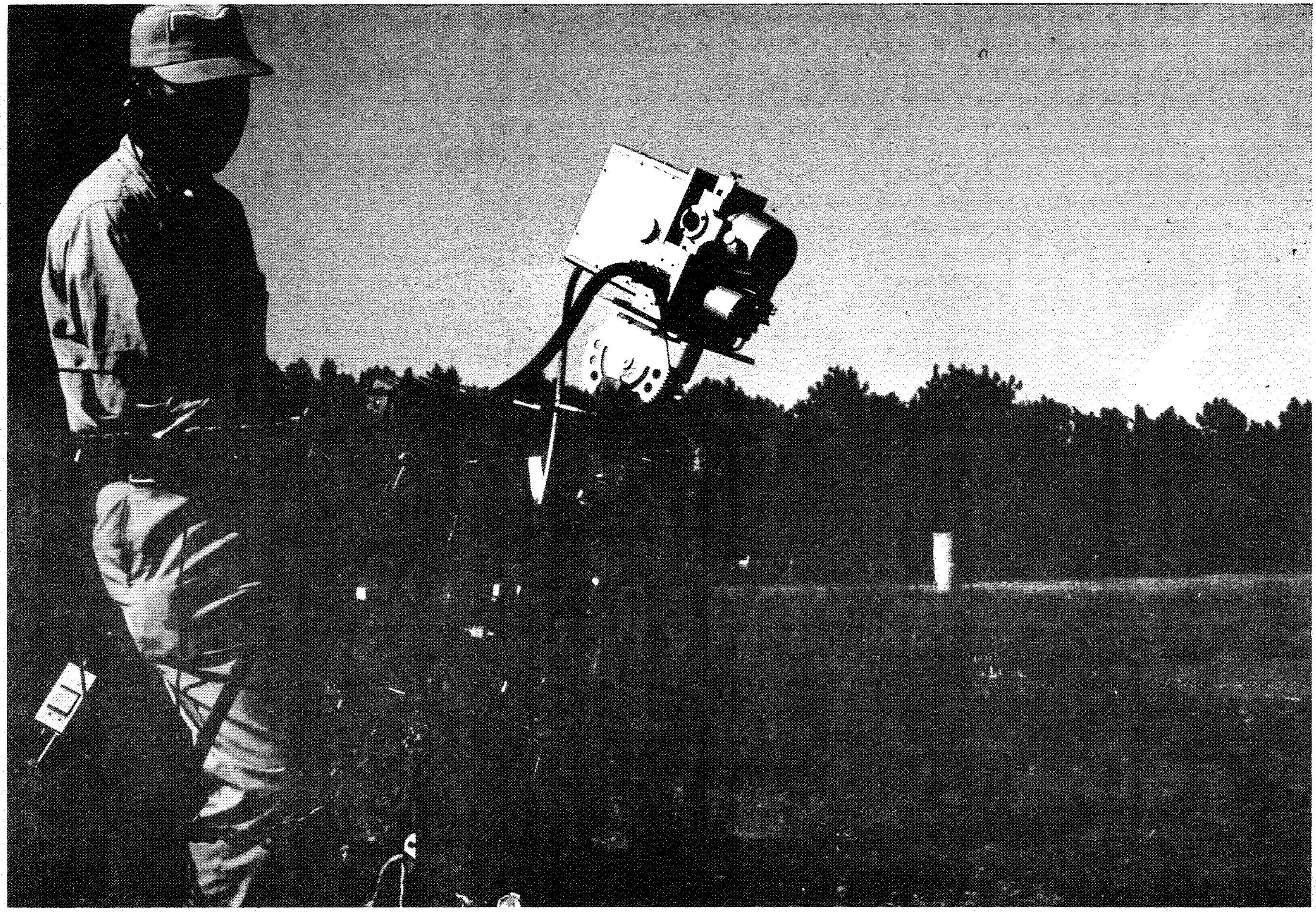

Fig. 3--Vic Myers, USDA/W slaco, preparing the SG-4 spectrometer for operation from the high-rise platform.

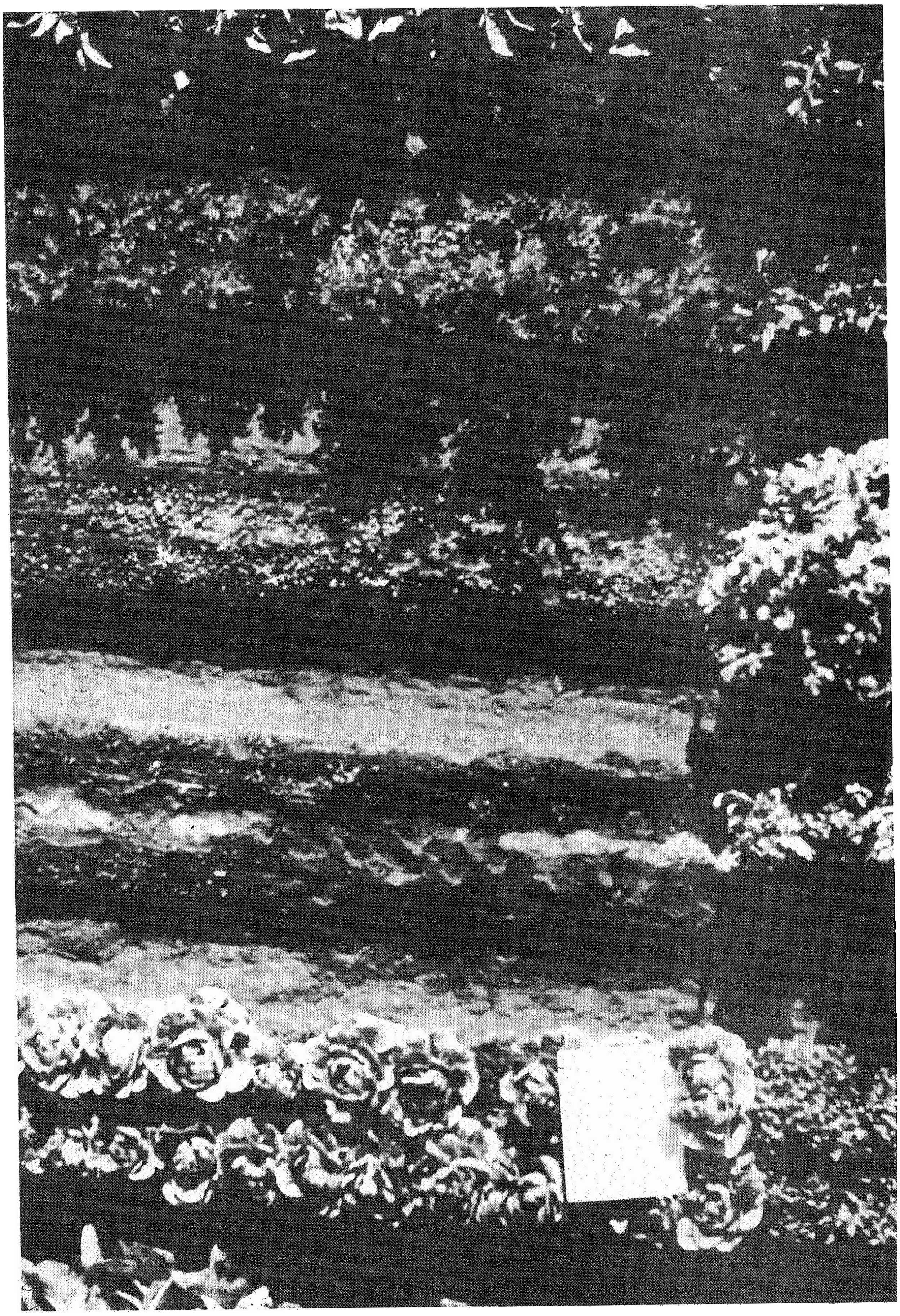

FIG.4--View from 60 feet above truck crops U.C. Davis site. Note irrigated soils and white card standard.

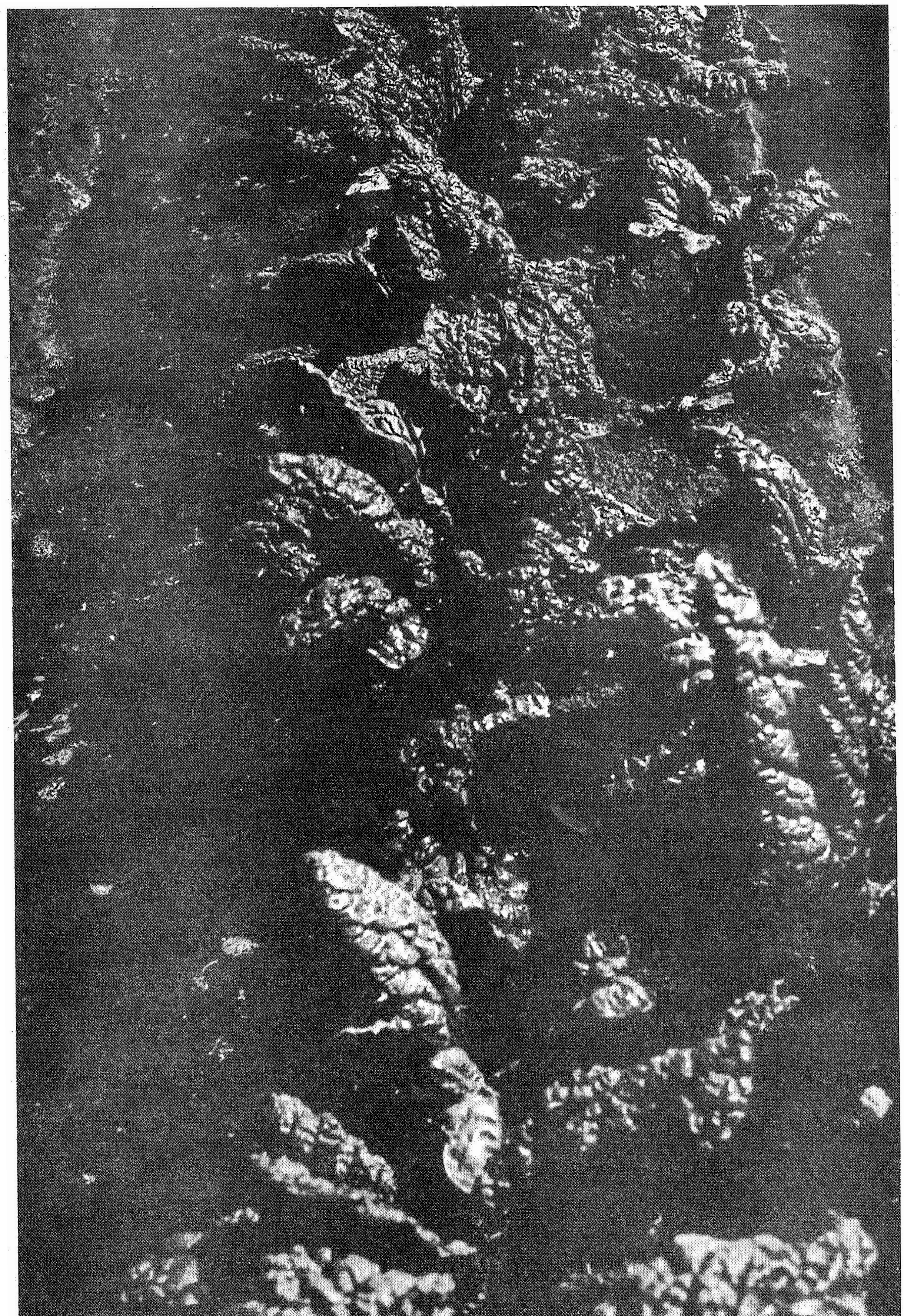

FIG. 5A--KALE, using regular Kodachrome II film. Compare with next figure of same scene using CD-False color film.

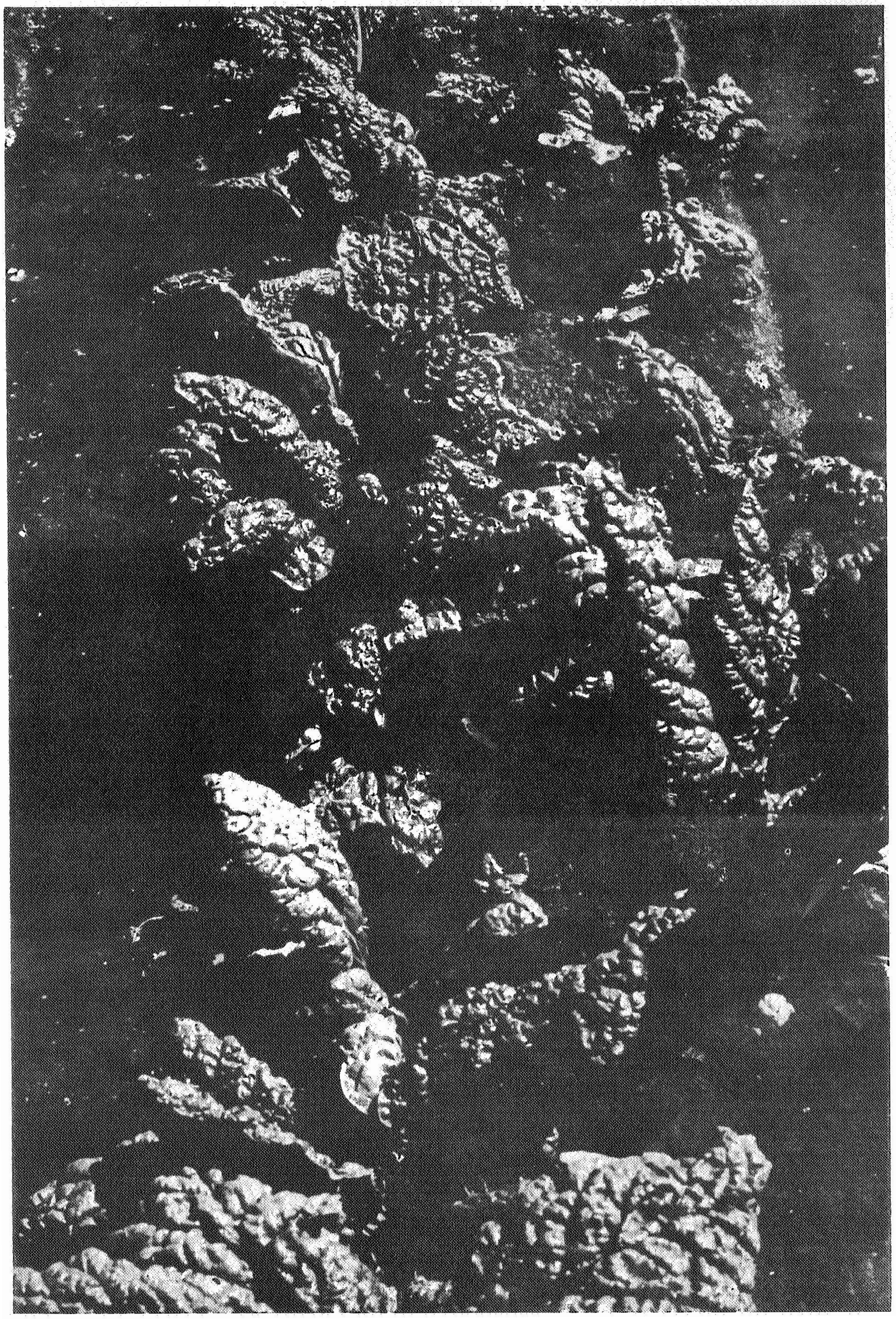

FIG. 5B--KALE using CD-False color film. Compare with previous figure using regular Kodaehrome II film.

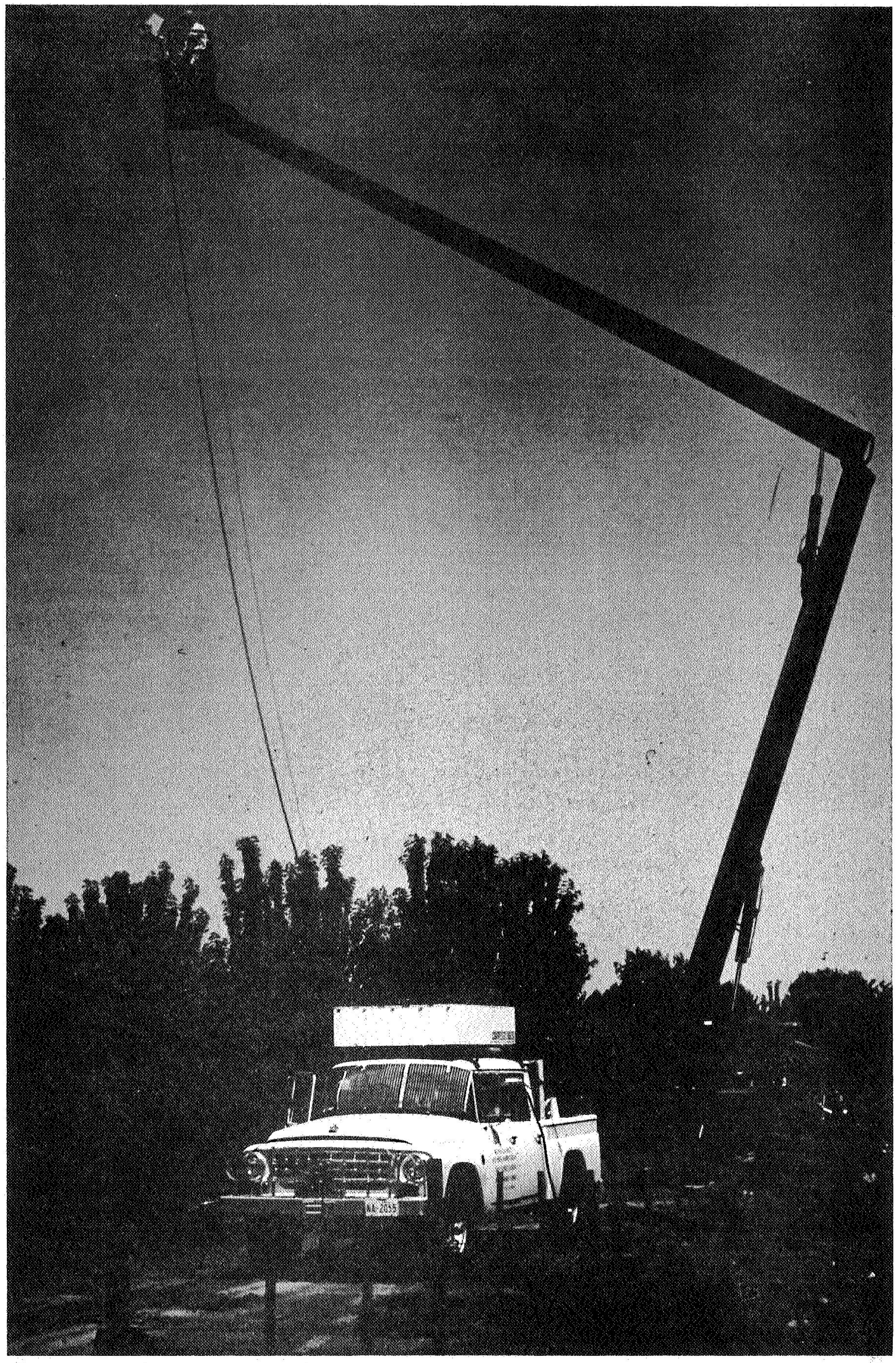

FIG. 6--Stanford Data Truck and the U.C.-Berkeley Cherry Picker units at Davis site. Note Spectrometer and Intrepid Operator 60 feet above vegetation.

The leaves were collected, placed immediately in "Saran Wrap" plastic foil and sent to the laboratory in Texas. This is a standard technique used by USDA-Weslaco. Analog chart recordings were received from Weslaco, hand digitized and a card-based library of spectra prepared for use in the Stanford computer. This was called library "B".

Finally, after the first 4 spectra in each of the 44 plant groups were run through the computer program (against library "B") we obtained a "mean spectrum" and ("+ 2 sigma" spectra) from those groups, to make up library "C").

In summary we found:

(i) Library "A" to be essentially useless

(ii) Library "B" was used to run the first 4 spectra of the 44 plant groups on Tape 11 and gave variable results

(iii) Library "C" gave the best results and was used for all the spectra run to date. The summary listings of the LMSC correlation program("CORRCO" see SRSL Tech. Letter 67-1) for all the spectra in the first 9 groups are shown on 2 pages in computer printout fom 'in Table VIII.

This listing shows across any horizontal line:

Column	Code	Examples	Code
1. Target Type	(TRGTYP)	Brocoli	BRCCLI
2. Location	(LOCN)	Davis, truck Crop #2	DVTC02
		Davis, grain field	DVGF01
3. Tape	(TAPE)	1100A	1100A
4. Day of Year	(DAY)	May 23	143 (Shown as "4" by mistake)
		May 24	144
5. Best fit (& CORRCO)	ANSR1 (R)	Broccoli (92%)	BRCCLI 92
6. 2nd best fit (CORRCO)	ANSR2 (R)	Lettuce (91%)	LTTUCE 91
7. 3rd best fit (CORRCO)	ANSR3 (R)	Potato* (85)	POTATO 85
8. 4th best fit (CORRCO)	ANSR4 (R)	Endive (85)	ENDIVE 85
9. 5th best fit (CORRCO)	ANSR5 (R)	Potato* (84%)	POTATO 84
10. 48th fit (2nd worst and CORRC)	ANSR 48 *(NR)*	Loose soil* (-75%)	LO SOIL -75
11. 49th fit (worst) & CORRCO	ANSR49 *(NR)*	Loose soil* (-76%)	LO SOIL -76
12. Polaroid Film #	(FILM)	not shown	

* Several types (and hence spectra) in the library used.

DAVIS TEST SITE — VEGETABLES, CROPS, TREES & VINES

STANFORD SPECTRAL MATCHING PROGRAM - MEANS LIBRARY

TARGTYP	DOCN	TAPE	DAY	ANSR1	R	ANSR2	R	ANSR3	R	ANSR4	R	ANSR5	R	ANSR49 NR	ANSR50 NR	FILM
BRCCLI	DVTC01	1100A	4	BRCCLI	92	LTTUCE	91	POTATO	85	ENDIVE	85	POTATO	84	LOSOIL-75	LOSOIL-76	
BRCCLI	DVTC01	1100B	4	BRCCLI	95	WHEAT9	88	LTTUCE	85	POTATO	82	POTATO	80	LOSOIL-79	LOSOIL-79	
BRCCLI	DVTC01	1100C	4	LTTUCE	91	BRCCLI	89	POTATO	89	POTATO	88	ENDIVE	87	LOSOIL-72	LOSOIL-72	
BRCCLI	DVTC01	1100D	4	BRCCLI	93	WHEAT9	91	POTATO	85	LTTUCE	84	HGRAPE	84	LOSOIL-78	RDSOIL-79	
BRCCLI	DVTC01	1100E	4	BRCCLI	91	LTTUCE	90	POTATO	88	ENDIVE	88	POTATO	84	RDSOIL-78	LOSOIL-81	
BRCCLI	DVTC01	1100F	4	BRCCLI	96	WHEAT9	90	LTTUCE	87	POTATO	84	HGRAPE	83	LOSOIL-80	LOSOIL-80	
BRCCLI	DVTC01	1100G	4	LTTUCE	92	POTATO	91	ENDIVE	90	POTATO	90	BRCCLI	90	RDSOIL-73	LOSOIL-75	
BRCCLI	DVTC01	1100H	4	BRCCLI	94	WHEAT9	93	POTATO	89	LTTUCE	88	POTATO	87	LOSOIL-81	RDSOIL-82	
BRCCLI	DVTC01	1100I	4	LTTUCE	93	POTATO	93	BRCCLI	92	ENDIVE	91	POTATO	90	RDSOIL-79	LOSOIL-8[illegible]	
KOLRBI	DVTC02	1104A	4	PEACH1	89	KOLRBI	88	TOMATO	84	SPEAR2	83	ALMOND	78	RDSOIL -8	CUSOIL-80	
KOLRBI	DVTC02	1104B	4	PEACH1	89	KOLRBI	84	TOMATO	80	SPEAR2	78	CGRAPE	72	RDSOIL 3	CUSOIL-56	
KOLRBI	DVTC02	1104C	4	PEACH1	89	KOLRBI	85	SPEAR2	80	TOMATO	78	ALMOND	72	RDSOIL -5	CUSOIL-60	
KOLRBI	DVTC02	1104D	4	PEACH1	88	KOLRBI	82	SPEAR2	77	TOMATO	75	ALMOND	68	RDSOIL -0	CUSOIL-59	
KOLRBI	DVTC02	1104E	4	PEACH1	88	KOLRBI	84	SPEAR2	78	TOMATO	76	ALMOND	71	RDSOIL -6	CUSOIL-92	
KOLRBI	DVTC02	1104F	4	PEACH1	86	KOLRBI	79	TOMATO	74	SPEAR2	74	WHEAT1	74	RDSOIL 4	CUSOIL-55	
KOLRBI	DVTC02	1104G	4	PEACH1	88	KOLRBI	87	SPEAR2	83	TOMATO	79	CGRAPE	76	RDSOIL-13	CUSOIL-63	
KOLRBI	DVTC02	1104H	4	PEACH1	87	KOLRBI	79	SPEAR2	74	TOMATO	72	CDSOIL	69	RDSOIL 2	CUSOIL-57	
KOLRBI	DVTC02	1104I	4	PEACH1	90	KOLRBI	85	SPEAR2	81	TOMATO	75	ALMOND	72	RDSOIL -7	CUSOIL-92	
TURNIP	DVTC02	1106A	4	KOLRBI	84	PEACH1	83	SPEAR2	82	CARROT	82	CGRAPE	79	RDSOIL-17	CUSOIL-64	
TURNIP	DVTC02	1106B	4	KOLRBI	96	ALMOND	91	CGRAPE	91	SPEAR2	91	POTATO	89	RDSOIL-38	CUSOIL-76	
TURNIP	DVTC02	1106C	4	CARROT	87	PEACH2	85	TURNIP	82	WHEAT1	80	WTSOIL	77	RDSOIL -6	CUSOIL-56	
TURNIP	DVTC02	1106E	4	KOLRBI	93	CARROT	91	CGRAPE	89	POTATO	89	SPEAR2	88	RDSOIL-36	CUSOIL-77	
TURNIP	DVTC02	1106F	4	KOLRBI	93	TOMATO	91	ALMOND	90	SPEAR2	88	CGRAPE	88	RDSOIL-21	CUSOIL-61	
TURNIP	DVTC02	1106G	4	TURNIP	91	PEACH2	89	WTSOIL	82	WHEAT1	80	DYSOIL	64	BRCCLI -2	CUSOIL-28	
TURNIP	DVTC02	1106H	4	TURNIP	96	WHEAT1	91	PEACH2	78	WTSOIL	69	CARROT	66	RDSOIL 10	CUSOIL-34	
ENDIVE	DVTC02	1108A	4	ENDIVE	94	RDBEET	92	POTATO	91	LTTUCE	89	POTATO	89	RDSOIL-63	CUSOIL-78	
ENDIVE	DVTC02	1108B	4	ENDIVE	96	POTATO	96	POTATO	95	RDBEET	95	LTTUCE	95	CUSOIL-80	RDSOIL-80	
ENDIVE	DVTC02	1108C	4	ENDIVE	97	RDBEET	94	POTATO	92	POTATO	92	LTTUCE	91	RDSOIL-68	CUSOIL-70	
ENDIVE	DVTC02	1108D	4	POTATO	95	POTATO	93	ENDIVE	93	WHEAT9	92	POTATO	92	CUSOIL-77	RDSOIL-80	
ENDIVE	DVTC02	1108E	4	CARROT	85	RDBEET	81	POTATO	80	POTATO	80	POTATO	80	RDSOIL-43	CUSOIL-77	
ENDIVE	DVTC02	1108H	4	BRCCLI	94	LTTUCE	92	POTATO	92	WHEAT9	91	ENDIVE	90	LOSOIL-85	RDSOIL-86	
ENDIVE	DVTC02	1108I	4	ENDIVE	95	LTTUCE	93	POTATO	92	RDBEET	91	POTATO	91	RDSOIL-77	LOSOIL-79	
ENDIVE	DVTC02	1108J	4	BRCCLI	93	POTATO	91	WHEAT9	90	LTTUCE	90	POTATO	90	LOSOIL-85	RDSOIL-86	
ENDIVE	DVTC02	1108K	4	ENDIVE	97	LTTUCE	95	RDBEET	93	POTATO	93	POTATO	92	RDSOIL-78	LOSOIL-78	
ENDIVE	DVTC02	1108L	4	BRCCLI	95	LTTUCE	92	POTATO	91	WHEAT9	90	ENDIVE	89	LOSOIL-86	RDSOIL-86	
LTTUCE	DTVC02	1109A	4	ENDIVE	89	RDBEET	87	LTTUCE	86	POTATO	86	CARROT	85	LOSOIL-61	CUSOIL-75	
LTTUCE	DVTC02	1109B	4	LTTUCE	96	POTATO	95	BRCCLI	95	ENDIVE	94	WHEAT9	94	LOSOIL-77	RDSOIL-79	
LTTUCE	DVTC02	1109F	4	POTATO	94	ENDIVE	93	LTTUCE	93	POTATO	93	BRCCLI	92	LOSOIL-84	RDSOIL-86	
CARROT	DVTC02	1110A	4	CARROT	94	KOLRBI	93	POTATO	88	ALMOND	88	SPEAR2	87	RDSOIL-29	CUSOIL-75	
CARROT	OVTC02	1110B	4	CARROT	93	PEACH2	79	CHERRY	77	POTATO	76	POTATO	76	RDSOIL-32	CUSOIL-73	
CARROT	DVTC02	1110C	4	RDBEET	86	POTATO	85	POTATO	85	POTATO	85	ENDIVE	84	RDSOIL-52	CUSOIL-70	
CARROT	DVTC02	1110D	4	CARROT	91	PEACH2	83	BDENIM	72	WHEAT1	72	TURNIP	71	LOSOIL-21	CUSOIL-59	
CARROT	DVTC02	1110E	4	CARROT	90	POTATO	90	POTATO	88	KOLRBI	87	CHERRY	86	RDSOIL-43	CUSOIL-77	
CARROT	DVTC02	1110F	4	PEACH2	92	WTSOIL	85	BDENIM	83	CARROT	82	TURNIP	76	RDSOIL 2	CUSOIL-49	
RDBEET	DVTC02	1111A	4	POTATO	96	POTATO	94	RDBEET	93	POTATO	93	POTATO	92	RDSOIL-78	CUSOIL-84	
RDBEET	DVTC02	1111B	4	ENDIVE	97	RDBEET	95	POTATO	94	POTATO	93	LTTUCE	92	RDSOIL-72	CUSOIL-76	
RDBEET	DVTC02	1111C	4	POTATO	96	RDBEET	95	POTATO	95	POTATO	94	WHEAT9	94	RDSOIL-74	CUSOIL-80	
RDBEET	DVTC02	1111D	4	RDBEET	93	ENDIVE	93	POTATO	92	CARROT	91	POTATO	90	RDSOIL-58	CUSOIL-81	
RDBEET	DVTC02	1111F	4	POTATO	91	POTATO	90	ENDIVE	89	POTATO	89	RDBEET	89	RDSOIL-59	CUSOIL-77	

DAWS TEST SITE PAGE 2 A 2

FLDGTYP	LOCN	TAPE	DAY	ANSR1	R	ANSR2	R	ANSR3	R	ANSR4	R	ANSR5	R	ANSR49 NO	ANSR50 NO	FILM
RDBEET	DVTC02	1111H	4	POTATO	94	POTATO	94	POTATO	93	RDBEET	92	POTATO	92	RDSOIL-61	CUSOIL-81	
WTSOIL	DVTC02	1112G	4	WTSOIL	83	RDSOIL	82	DYSOIL	81	SOILHI	81	PEACH2	78	CUSOIL-18	BRCCLI-32	
WTSOIL	DVTC02	1112H	4	WTSOIL	96	PEACH2	89	DYSOIL	84	BDENIM	83	RDSOIL	79	CUSOIL-20	BRCCLI-31	
WTSOIL	DVTC02	1112I	4	WTSOIL	98	DYSOIL	90	PEACH2	86	RDSOIL	85	BDENIM	82	LTTUCE-22	BRCCLI-43	
WTSOIL	DVTC02	1112J	4	PEACH2	93	WTSOIL	90	BDENIM	84	DYSOIL	73	CARROT	71	BRCCLI -8	CUSOIL-23	
WTSOIL	DVTC02	1112K	4	WTSOIL	90	PEACH2	86	DYSOIL	80	BDENIM	77	PEACH1	75	BRCCLI -8	CUSOIL-33	
WTSOIL	DVTC02	1112L	4	WTSOIL	90	DYSOIL	85	PEACH2	83	BDENIM	78	RDSOIL	74	WHEAT9-23	BRCCLI-37	
WTSOIL	DVTC02	1112M	4	TOMATO	77	DYSOIL	65	WTSOIL	61	KOLRBI	61	PEACH2	60	BRCCLI 5	CUSOIL-22	
WTSOIL	DVTC02	1112N	4	WTSOIL	90	BDENIM	87	RDSOIL	85	PEACH2	83	CDSOIL	83	BRCCLI-23	CUSOIL-28	
WTSOIL	DVTC02	1112O	4	WTSOIL	91	PEACH2	82	BDENIM	78	DYSOIL	76	TURNIP	72	BRCCLI-16	CUSOIL-20	
WTSOIL	DVTC02	1112P	4	WTSOIL	95	BDENIM	89	PEACH2	88	DYSOIL	87	RDSOIL	81	CUSOIL-18	BRCCLI-27	
WTSOIL	DVTC02	1112Q	4	WTSOIL	86	PEACH2	81	DYSOIL	75	TOMATO	70	CARROT	69	BRCCLI -2	CUSOIL-22	
DYSOIL	DVTC02	1114A	4	DYSOIL	90	RDSOIL	80	SOILHI	78	WTSOIL	78	BCSOIL	77	LTTUCE-37	BRCC I-54	
DYSOIL	DVTC02	1114B	4	DYSOIL	94	RDSOIL	86	BCSOIL	84	SOILHI	84	CDSOIL	82	LTTUCE-47	BRCC I-65	
DYSOIL	DVTC02	1114C	4	DYSOIL	91	RDSOIL	84	SOILHI	83	BCSOIL	83	LDSOIL	82	LTTUCE-47	BRCC I-60	
DYSOIL	DVTC02	1114D	4	DYSOIL	96	RDSOIL	91	WTSOIL	88	CDSOIL	87	SOILHI	87	LTTUCE-44	BOCCLI-02	
DYSOIL	DVTC02	1114E	4	RDSOIL	93	DYSOIL	91	SOILHI	89	CDSOIL	89	BCSOIL	87	LTTUCE-41	BRCCLI-01	
DYSOIL	DVTC02	1114F	4	DYSOIL	94	RDSOIL	89	WTSOIL	88	CDSOIL	84	SOILHI	83	WHEAT9-41	BRCCLI-60	
DYSOIL	DVTC02	1114G	4	DYSOIL	93	RDSOIL	91	SOILHI	86	CDSOIL	85	WTSOIL	85	LTTUCE-43	BRCCLI-58	
DYSOIL	DVTC02	1114H	4	DYSOIL	96	RDSOIL	88	WTSOIL	87	SOILHI	85	BCSOIL	84	LTTUCE-41	BRCCLI-57	

BMD02D Stepwise Discriminant Program

The stepwise discriminant program (BMD02D) is fully described in Sections IIID.4 and Appendix A. In this application we have used 99 plant and soil spectra taken at Davis, California test site during May 23-26, 1966. These spectra covered the range 0.750 to 2.050 microns, digitized in 0.025 micron incremental wavelengths.

The 99 spectra were broken into training groups - potatoes (23P), wheats (20W), and a group of "dry soils" of the Yolo silt type (.20S). A "test group" of 28 soils-T (including 4 wet soils) was used, along with a test group of 8 almond spectra (A). The resultant plot (Fig. 7) shows them nicely segregated into three main groups with a subsidiary wet soil class. The almonds (A) however vary widely in this classification attempt.

One of the most powerful aspects of this program is shown in the following flow pattern.

1. The spectra are really 53 channels wide

2. The program searches initially for the first wavelength with which it can make the best discrimination (called step 1) and prints out its decisions.

3. It then sequentially chooses the best paid (Step 2), the best trio (step 3) etc., until a halt is called at step 5.

The analysis of these 99 spectra shows that one single wavelength (1.05μ) of the 53 is all that is needed to make a 97% decision out of 5 possibilities. Even adding 4 more wavelength only creases the decision to 98% correct. Significantly this is ~~not~~ one of the bands used for wheat analysis by Purdue University with the University of Michigan airborne scanner data over the Purdue cereal farm (LARS report 21567, dated March 1967).

WHEAT

Purdue 4 bands---------9%
(0.44 - .46μ)
(+ 0.52 - .55μ)
(+ 0.62 - 66μ)
(+ .72 - .80μ)

WHEAT ONLY

Stanford 1 band (1.05μ)-----95%
(bandpass 4 bands .(in ranking)--95%
0.025μ) (1.05μ, 0.925μ, 1.975μ,
1.375μ, 1.500μ

ALL 99 SPECTRA
1 band 97%
4 bands 98%

It should be realized however, that this is only an analysis of 99 spectra whereas the Purdue study covers probably several thousand and is based therefore on better estimates of success.

DAVIS P1&2

IR AND WEATHER DATA 1966 FIELD SEASON
DAVIS,CALIF., AGRICULTURAL TESTSITE
LAT 38 49DEG LONG 121 72DEG ALT HUNTSVILLE GRATING 6.2 MIN 19.2 DEG MAX COOLED PBS FILTER # 2

VAL	TARGET	LOCN	TAPE	DAY	TIME	LAPSE	BB	ROCK	SAND	WATER	AIR	RH	WIND	VIEW	TILT	AID	ARO	GN	BA	OSET	GNR	RDE	RANGE	SOL
N	900006	DVTC01	1100	143	1235	25	56	0	40	0	35	14	1	0	0	0	14	19	25	0	0	0	0	0
N	900006	DVTC01	1100	143	1238	28	57	0	44	0	35	11	3	0	0	0	14	19	25	0	0	0	0	0
N	900006	DVTC01	1100	143	1241	31	56	0	45	0	34	11	2	0	0	0	14	19	25	0	0	0	0	0
N	900006	DVTC01	1100	143	1244	34	57	0	44	0	34	11	2	0	0	0	14	19	25	0	0	0	0	0
N	900006	DVTC01	1100	143	1247	37	56	0	46	0	35	11	5	0	0	0	14	19	25	0	0	0	0	0
N	900006	DVTC01	1100	143	1250	40	56	0	47	0	35	11	1	0	0	0	14	19	25	0	0	0	0	0
N	900006	DVTC01	1100	143	1253	43	55	0	46	0	34	10	3	0	0	0	14	19	25	0	0	0	0	0
	STDCRD	DVTC01	1099	143	1547	0	0	0	0	0	0	0	0	0	0	0	25	19	25	0	0	0	5	0
	BRCCLI	DVTC01	1100	143	1554	0	0	0	0	0	0	0	0	0	0	0	25	19	25	0	0	0	5	0
	STDCRD	DVTC02	1101	143	1701	0	0	0	0	0	0	0	0	0	0	0	14	19	25	0	0	0	0	0
	STDCRD	DVTC02	1102	143	1720	19	0	0	0	0	0	0	0	0	0	0	14	19	25	0	0	0	0	0
	STDCRD	DVTC02	1103	143	1723	22	0	0	0	0	0	0	0	0	0	0	14	19	25	0	0	0	0	0
	KOLRBI	DVTC02	1104	143	1728	27	0	0	0	0	36	0	0	0	0	0	14	19	25	0	0	27	0	0
	STDCRD	DVTC02	1105	143	1733	32	0	0	0	0	36	0	0	0	0	0	14	19	25	0	0	30	0	0
	TURNIP	DVTC02	1106	143	1737	36	0	0	0	0	0	0	0	0	0	0	14	19	25	0	0	0	0	0
N	900006	DVTC02	1100	143	1742	41	45	0	40	0	36	17	5	0	0	0	14	19	25	0	0	0	0	0
	STDCRD	DVTC02	1107	143	1746	45	0	0	0	0	0	0	0	0	0	0	14	19	25	0	0	0	0	0
	ENDIVE	DVTC02	1108	143	1752	51	0	0	0	0	36	[illegible]	0	0	0	0	14	21	25	0	0	30	0	0
	LTTUCE	DVTC02	1109	143	1804	63	0	0	0	0	36	0	0	0	0	0	14	21	25	0	0	30	0	0
	CARROT	DVTC02	1110	143	1808	67	0	0	0	0	36	0	0	0	0	0	14	21	25	0	0	30	0	0
	RDBEET	DVTC02	1111	143	1811	70	0	0	0	0	36	0	0	0	0	0	14	21	25	0	0	28	0	0
	WTSOIL	DVTC02	1112	143	1819	78	0	0	0	0	0	0	0	0	0	0	14	21	25	0	0	0	0	0
	STDCRD	DVTC02	1113	143	1825	84	0	0	0	0	0	0	0	0	0	0	14	21	25	0	0	0	0	0
	DYSOIL	DVTC02	1114	143	1830	89	0	0	0	0	36	0	0	0	0	0	14	21	25	0	0	28	0	0
	STDCRD	DVGF01	1115	144	1007	0	0	0	0	0	0	0	0	133	0	0	20	19	25	0	0	0	0	0
	DYSOIL	DVGF01	1116	144	1013	6	0	0	0	0	0	0	0	133	0	0	20	19	25	0	0	0	0	0
	STDCRD	DVGF01	1117	144	1110	25	0	0	0	0	0	0	0	115	0	0	20	18	25	0	0	0	0	0
	WHEAT0	DVGF01	1118	144	1114	29	0	0	0	0	0	0	0	122	0	0	20	18	25	0	0	0	0	0
	WHEAT9	DVGF01	1119	144	1122	37	0	0	0	0	0	0	0	125	0	0	20	18	25	0	0	0	0	0
	WHEAT1	DVGF01	1120	144	1128	43	0	0	0	0	0	0	0	0	0	0	20	18	25	0	0	0	0	0
	WHEAT8	DVGF01	1121	144	1133	48	0	0	0	0	0	0	0	118	0	0	20	18	25	0	0	0	0	0
	WHEAT3	DVGF01	1122	144	1139	54	0	0	0	0	0	0	0	135	0	0	20	18	25	0	0	0	0	0
	SOIL	DVPP01	1123	144	1435	15	54	0	62	0	37	12	3	0	0	0	0	0	0	0	0	60	0	0
	STDCRD	DVPP01	1124	144	1457	22	0	0	0	0	0	0	0	0	0	0	16	18	25	0	0	0	0	0
	POTATO	DVPP01	1125	144	1503	28	0	0	0	0	0	0	0	0	0	0	16	18	25	0	0	0	0	0
	POTATO	DVPP01	1126	144	1513	38	0	0	0	0	0	0	0	145	0	0	16	18	25	0	0	0	0	0
	POTATO	DVPP01	1127	144	1518	43	0	0	0	0	0	0	0	0	0	0	16	18	25	0	0	0	0	0
	POTATO	DVPP01	1128	144	1523	48	0	0	0	0	0	0	0	164	0	0	16	18	25	0	0	0	0	0
	POTATO	DVPP01	1129	144	1534	59	0	0	0	0	0	31	0	164	0	0	16	18	25	0	0	32	0	0
	POTATO	DVPP01	1130	144	1544	69	0	0	0	0	0	0	0	123	0	0	16	18	25	0	0	0	0	0
	STDCRD	DVPP01	1131	144	1550	75	0	0	0	0	0	0	0	123	0	0	16	18	25	0	0	0	0	0
	RGSOIL	DVPP01	1132	144	1553	78	0	0	0	0	0	0	0	118	0	0	16	18	25	0	0	0	0	0
	STDCRD	DVPP01	1133	144	1609	94	52	0	60	0	37	13	0	125	0	0	16	18	25	0	0	52	0	0
	LOSOIL	DVPP01	1134	144	1614	99	54	0	60	0	37	13	0	125	0	0	16	18	25	0	0	0	0	0
	LOSOIL	DVPP01	1135	144	1620	105	0	0	0	0	0	0	0	151	0	0	16	18	25	0	0	0	0	0
	RDSOIL	DVPP01	1136	144	1632	117	0	0	0	0	0	0	0	128	0	0	16	18	25	0	0	0	0	0
	TOMATO	DVPP01	1137	144	1643	128	54	0	62	0	37	12	3	0	0	0	16	18	25	0	0	60	0	0
	CUSOIL	DVPP01	1138	144	1647	132	0	0	0	0	0	0	0	155	0	0	16	18	25	0	0	0	0	0
	STDCRD	DVPP01	1139	144	1654	139	0	0	0	0	0	0	0	155	0	0	16	18	25	0	0	0	0	0

Ground Truth Data

Weather and temperature data, collected during the field study at Davis is displayed in computer output format in Tables IX A & B. This is a direct readout from input cards, which are generated from field data sheets (actually IBM coding forms with added basic annotations). Two examples of these sheets are given in the text for Sections IIIC.2 and 3, the field trips to Mesquite, Arizona and Pisgah, California test sites.

On these tables (IX A & B) any horizontal line may be read as follows:

Column		Code	Examples	Code
1.	Value	(VAL)	Not sampled	N
2.	Target	(TARGET)	Standard card	STDCRD
3.	Location	(LOCN)	Davis, Truck Card #1	DVTC01
4.	Tape No.	(TAPE)	1100 A-D	1100 (A not used)
5.	Day No.	(DAY)	May 23	143
6.	Time now	(TIME)	12:35 P.M.	1235
7.	Lapsed time since start of cooling	(LAPSE)	43 minutes since coolant added	43
8-12.	Temperatures	(BB,ROCK...AIR)	40°C	40
13.	Relative Humidity	(RH)	14%	14
14.	Wind Velocity	(WIND)	none	0
15.	View angle of spectrometer	(VIEW)	57° depression	133
16.	Tilt	(TILT)	Not applicable	
17.	Dip	(DIP)	Not applicable	
18.	Spectrometer Period	(PRD)	Spectral period 24 seconds	25
19.	Spectrometer Gain	(GN)	Gain setting 1.9	19
20.	Spectrometer Bandpass	(BP)	Bandpass-out 25 cycles	25
21.	Radiometer offset	(OSET)	Offset reading	not used
22.	Radiometer Gain	(GNR)	Gain reading	not used
23.	Radiometer Reading (Barnes IT3)		Radiometer reading 27°C	27
24.	Range to Target	(RANGE)	(Generally 75' sloping)	not noted
25.	Solarimeter reading	(SOL)	Solar reading in millivolts)	not used

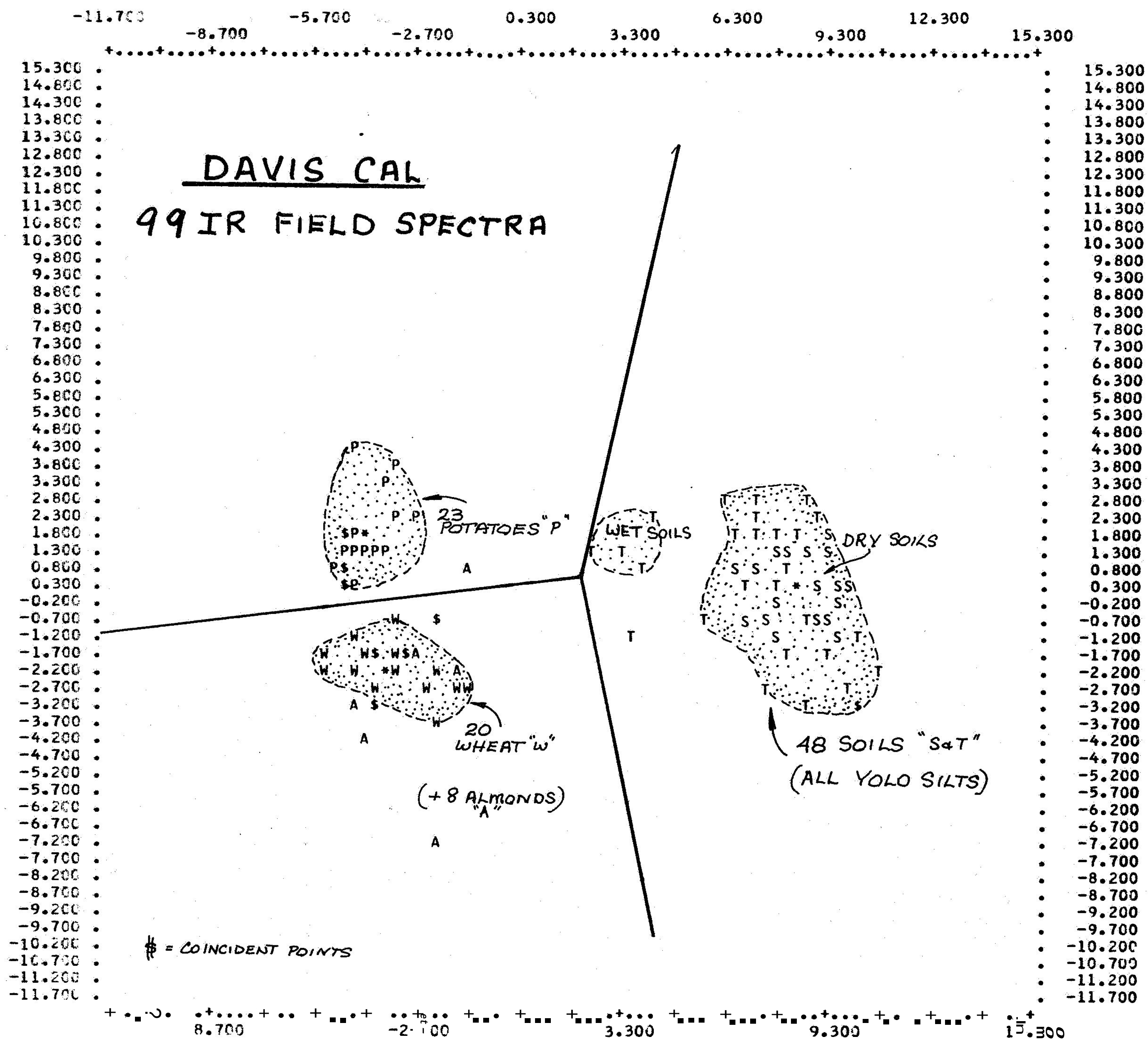
DAVIS CAL
99 IR FIELD SPECTRA
23 POTATOES "P"
WET SOILS
DRY SOILS
20 WHEAT "W"
(+ 8 ALMONDS "A")
48 SOILS "S&T"
(ALL YOLO SILTS)
$ = COINCIDENT POINTS

DAVIS p.282

Ia aND WEATHER DATA 1966 FIELD SEASON

DAVIS, CALIF., AGRICULTURAL TESTSITE

LAT 38.49DEG LONG 121.7ZDEG aLT HUNTSVILLE GRATING 6.2 MIN 19.2 DEG MaX COOLED PBS FILTER # 2

VAL	TARGET	LOCN	TAPE	Da*	TImE	LaaΞE	BΞ	ROCK	SaND	WaTEa	aIa	aH	WIND	VIEW	TILT	DIP	PXD	aN	ΞP	OSET	ENa	aOG	aANGE	SOL
	STDCRD	DVSF01	1140	145	1049	42	0	0	0	0	0	0	0	123	0	0	23	18	25	0	0	0	75	0
	GRAPES	DVSF01	1141	145	1054	47	0	0	0	0	0	0	0	123	0	0	23	18	25	0	0	0	75	0
	GRAPES	DVSF01	1142	145	1103	55	0	0	0	0	0	0	0	151	0	0	23	18	25	0	0	0	100	0
	BDENIM	DVSF01	1143	145	1108	61	0	0	0	0	0	0	0	123	0	0	23	18	25	0	0	0	75	0
	CUSOIL	DVSF01	1144	145	1118	71	0	0	0	0	0	0	0	129	0	0	23	18	25	0	0	0	75	0
	RGSOIL	DVSF01	1145	145	1123	76	0	0	0	0	0	0	0	172	0	0	23	18	25	0	0	0	Ξ00	0
	RGSOIL	DVSF01	1146	145	1126	79	0	0	0	0	0	0	0	172	0	0	23	25	25	0	0	0	Ξ00	0
	CUSOIL	DVSF01	1147	145	1127	80	0	0	0	0	0	0	0	172	0	0	23	25	25	0	0	0	Ξ00	0
	STDCRD	DVSF01	1148	145	1153	8	0	0	0	0	0	0	0	123	0	0	23	18	25	0	0	0	65	0
	ALMOND	DVSF01	1149	145	1157	12	0	0	0	0	0	0	0	140	0	0	23	18	25	0	0	0	70	0
	PEACH1	DVSF01	1150	145	1201	16	0	0	0	0	0	0	0	140	0	0	23	18	25	0	0	0	70	0
	PEACH3	DVSF01	1151	145	1205	20	0	0	0	0	0	0	0	120	0	0	23	18	25	0	0	0	70	0
	PEAR63	DVSF01	1152	145	1210	25	0	0	0	0	0	0	0	115	0	0	23	18	25	0	0	0	57	0
	STDCRD	DVSF01	1153	145	1214	29	0	0	0	0	0	0	0	118	0	0	23	18	25	0	0	0	65	0
	PEAR73	DVSF01	1154	145	1220	35	0	0	0	0	0	0	0	112	0.	0	23	18	25	0	0	0	0	0
	DYSOIL	DVSF01	1155	145	1224	39	0	0	0	0	0	0	0	0	0	0	23	18	25	0	0	0	0	0
	CHRY12	DVSF01	1156	145	1238	53	0	0	0	0	0	0	0	0	0	0	23	18	25	0	0	0	0	0
	CHRY59	DVSF01	1157	145	1245	60	0	0	0	0	0	0	0	0	0	0	23	18	25	0	0	0	0	0
	DYSOIL	DVSF01	1158	145	1259	74	0	0	0	0	0	0	0	0	0	0	23	18	25	0	0	0	0	0
	DYSOIL	DVSF01	1159	145	1304	79	0	0	0	0	0	0	0	119	0	0	23	18	25	0	0	0	60	0
	ALMOND	DVSF01	1160	145	1308	83	0	0	0	0	0	0	0	177	0	0	23	18	25	0	0	0	276	0
	STDCRD	DVSF01	1161	145	1317	92	0	0	0	0	0	0	0	123	0	0	23	18	25	0	0	0	60	0

When all of the spectra in tape 11 are run we will perform a "shot-gun" correlation study of the weather data and **CORRCO** results, as we did in the next Section (IIID.3) for the 1965 field data.

3. Computer Analysis of Ground Truth Data

Analysis of 1965 meteorological data has been made by cross correlation methods. Several attempts have been made previously to search for meaningful patterns in our 1700 sets of ground truth data, which would relate directly to the results of the infrared spectral matching process. One such report appeared in our first semi-annual report a year ago (May 10, 1966, p. 15) and another was summarized in the First Annual Report (Nov. 1, 1966) on page 4 and in detail on pages 54-56 of that report. At the latter time we felt that we could see <u>no effect on the outcome of the spectral matching process which would be directly related to meteorological conditions</u> present at the time the spectra were taken.

Intuitively this seems to be the wrong conclusion, and so we have made a further, more more detailed analysis of these field data. One answer to which we attribute some credence is that the spectra are themselves so noisy, due to the microphonic condition of the Cu:Ge detector (See SRSL Tech Report 67-3) that any further perturbations introduced by "noise" in the weather variables cannot be seen. In this maner one can truthfully say that...."the use of the ... [weather] ... variables did not lead to a significantly better classification into rock types". (1st Annual Report, p. 4)

The present study was to all intents and purposes a "shot-gun" approach. We collected all the available data and found we had 2 groups.

Group I Those with data for 17 variables (275 samples)

Group II Those with data for 23 variables (252 samples)

A cross correlation program was run in the computer with these groups of data and a triangular coefficient matrix prepared for each group (Figs. 8 and 9). Suitable stippled patterns indicate the 0.25, 0.4 and 0.6 coefficient levels. No confidence level was run by this program so we are not sure which numbers are significant at the 95% level, for example. A quick glance will show that for 250 samples of 17 or 23 variables each, the stippled levels are conservative.

Of more significance is the analysis following in Tables X A & B, where we have tried to segregate relationships which have obvious character (even redundancy in some cases) from those which might have experimental signficance. Many associations can be explained by the temporal pattern of daily or yearly activity (geographical locations or altitudes for example) as we moved from test site to test site.

Sequence of Test Sites - 1965 Field Period

Date (1965)	(Day)	Location (California)		Altitude/S.L.	Rock Type	Tape No.
8/12	(224)	Pacific Coast	(PGLH01)	30	Granite	1
8/13	(225)	Pacific Coast	(PGLP01)	30	Granite	2
8/18	(230)	Donner Pass	(DPGC01	6825	Granite	2
9/25	(268)	Mono Lake	(MCAB01)	7310	Granite	3
9/26	(269)	Mono Lake	(MCSC01)	8680	Rhy. Pumice	3
9/27	(270)	Mono Lake	(MCSC05)	8680	Rhy. Pumice	4
9/28	(271)	Mono Lake	(MCNC01)	6800	Rhy. flows	4
10/1	(274)	Mono Lake	(MCNC01)	6800	Rhy. flows	4
10/2	(275)	Mono Lake	(MCCC01)	7629	Bas. Cinder	5
10/3	(276)	Mono Lake	(MCSC05) (MCSC10)	8680	Rhy. Pumice	6
10/4	(277)	Mono Lake	(MCSB01)	6440	Pum. Beach	6
10/14	(287)	Tioga Pass	(TPOP01) (TPLD01)	8500	Granite	7
10/15	(288)	Mono Lake	(MCBP01)	6520	Basalt Cone	8
10/23	(296)	Pisgah Crater	(PCWR01,02,03)	2515	Basalt Cone	8,9
10/24	(297)	Pisgah Crater	(PCTP01) (PCER01,02)	2543	Basalt Cone	9,10
10/25	(298)	Pisgah Crater	(PCLL12,13,14)	1888	Basalt flows	10
10/26	(299)	Pisgah Crater	(PCLL15)	1888	Basalt flows	10

DAY	LAPSE	RANGE	ALT	ROCK T	BB	SAND T	AIR T	RH	WIND V	PRD	GN	BP	QTZ	VOID	TAPE	SPEC	
	-01	.12	.007	.15	.20	.15	.28	-.78	-.01	-.34	.60	.03	-.35	.04	.89	.20	DAY
		.25	.21	-.20	-.20	-.28	-.26	-.04	-.21	-.12	.12	-.14	-.10	-.14	-.15	.38	LAPSE
			.12	-.16	-.16	-.10	-.14	-.03	-.14	-.04	-.03	-.04	-.10	-.12	.10	-.0	RANGE
				-.42	-.67	-.59	-.62	-.20	-.16	-.25	.30	-.32	-.02	-.23	-.32	.05	ALT
					.76	.81	.73	-.14	.19	-.01	-.02	.27	.04	.29	.21	-.02	ROCK T
						.84	.85	-.06	.13	.10	-.10	.35	.00	.24	.36	.03	BB
							.84	-.09	.18	.08	-.20	.21	.09	.32	.29	-.10	SAND T
								-.16	.10	.06	-.04	.25	.03	.24	.44	.10	AIR T
									-.01	.30	-.49	.20	.28	-.02	-.60	-.24	RH
										.01	-.13	-.24	.05	.04	.03	-.19	WIND V
											-.19	-.22	.10	.09	-.27	-.16	PERIOD
												-.18	-.19	-.10	.36	.32	GAIN
													-.01	.00	.23	-.16	BND PASS
														-.14	-.33	-.12	QTZ
															.07	-.19	VOID
																.08	TAPE
																	SPEC

WEATHER DATA, INSTRUMENT VARIABLES,
MODAL ANALYSIS AND CROSS-CORRELATION RESULTS

GROUP I - 17 VARIABLES

	DAY	LAPSE	RANGE	ALT	ROCK T	BB T	SAND T	AIR T	RH	WIND VEL	SG-4 PRD	SG-4 GAIN	SG-4 BP	QTZ	VOIDS	Ē	E var	CORRCO	TAPE	SPECTR.
DAY		.02	.15	.04	.1	.19	.14	.27	-.79	-.02	-.34	.63	.02	-.35	.05	.01	.10	-.27	.90	.22
LAPSE			.22	.20	-.17	-.19	-.27	-.24	-.05	-.18	-.14	.14	-.13	-.11	-.15	-.28	-.09	.15	-.11	.43
RANGE				.10	-.11	-.09	-.05	-.10	.01	-.11	-.05	.10	-.01	-.10	-.13	-.18	-.05	-.12	.14	.03
ALT.					-.41	-.67	-.60	-.62	-.21	-.16	-.26	.32	-.32	-.02	-.23	.06	.05	.03	-.30	.05
ROCK T						.76	.81	.73	-.14	.18	-.01	-.03	.27	.04	.31	-.04	-.07	-.08	.19	.005
BB T							.86	.86	-.08	.13	.10	-.13	.35	-.005	.24	.01	-.09	-.07	.36	.08
SAND T								.84	-.09	.18	.08	-.22	.21	.09	.34	.04	-.01	-.12	.29	-.08
AIR T									-.16	.10	.06	-.06	.25	.03	.25	-.04	.04	-.13	.43	.13
RH										-.003	.31	-.53	.20	.28	-.04	-.18	-.17	.10	-.63	-.25
WIND VEL											.02	-.16	-.26	.06	.05	.10	-.07	-.06	.02	-.21
PERIOD SG-4												-.22	-.22	.10	.10	.17	-.01	.003	-.27	-.16
GAIN SG-4													-.20	-.20	-.10	-.03	.14	-.13	.39	.36
BP SG-4														-.02	-.01	-.29	-.19	-.03	.22	-.17
QTZ															-.16	-.25	-.07	.18	-.35	-.13
VOID																.29	.14	-.17	.08	-.20
E Bar																	.23	-.24	.02	-.17
E var																		-.17	.08	-.05
CORRCO																			-.34	.16
TAPE																				.10
SPECTR																				

WEATHER DATA, INSTRUMENT VARIABLES,
MODAL ANALYSIS, COMPUTER OUTPUT
AND CROSS-CORRELATION RESULTS

GROUP II - 20 VARIABLES

The tables A-K which have been prepared from this analysis are as follows. Experimentally significant tables are indicated by an asterisk(*).

A. Logically explainable by parameter involved

B. Explainable by relationships between meteorological and rock temperature.

C.* Experimentally significant relationships not immediately explainable.

D. Directly related to the yearly sequence of site chosen for field work.

E. Related to daily work pattern at sites.

F. Related to sequential breakdown of detector in SG-4.

G.* Instrumental Relationship

H. Modal Quartz percentage

I. Emissivity average (E Bar)

J. LMSC correlation coefficient (CORRCO)

K. Correlations ranked by value (over 0.24).

The following notes are important to the analysis of tables A-K:

1. Tape No. - Serially from Tape 1 to Tape 10
2. Day - day of the year, see sequence table above
3. Temperatures (Sand) (BB) (Rock) - all contract, using DIGITEC thermistor probes, in °C
4. Air Temperature - 6 inches off ground in shade, DIGITEC thermistor
5. Relative Humidity - Percentage, Honeywell RH Indicator meter, type W611A used with 5 ranges of probes
6. Altitude - taken from topographic maps
7. SG-4 parameters (Gain) (Period) (Bandpass) - electronic settings off unit, period in seconds
8. Spectrum No. - sequential spectral group along any one tape
9. Lapse Time - time in minutes since last filling of liquid helium cryogenics (appeared to be directly related to noise increases in the field)

10. Quartz - modal analysis, prepared by counting 1500 grains in a thin section under the microscope, can be considered to be an approximation of rock type

11. CORRCO - See footnote table K, correct answer for that rock type target was used, not the highest value

12. VOIDS - modal analysis as for quartz. Both Pisgah basalts and Mono Crater pumice had high void values which may have acted to cut down "spectral contrast".

13. E BAR - average emittance ratio values in LMSC program

14. E Var - variance of emittance ratio in LMSC program

15. Wind velocity - in miles per hour, hand held "venturi" gauge

16. Range - in feet, if over 1000, taken from maps.

TABLE X

CORRELATION STUDIES ON 1965 FIELD DATA

A, LOGICALLY EXPLAINABLE BY PARAMETER INVOLVED

	Simply Explainable	Correlation Coefficient
1.	Tape No. vs. Day of Year	(.90)
2.	Sand Temperature vs. BB Temp.	(.86)
3.	Sand Temperature vs. Rock Temp.	(.81)
4.	BB Temperature vs. Rock Temp.	(.76)
5.	Sand Temperature vs. Void %	(.34)
6.	Rock Temperature vs. Void %	(.31)
	Not so obviously related	
1.	Sequential spectrum no. vs. lapse time	(.43) (should be higher but lapse Time returns often to zero)

B. EXPLAINABLE BY RELATIONSHIPS BETWEEN METEOROLOGICAL & ROCK TEMPERATURES

	Simply Explainable	
1.	Air Temperature vs. BB Temp.	(.86)
2.	Air Temperature vs. Sand Temp.	(.84)
3.	Air Temperature vs. Rock Temp.	(.73)
4.	Air Temperature vs. Altitude Temp.	(- .62)
5.	Average Emissivity ($\bar{E}$) vs. Void %	(.29)
6.	Lapse time vs. BB, rock, air, Temp.	(-.17 to -.27)
	Not so obviously related	
1.	BB Temperature vs. Altitude	(- .67)
2.	Sand Temperature vs. Altitude	(- .60)
3.	Rock Temperature vs. Altitude	(- .41)
4.	SG-4 Gain vs. Altitude	(.32)
5.	Air Temperature vs. Day	(.27)
6.	SG-4 Bandpass vs. Altitude	(-. .32)

C. EXPERIMENTALLY SIGNIFICANT RELATIONSHIPS NOT IMMEDIATELY EXPLAINABLE

	Correlation Coefficient
1. LMSC Correlation Coefficient vs. Tape No.	(-.34) (Why?)
2. SG-4 Gain vs. BB Temperature	(.35) (Why not negative?)
3. Average Emissivity ($\bar{E}$) vs. SG-4 Bandpass	(-.29)
4. Average Emissivity ($\bar{E}$) vs. Void %	(-.29)
5. Quartz % vs. RH	(.28)
6. Quartz % vs. Day of Year	(-.35)
7. Average Emissivity ($\bar{E}$) vs. Lapse Time	(-.28)

D. RELATED TO THE YEARLY SEQUENCE OF SITES CHOSEN FOR FIELD WORK

1. Day No. vs. Relative Humidity	(-.79)
2. Tape No. vs. Relative Humidity	(-.63)
3. Tape No. vs. Air Temp.	(.43)
4. Tape No. vs. BB Temp.	(.36)
5. Quartz content vs. Day of Year	(-.35)
6. Tape No. vs. Altitude	(-.30)
7. Tape No. vs. Sand Temp.	(.29)

E. RELATED TO THE DAILY WORK PATTERN AT SITES

1. SG-4 gain vs. Sequential Spectrum No.	(.36) (not clear)
2. SG-4 period vs. Day of Year	(-.34)

F. RELATED TO SEQUENTIAL BREAKDOWN OF DETECTOR IN SG-4

1. SG-4 gain vs. Day of Year (whereas BBT vs. day is (.19))	(.63)
2. SG-4 gain vs. Tape No.	(.39)
3. SG-4 gain vs. Sequential Spectrum No.	(.36)

Uncertain Why Relationship Exists

1. SG-4 gain vs. Relative Humidity (Day vs. RH is -.79) (Day vs. SG-4 gain is .63)	(-.53)

Uncertain Why Relationship Exists	Correlation Coefficient
2. SG-4 Period vs. Day of Year	(-.34)
3. SG-4 Period vs. Rel. Humidity	(.31)

G. INSTRUMENTAL RELATIONSHIPS

Clearly Related	
1. SG-4 Bandpass vs. BB Temp.	(.35) (not so clear)
2. SG-4 Period vs. SG-4 Bandpass	(-.22)
3. SG-4 Gain vs. SG-4 Bandpass	(-.20)
Clearly related and should be of other sign	
1. SG-4 Gain vs. BB Temperature	(-.13) (why negative?)
Unclear but probably should be of other sign	
1. SG-4 Gain vs. SG-4 Reriod	(-.22)

H. MODAL QUARTZ PERCENTAGE

Relationship Found	Correl. Coeff	Reason
1. Quartz vs. Day	(-.35)	Day vs. Tape (.90)
2. Quartz vs. Tape	(-.35)	
3. Quartz vs. RH	(.28)	Day vs. R.H. (-.79)
4. Quartz vs. E Average	(-.25)	

I. EMISSIVITY AVERAGE ($\bar{E}$)

$\bar{E}$ vs. Voids	(.29)
$\bar{E}$ vs. SG-4 Bandpass	(-.29)
$\bar{E}$ vs. Time Lapse	(-.28)
$\bar{E}$ vs. Quartz	(-.25)
$\bar{E}$ vs. LMSC CORRCO	(-.24)
E vs. E variance	(.23)
$\bar{E}$ vs. Range	(-.18)

J. LMSC CORRELATION COEFFICIENT (CORRCO)

	Correl. Coeff.
CORRCO vs. Tape No	(-.34)
CORRCO vs. Day	(-.27)
CORRCO vs. E	(-.24)
CORRCO vs. Quartz	(.18)
CORRCO vs. Voids	(-.17)
CORRCO vs. E variance	(-.17)
CORRCO vs. Spectral Sequence	(.16)

CORRELATIONS RANKED BY VALUES	Group II (23 variables includes LMSC output)	Group I (17 variables)
Tape number vs. Day	.90	.89
Sand T vs. BB Temp	.86	.84
Air T. vs. BB Temp	.86	.85
Air T. vs. Sand Temp	.84	.84
Sand T. vs. Rock Temp	.81	.81
RH vs. Day	-.79	-.78
BB Temp vs. Rock Temp	.76	.76
Air Temp, vs. Rock Temp	.73	.73
BB Temp vs. Altitude	-.67	-.67
SG-4 Gain vs. Day	.63	.60
Tape No. vs. R.H.	-.63	-.60
Air Temp vs. Altitude	-.62	-.62
Sand Temp vs. Altitude	-.60	-.59
SG-4 Gain vs. R.H.	-.53	-.49
Tape No. vs. Air Temp	.43	.44
Spectrum no. vs. Lapse Time	.43	.38
Rock Temp vs. Altitude	-.41	-.42
Tape No. vs. SG-4 Gain	.39	.36
Tape No. vs. BB Temp	.36	.36
Spectrum No. vs. SG-4 Gain	.36	.32
SG-4 Bandpass vs. BB Temp	.35	.35
Quartz vs. Day	-.35	-.35
Voids vs. Sand Temp	.34	.32
SG-4 Period vs. Day	-.34	-.34
Tape No, vs. CORRCO(*)	-.34	(not used in Group I)
SG-4 Gain vs. Altitude	.32	.30
SG-4 Bandpass vs. Altitude	-.32	-.32
Voids vs. Rock Temp	.31	.29
SG-4 Period vs. R.H.	.31	.30
Tape vs. Altitude	-.30	-.32
Tape vs. Sand Temp	.29	.29
$\bar{\bar{E}}$ vs. SG-4 Bandpass	-.29	
$\bar{\bar{E}}$ vs. Voids	.29	
Quartz vs. R.H.	.28	.28
$\bar{\bar{E}}$ vs. Lapse Time	-.28	
Air vs. Day	.27	.28
SG-4 Bandpass vs. Rock Temp	.27	.27
CORRCO(*) vs. Day	-.27	
Sand Temp vs. Lapse	-.27	-.28
Tape No. vs. SG-4 period	-.27	-.27
SG-4 Period **vs.** Altitude	-.26	-.25
SG-4 Bandpass vs. Wind Vel.	-.26	-.24
SG-4 Bandpass vs. Air Temp,	.25	.25
Voids vs. Air Temp	.25	.24
Spectral No. vs. R.H.	-.25	-.24
$\bar{\bar{E}}$ vs. Quartz	-.25	

*CORRCO - Correlation coefficient used was from the LMSC output. The value used was that which correctly matched the target rock type, for the same rock type in the library, and not necessarily the maximum value of CORRCO.

4. Mineral Analysis Programs

Some of the prime objectives in the course of research carried out by geologists are to identifiy and classify rocks, and to show their location on a suitable map. The geologist uses long-established rules and criteria to complete this work. For example, rocks are grouped into various classes and given a varietal name on the basis of such properties as rock texture and mineral composition. Three general groups of rocks are igneous, metamorphic, and sedimentary, each of which is characterized by a fairly unique texture. Varieties of rocks within these three general groups are based on the presence (or absence) and proportions of the constituent rock-forming minerals.

The advent of remote sensing of earth surface materials has brought about a rather unique problem for the geologist. The properties of rocks observed by the remote sensor are not necessarily texture and mineral composition per se, but such things as average reflectance, average emittance, surface temperature, etc. Because rocks are classically defined in terms of texture and mineral composition, the problem faced by the modern geologist is to redefine the criteria by which rocks are identified and classified in terms of the properties observed by a remote sensor.

Let us take an example to illustrate this point. Suppose an airborne infrared spectrometer is used to scan a terrain composed of granite in an overflight. The spectrometer will yield a series of spectral emittances in the 8-13 micron region taken at intervals along the flight line, each one corresponding to a patch of given size (typically 20-40 ft. square) on the ground. Assuming no a priori knowledge exists of the composition and texture of the rocks, then the spectra will provide the only criteria by which the rock may be identified. We would hope in this case that the spectra of the granitic rocks would be similar to other spectra taken of other rocks and known to be granites. If the flight line were to be extended to pass over an area in which basalts were exposed, another series of spectra would be produced of that section of the flight line. Hopefully, the basalt spectra would be similar to other spectra of rocks known to be basalts and different from the spectra of the granitic rocks.

The above description suggests a method by which the identification of rock type based on spectra alone can be made. A "library" of spectra of known rock types is produced under simulated field conditions. Spectra of unknown rocks are then compared statistically with the "library". The statistical comparison might take the form of a fitting procedure in which the unknown and known spectra are compared and the results might take the form of a correlation statistic. Spectra taken over a granitic terrain should correlate strongly with known granite spectra and poorly with known basalt spectra. This procedure has been used with success in the Stanford Remote Sensing Program.

The above rock identification procedure is not the only one available, It is possible to mathematically determine the proportion of rock-forming minerals in the rock scanned from the spectra alone with a fair degree of accuracy, This method yields criteria which are exactly those used by $he geologist to identify the rock. This method of identification of rock type from spectrum analysis has been used in the Stanford program previously and has met with limited success. Briefly, the method is based on the assumption that a rock spectrum is a linear combination of its component mineral spectra. Using this mathematical model, it is possible to obtain least squares estimates of individual weighted component mineral spectra, The calculated mineral spectra are then combined in various proportions by a least squares method to give an optimum "fit" to the rock spectrum, The statistically derived mineral composition of the rock is taken to be the various percentages of individual mineral spectra whose combined spectrum give the best "fit" to the original rock spectrum. This method of analysis has been performed on 22 "library" rock samples for which both CIPW Norms (Normative Mineral Composition) and infrared spectra were available. A complete description of this analysis is given in the 1st Annual Report. We plan to use the same method of analysis on a series of spectra taken recently in the Stanford Remote Sensing Laboratory of many different kinds of rocks for which modal compositions will be soon available. The results of this study will be published at a later time.

A third method of identification of rock types from infrared spectra is available to us at this time. This method involves the use of multiple linear discriminant analysis in discriminating between rock types and classifying each spectrum (rock) into one of several groups on spectral properties alone. The major drawback of this system of analysis is that spectra (rocks) are classified into pre-assigned groups, the assignment of groups made before the statistical analysis. This pre-supposes that the various types of rocks for which spectra were taken are known in general before hand, possibly through geological ground analysis of the sites scanned. A test group of spectra from each of the pre-assigned groups is used as a basis for comparison with the spectra from unknown rocks. The computer program used in this analysis (BMD07M) treats each rock class as a square covariance matrix, the size (N) of the matrix depending upon the number of individual wavelengths judged. to give the best classifying power. Each spectrum of an unknown rock is then placed in N dimensional space based on the N critical wavelengths by the computer program and the "Mahalanobis distance" from each individual rock spectrum to the center of gravity of each of the pre-assigned classes is then computed, The rock is then assigned to the class (rock type) that to which it is nearest, based on the Mahalanobis distance (See Appendix "A"). The program also computes canonical variables, which are used as an aid in graphically showing the discriminating power of this type of analysis. A description of the use of this analytical procedure is given in the 1st Annual Report. The mathematical rationale for the use of this method of analysis and. a detailed description of the computational procedures contained in the BMD07M program are given in Appendix A of this report.

a

5. New Computer Programs

a. Interim-"360" Programs for Infrared Spectral Analysis

A new set of computer programs has been written to replace the modified LMSC programs of 1965. These new programs are in essence still another modification of the LMSC programs, however, they are sufficiently different to warrant new names.

The main reason for creation of a new set of programs is that the Stanford University Computation Center is installing new third-generation IBM computing equipment. The old LMSC programs, even when modified, are still machine dependent. Thus an IBM 360 program, called NSCP2, has been written in FORTRAN IV which can be used on either the IBM 7090 or 360-67 (with appropriate modifications) to process spectral data.

NSCP presently expects input data on magnetic tape which is blocked in logical records which contain information for one (and only one) spectrum, It is anticipated that when spectral data generated by new infrared hardware in the 360 format is obtained, minor changes in the program will be required,

Some characteristics of NSCP2 are as follows:

(1) Any new library of several spectra can be stacked with the job. A new library tape in a binary format is written, This tape can then be saved or discarded as desired.

(2) The binary format of the library tape permits rapid reading of the library in processing.

(3) The program reads each spectrum sequentially. A control character indicates to the program that any specific spectrum is that of a blackbody, All blackbody spectra are then averaged (that is, more than 4 can now be used) until a non-blackbody spectrum is encountered, Then this averaged blackbody spectrum is used to compute all subsequent spectra, until a new blackbody spectrum is encountered.

(4) Emittance ratio values are generated for each spectrum and punched out on cards in 7F10.7 format for subsequent plotting or processing, Average emittance cards can also be punched.

(5). Spectral correlation coefficients (CORRCO) are computed by comparing the spectrum with the library. This is the same as in the modified LMSC program.

Another program was written to prepare the data for use in conjunction with NSCP2. This program is called TPTP. This program to a great extent contains elements of the old modified LMSC programs.

The purpose of TPTP is

(a) to read the TRIFID input tapes

(h) to write a tape in blocked form with one spectrum to a logical record.

Some of the more salient characteristics of TPTP are

(a). Start-s-top times and calibration times are still required for each spectra as with the LMSC program. These are manually prepared but are now taken from a digital tape-dump instead of from analog scrolls.

(b). As many spectra as desired can be stacked back to back and processed. A blackbody is identified by the work BLACK in columns 922 to 27 (or the word STDCRD **if** the spectrum is in the short wavelength range - MSFC unit). Any other symbol in columns 22 to 27 of the spectrum card identifies the data as a spectrum and not a blackbody.

(c) If new calibration times are required for a second set of data, a blank card is inserted and a complete set of data as in the beginning is required behind this blank card.

(d). The number of spectral points is determined by the variable IIN (read in on the first card).

Collectively these two programs are called "Interim 360 Program", Parts B & A.

6. Analysis of USGS IR Spectra - Tech Letter #13

Daniels (1966)* has published infrared emittance spectra (8 - 14 microns) of 13 rock samples from the Pisgah Crater and Mono Craters test sites. The samples include felsic plutonic and volcanic rocks from Mono Craters and mafic volcanic rocks from Pisgah Crater. Specifically, spectra were taken of the following samples:

Mono Craters

- (2) obsidian
- (2) rhyolite pumice
- (2) Bishop tuff
- (1) quartz monzonite

Pisgah Crater

- (2) pahoehoe olivine basalts
- (4) aa olivine basalts

The 13 spectra were taken of heated samples with a Block Engineering Model I-4T interferometer spectrometer equipped with an ambient temperature thermistor bolometer detector.

We have digitized the 13 spectra by hand at a 0.1 micron interval from 7.8 to 13 microns and statistically analyzed the data according to our now, fairly routine algorithms.

a. Correlation Coefficient Ranking (CORRCO) Program

We have prepared secondary entry points in the LMSC CORRCO program (See SRSL Tech Report 67-2, p. 41) so that spectral emittance ratios taken from other sources, as from Daniels for example, can be used and compared against our library of 19** rocks in the memory of the computer.

In order to conserve space we have only presented the five rocks which best fit (i.e. top five rankings) and the two which are the worst

---

* Daniels, D.L., 1966 "Infrared Spectral Emittance of Rocks from Pisgah Crater and Mono Craters area, California", USGS Technical Letter NASA-13, pp 1-20,

** Changed from 50 to 19 because of redundancy in the rock types.

fit (i.e. lowest two rankings) for each of the 13 input spectra. The data are summarized in Table XI which shows that the correct rock type was chosen first only 4 times.

TABLE XI

SPECTRAL MATCHING SUMMARY

USGS #	ROCK TYPE	CORRCO RANKING OUT OF 19 CHOICES
	Mono Lake, California	
73	Obsidian, grey	2nd
74	Obsidian, black	2nd
85	Rhyolite pumice, weathered	1st
75	Rhyolite pumice, weathered	1st
79	Bishop Tuff (upper)	1st
80	Bishop Tuff (lower)	3rd
78	Quartz Monzonite, weathered	3-4th
	Pisgah Crater, California	
71	Basalt, pahoehoe, weathered	10th
72	Basalt, pahoehoe, sawed	2nd
89	Basalt, aa, weathered	13th
86	Basalt, aa, weathered	5th
91	Basalt, aa, weathered	9th
90	Basalt, aa, rough	1st

The detailed listing in Table XII however shows that a "reasonable fit" (i.e. obsidian for rhyolite pumice) was made in 10 out of the 13 cases. The other 3 chose a single mineral (K-feldspar) rather than the rock.

The discrimination is good, but not excellent. There is some doubt about the basalt spectra, and when one redigitizes spectra, which are already drafted, there is a problem of obscuring information which may have been present in the original spectra.

TABLE XII

DETAILED SPECTRAL MATCHING - USGS SAMPLES

USGS 73 Obsidian, gray smooth, Mono Craters (Obsidian ranked 2nd in 19)

Rhyolite pumice	97%
Obsidian	97
Pyrox aplite	92
Welded tuff	91
Granite, rough	88
Meteorite	- 14
Dunite Rough	- 23

USGS 74 Obsidian, black smooth, Mono Crater (Obsidian, ranked 2nd in 19

Rhyolite pumice	98%
Obsidian	97
Pyrox. aplite	93
Welded tuff	91
Granite, rough	88
Meteorite	- 9
Dunite	- 17

USGS 85 Rhyolite pumice, weathered rough, Mono Crater (Rhy. pumice ranked 1st in 19)

Rhyolite pumice	90%
Obsidian	83
Hyp. andesite	80
Welded tuff	79
Aug. diorite rough	79
Polystyrene	7
Dunite rough	7

USGS 75 Rhyolite pumice, weathered rough, Mono Crater (Rhyolite pumice ranked 1st of 19)

Rhyolite pumice	95%
Obsidian	91
Welded tuff	91
Pyrox. aplite	89
Granite rough	86
Farmington meteorite	- 16
Dunite rough	- 26

USGS 79 Bishop tuff, upper unit rough, Mono Crater (welded tuff ranked 1st in 19)

Welded tuff	96%
Rhyolite pumice	95
Pyrox aplite	94
Granite rough	93
Obsidian	92 -
Farm. Meteorite	- 15
Dunite rough	- 24

USGS 80 Bishop tuff, lower unit rough, Mono Crater (welded tuff ranked 3rd in 19

Rhyolite	96%
Obsidian	92
Welded tuff	89
Pyrox aplite	88
Granite rough	85
Farm. meteorite	- 14
Dunite rough	- 23

USGS 78 Quartz monzonite, weathered Mono Crater (QMP rough ranked between 3 & 4 in 19)

Pyrox. aplite	98%
Welded tuff	96
Granite rough	96
Obsidian	94
Rhyolite pumice	93
Farm. meteorite	- 17
Dunite rough	- 23

USGS 71 Basalt, pahoehoe, weathered rough, Pisgah Crater (ranked 10th in 19)

K-feldspar, rough	94%
Augite diorite, rough	90
Quartz diorite	87
Andesite	85
Neph. syenite	84
Caleite	15
Dunite, rough	12

Table XII (continued)

USGS 72 Basalt, pahoehoe, sawed, Pisgah Crater (ranked 2nd in 19)

Q. diorite	88%
Basalt	87
Serpentine	86
Hyp. andesite	86
K-feldspar, rough	85
Calcite	22
Qtz. beach sand	- 4

USGS 89 Basalt, AA weathered, v. rough Pisgah Crater (ranked 13th in 19

Andesite	90%
Neph. syenite	88
Aug. diorite, rough	86
K-feldspar, rough	84
Obsidian	83
Meteorite	8
Dunite, rough	- 8

USGS 86 Basalt, AA, weathered v. rough, Pisgah Crater (basalt ranked 9th in 19)

K-feldspar rough	87%
Aug. diorite rough	80
Hyp. andesite	75
Quartz diorite	71
Basalt	71
Polystyrene std.	12
Calcite	10

USGS 91 Basalt, AA, weathered v. rough, Pisgah Crater (basalt ranked 9th in 19)

K-feldspar rough	97%
Aug. diorite rough	91%
Quartz diorite	84
Hyp. andesite	83
serpentine	83
Polystyrene std.	21
Calcite	7

USGS 90 Basalt, AA, rough broken, Pisgah Crater (basalnt ranked 1st in 19)

Basalt	91%
Hyp. andesite	87
Serpentine	83
K-feldspar rough	81
Quartz diorite	80
Polystyrene standard	- 1
Quartz beach sand	- 13

b. Step-wise Discriminant Program

A second method of analysis concerns the discrimination of the various rock types represented by the spectra. This analysis is more satisfactory than computed modes because within sample (rock type) spectral variation, while large per se, is less than between-sample spectral variation and the discrimination analysis is able to discriminate between rock types rather well in certain respects. All felsic volcanic rocks from Mono Craters cluster closely, and apart from the cluster of the basalts from Pisgah Crater. (See Fig. 10) The 13 test spectra were classified into one of three groups (granite, basalt, pumice), the 3 groups previously set up with our own spectra. In this respect, the program is less than satisfactory. Most of the felsic volcanic rocks would be classified by most geologists as pumices, yet the program classifies them as granites. It should be noted however that the felsic rocks correspond quite closely to granite in composition, but differ markedly in texture. The program classified 4 out the 6 basalt spectra correctly as basalt, the two incorrect classifications being assigned to the granite class.

c. Mineral Ratios Program

The third method of statistical analysis consisted of an attempt to compute modal analyses for the 13 rocks from the library mineral spectra compiled from our 22 library samples. This analysis has proved to be less than satisfactory. We have found that the standard error of each of the computed component minerals is incredibly large, and then the computed modal analyses are essentially meaingless. We attribute this factor to the high "noise level" of the 13 spectra and the general lack of similar shape in spectra from compositionally and texturally similar rocks.

In summary, it is encouraging to note that the step-wise discrimination program (b) is able to sort out and cluster spectra of similar rock types (Fig. 10) but the classification performed by the program (c) in this case is not adequate. We attribute this factor to the generally poor quality of the 13 spectra. We must also note however that the "training" spectral groups used in this program were produced from our own field spectra, taken under very different conditions and with different equipment than the U.S.G.S. spectra.

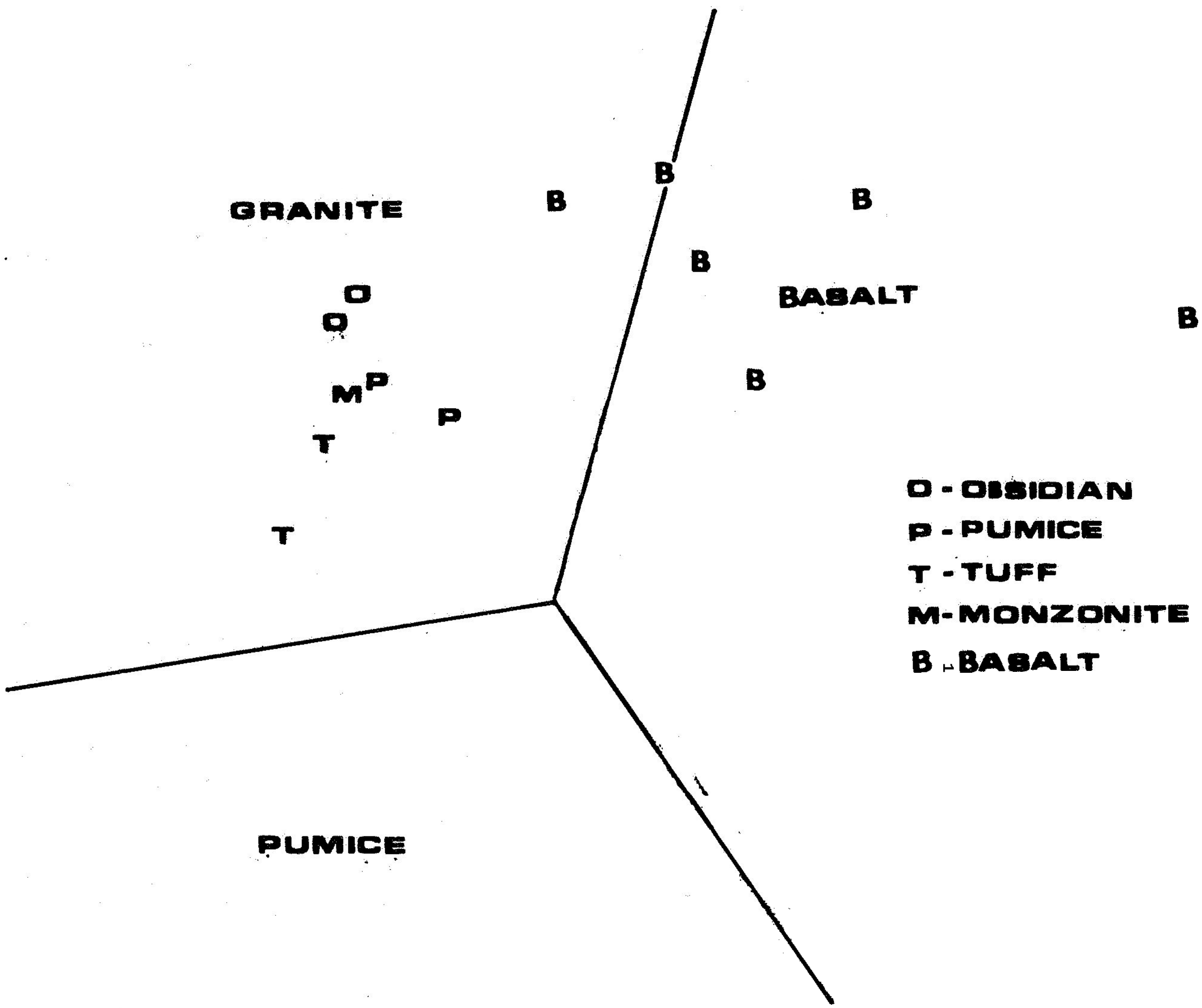

FIGURE 10 - Classification of U.S.G.S. spectra into 3 rock Groups with Use of Discriminant Analysis.

7. Academic Research Projects using Partial Grant Support

a. Experiment in Infrared Scanning of Water Surfaces
(Keenan Lee, Graduate Student)

The experiment is designed to resolve and quantify water surface temperatures by infrared scanning. The present approach is through a model study using small, contained water bodies of various characteristics and scanning them with a Barnes Infrared Camera (5-20μ). The results should indicate the feasibility of using this slow and relatively non-sophisticated system to detect and map shoreline groundwater discharge areas, and the data reduction methods developed should also be applicable to airborne scan imagery.

The scanning system used is the Barnes Infrared Camera, Model T-4A. This fixed-position unit has a horizontally oscillated scanning mirror which reflects incoming radiation through a Cassegrain optical system to the detector. The thermistor detector is sensitive from 2-20μ, and was used with a cut-on filter at 5μ. Incoming radiation is chopped against a reference blackbody of known temperature, and the response from the detector is converted to a visible light output subsequently recorded on Polaroid Positive-Negative film. Scanning time is six minutes, with a 10" x 20° field of view and 1 milliradian resolution. For this experiment, the unit was mounted on a fire escape 6.7 meters above the targets with a look angle of 14-24" depression.

Targets scanned include two-temperature static water bodies separated by impermeable and permeable dividers, saline vs. fresh water bodies, and point discharges of warm water into ambient-temperature standing water. With static water bodies, the system can discriminate temperature differences of less than 0.5°C in a field range of 10°C. Imagery of the saline (approximately 34°/oo) vs. fresh water surfaces suggests that an assumed equal emissivity for both bodies leads to no significant error. Fig. 11 is an example of imagery of a constant point discharge of warm water into a standing body. The warm current is clearly visible as the bright area spreading out from the source at bottom. The slight asymmetry of the warm surface pattern, with feathering to the left near the bottom and to the right at top, is attributable to a weak residual clockwise current from earlier stirring. The linear pattern of apparently warmer water on the right is due to the reflection of a roof overhang (roof, about +12.8°C; sky, less than -12.2°C).

An attempt was made to scan a lake surface where a tributary stream enters. Although the imagery is poor due to instrumental difficulties, a pattern of cooler water at the stream's mouth was evident.

A data reduction program is now being developed. Basic steps involve optical densitometer profiles of image negatives, digitizing of the profiles, conversion of data to electronic output and then to apparent (or "brightness") temperatures, and correction for atmospheric attenuation and reflection to yield true target temperatures. Data points will then be plotted to give isothermal maps and used to construct trend surfaces and thermal. residual maps.

Preliminary, and decidedly inconclusive results suggest that this scanning system might be used with moderate success to detect and map shoreline springs. However, its use would be restricted by these requirements:

1. A high-relief coastline or the availability of high structures from which to scan.
2. Spring discharges with ± 5°C contrast to standing body, or perhaps somewhat less contrast if the discharge is great.
3. Bandpass filters to narrow range at least to 8-13μ.
4. Frequent re-calibration of the system.

Present effort is directed toward digitizing available density profiles and writing a computer program to quantify and map temperature data.

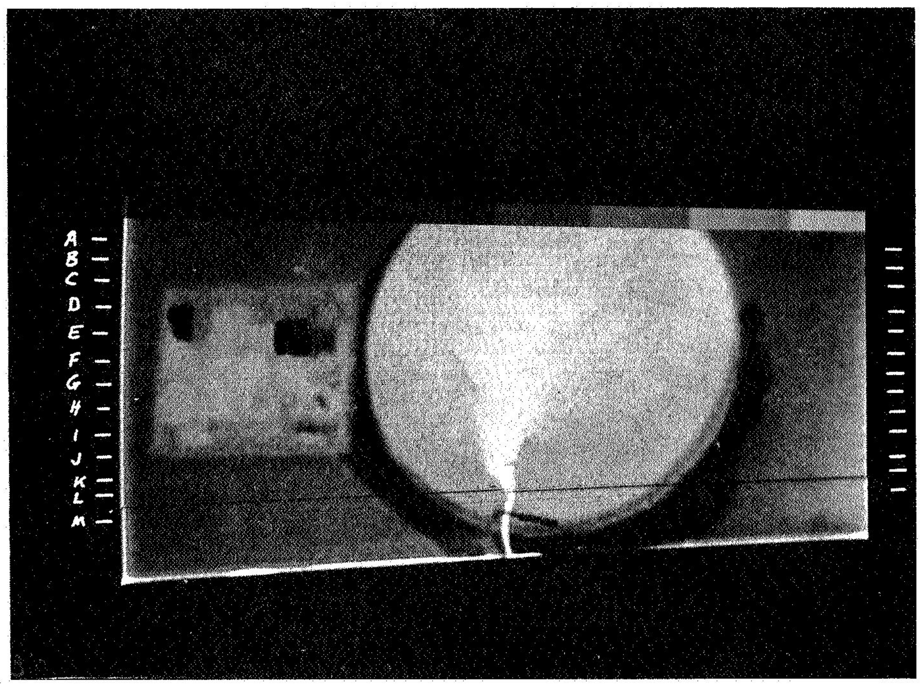

a

b. Analysis of NIMBUS HR IR Imagery (William Liggett, Undergraduate Student)

The Nimbus II weather satellite has produced infrared photographs of the earth's surface which distinguishes cloud masses and water bodies by photographic densities corresponding to their relative temperatures. Six NIMBUS photographs showing the North American (eastern) coastline were examined for evidence suggesting the behavior of the contact between cool coastal water and the warmer Gulf Stream. These two water masses are distinguishable on all six photos - the Gulf Stream is considerably darker than the coast water. This contact is roughly constant although its meandering character discussed by Stommel is apparent.' The continent is darker (warmer) than the ocean for daytime shots and lighter in the night exposures. The land features visible in the six photos are listed below:

1. Pass 238--Shows Delaware and Chesapeake Bays, also Gulf Stream.
2. Pass 1995--Chesapeake Bay (left center) hints of Gulf Stream Margin.
3. Pass 1942--Shows Chesapeake Bay, Delaware Bay, and Long Island. Cloud cover follows Gulf Stream? (Lake Erie).
4. Pass 510/511--Taken over U.S., shows tip of Lake Michigan, Lake Huron, and Lake Erie. Also Chesapeake Bay, Long Island.
5. Pass 110/111--Chesapeake Bay, Great Lakes, Cape Cod, Nova Scotia--note dark area paralleling the coast.
6. Pass 123/124--Coastline shows Cape Cod, Long Island, Nova Scotia and Newfoundland.

Photographs Nos. 2 and 6 show an area of warm water surrounded by the cooler near-shore water between Cape Cod and Nova Scotia. This is especially clear in photo No. 6 reproduced here with an overlay (Fig.12). A definite clockwise rotation in this eddy feature is evident. It was suggested that this water mass is an eddy which simply broke from the Gulf Stream and migrated into the cooler coast water. Although the source for this warmer water probably was the Gulf Stream, the clockwise sense of rotation is not the expected result of a north flawing current. A more complicated system of turbulence must be involved. H.U. Sverdrup

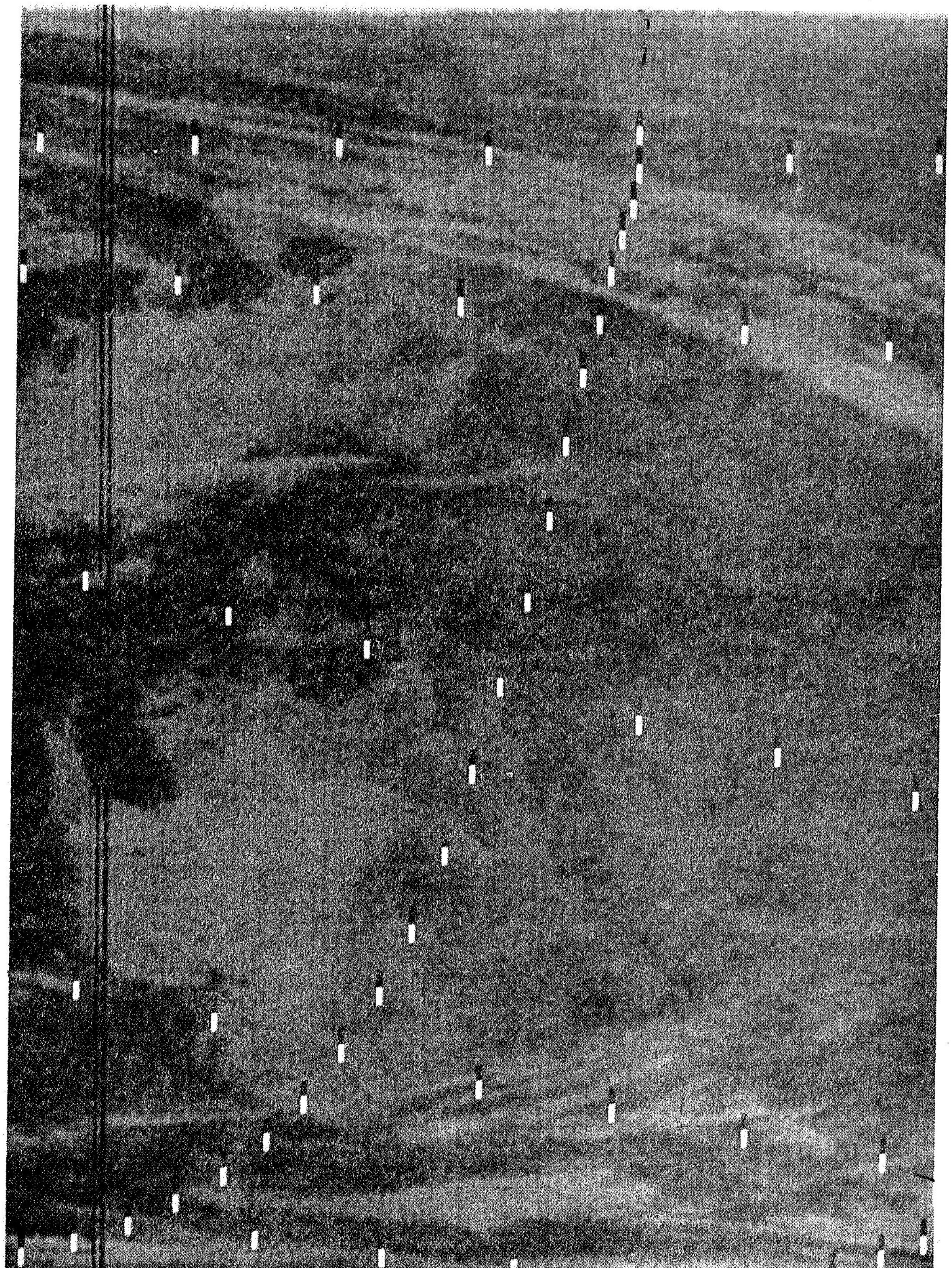

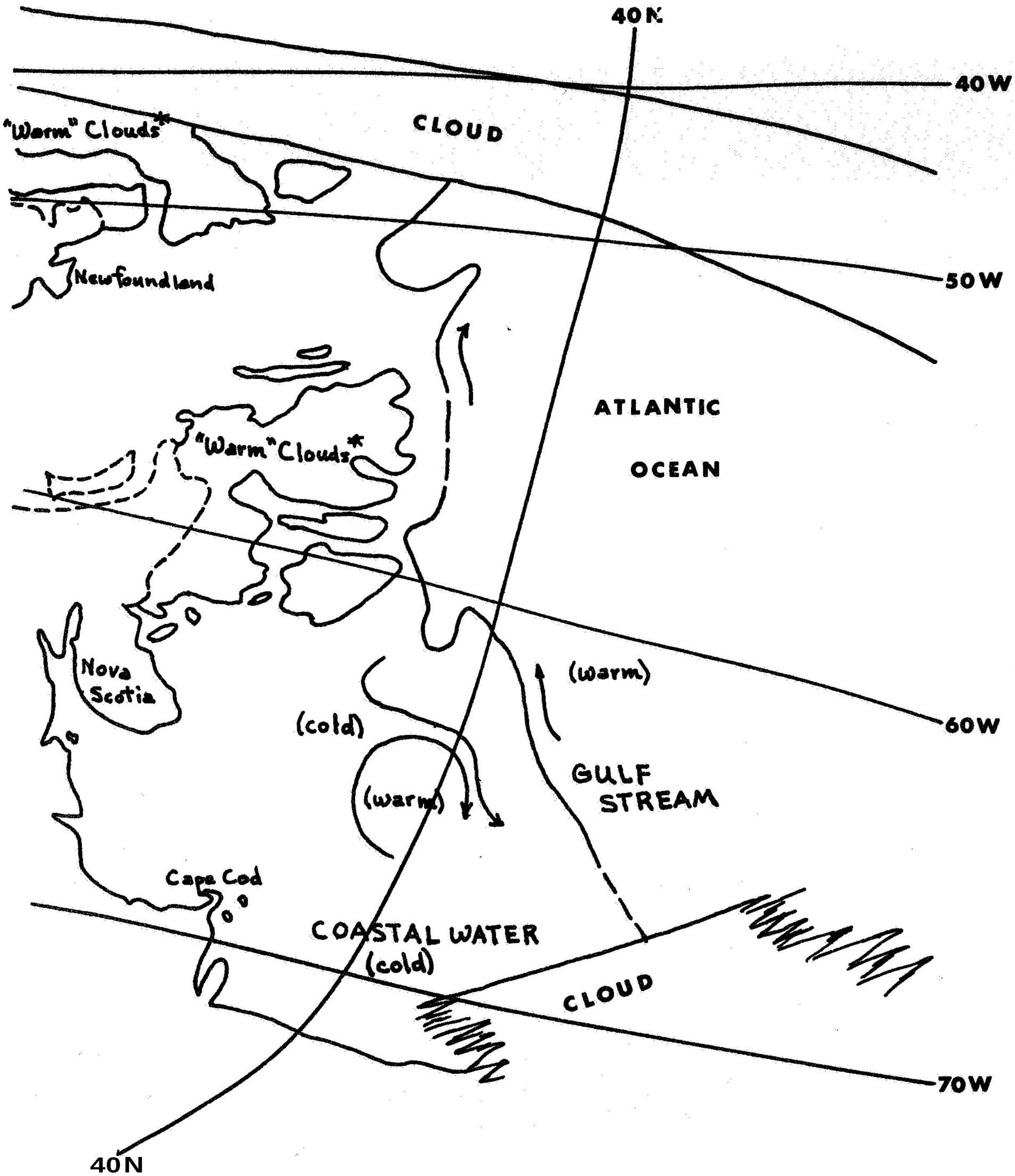

FIG. 12 Shows clockwise eddy in coastal water and the meandering **Gulf** Stream.
***Dark** color indicates warm.

discusses this phenomenon in the Oceans:

> "Such an eddy, rotating clockwise, has repeatedly been observed to the south of Nova Scotia (Iselin, 1936), but the clockwise rotation has been difficult to explain because the eddy was considered an offshoot of the Gulf Stream. The direction of rotation is better understood, on the other hand, if the eddy is considered as a part of the slope-water gyral.[2]

Figure 13 is a diagramatic representation of the turbulence suggested by Sverdrup[3]. The south-flowing coastalwater and the slope water gyral are not discernable on the NIMBUS photo presumably because they involve uniformly cold water. The eddy is visible only because water of two temperatures are involved.

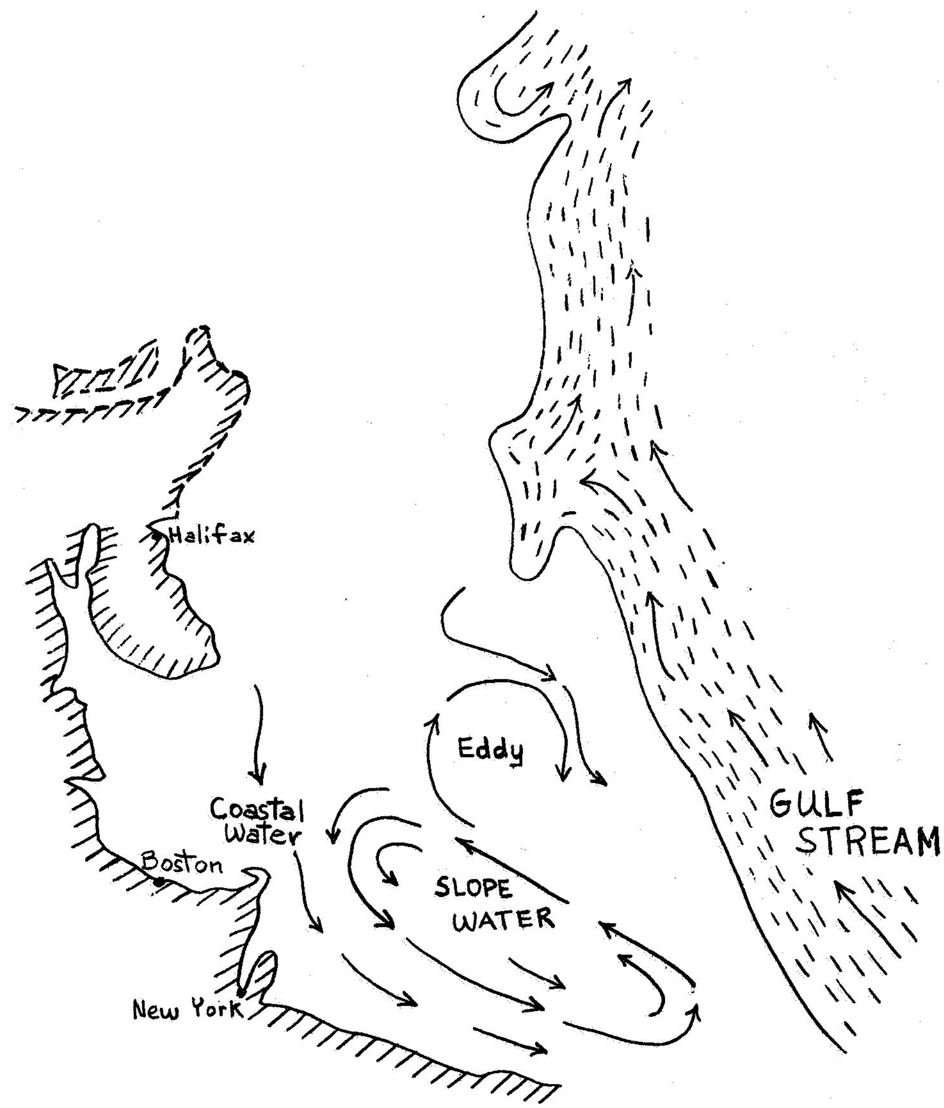

FIGURE 13

Several dark patches labeled "warm" clouds in Fig. 12 appear on photo nos. 5 and 6 and are difficult to account for. Their dark color indicates bodies with temperatures as high as the land during the day yet their shape and position can only be that of cloud or very warm water masses. The term "warm" cloud comes from a possible explanation as a cloud mass with very high reflectivity of solar radiation. Further investigation of these patches is essential, as this is a most unexpected situation. These NIMBUS photographs demonstrate the value of satellites in plotting major ocean currents and the application of this technique to related oceanographic problems.

---

[1] Henry Stommel, The Gulf Stream, Physical and Dynamical Description, (Berkeley, 1965), p. 51.

[2] H.U. Sverdrup, M.W. Johnson, R.H. Fleming, The Oceans, (New York, 1942), p. 679.

[3] H.U. Sverdrup, M.W. Johnson, R.H. Fleming, The Oceans, (New York, 1942), figure 185, p. 680.

c. Photoelectric Analysis of Stained Rocks (William Liggett, u/grad student)

Geologic investigations often require the determination of percentages of various minerals in rock specimens. A common procedure which has proved inexpensive and uncomplicated for rough analyses involves cutting the specimen and applying stains. A solution of sodium cobaltinitrate produces a yellow stain in the potassium feldspars. An organic dye, amaranth, stains the sodium feldspar pink. Traditionally, a large number of distinct points (600-1000) of stained minerals are counted on the rock surface and percentages calculated. The point counting procedure is done manually under a microscope or lens and requires from one-half hour to one hour to count a coarse crystalline rock.

The purpose of this investigation is to reduce the time and labor involved in obtaining mineral percentages from the stained rock and to increase the accuracy of the measurements.

A simple photocell-meter instrument is used in conjunction with colored filters to discriminate the relative amount of rock surface covered by the minerals. 35mm colored slides are used in an intermediate step because of their convenience and placed in a photocell device (a Hach Chemical Co. colorimeter) to be read. A spectroradiometer is currently being used to obtain curves of the integrated reflected radiation from the stained rocks and the transmitted radiation through the colored. slides. Based on these spectra, filters with the appropriate pass-width will be obtained. The time saved by using photoelectric device in rock analysis should be significant. Also, the accuracy of this method should prove higher than that of point counting since the entire rock surface or slide is measured rather than discontinuous points.

d.. <u>Multivariate Analysis of Multiband Photography (Gary Ballew, Graduate Student)</u>

The basis of NASA's program of remote sensing of environment is that the nature of the earth, or any other planet, can be deduced by sampling as many regions of the electromagnetic spectrum as possible. The geological applications of such a program are obvious, yet much work remains in the field of data reduction and geologic classification of resulting spectra*. The following data are relative reflectance spectra derived from six of the nine filtered "bands" of the Multiband camera, each spectrum having been classed as being rhyolite, pumice or shadow. This classification was arrived at by photographic and field inspection of the region of interest at Mono Lake, California.

As each of the six bands may be considered a variable and each of the three possible terrain types may be considered a group, the method of multivariate analysis can be used and the resulting classification checked against actual conditions. First, a "perfect" spectrum for each terrain group is decided upon--the mean of each group--and is calculated thus:

$$H^R \quad {}^{R}_{1},\ h^R_2, \ldots, h^R_6);\ h^R_i \quad \sum_{j=1}^{n}\left(b^R_{ij}\right)\ ;\ \text{e.g. } h^R_1 = \frac{1}{18}\sum_{j=1}^{18}\left(b^R_{1j}\right) = 0.65167$$

$$H^S = (h^S_1,\ h^S_2, \ldots, h^S_6);\ h_i = \frac{1}{n_S}\sum_{j=1}^{n}\left(b^R_{ij}\right)\ ;\ \text{e.g. } h^S_1 = \frac{1}{15}\sum_{j=1}^{15}\left(b^S_{1j}\right) = 0.40000$$

$$H^P = (h^P_1,\ h^P_2, \ldots, h^P_6);\ h_i = \frac{1}{n_P}\sum_{j=1}\left(b^R_{ij}\right)\ ;\ \text{e.g. } h^P_1 = \frac{1}{46}\sum_{j=1}^{46}\left(b^P_{1j}\right) = 0.54696$$

where H^R, H^S, H^P are each a set of 6 band means for rhyolite, shadow or pumice; h^R_i, h^S_i, h^P_i are the means of an individual band i; n_R, n_S, n_P are the number of spectra in each of the three groups; and b^R_{ij}, b^S_{ij}, b^P_{ij} are the relative reflectancevalues of an individual band in an individual spectrum j.

* The three bands of' IR film were not available for this flight.

a

By using these means as the most probable estimates we may also assume that any variation within an individual band is not completely random, but may be approximated by a Gaussian function of some type. This implies that the three distributions in a given band are each represented by a characteristically shaped normal curve with its peak at the mean of that band. Unknown spectra may then be compared to these

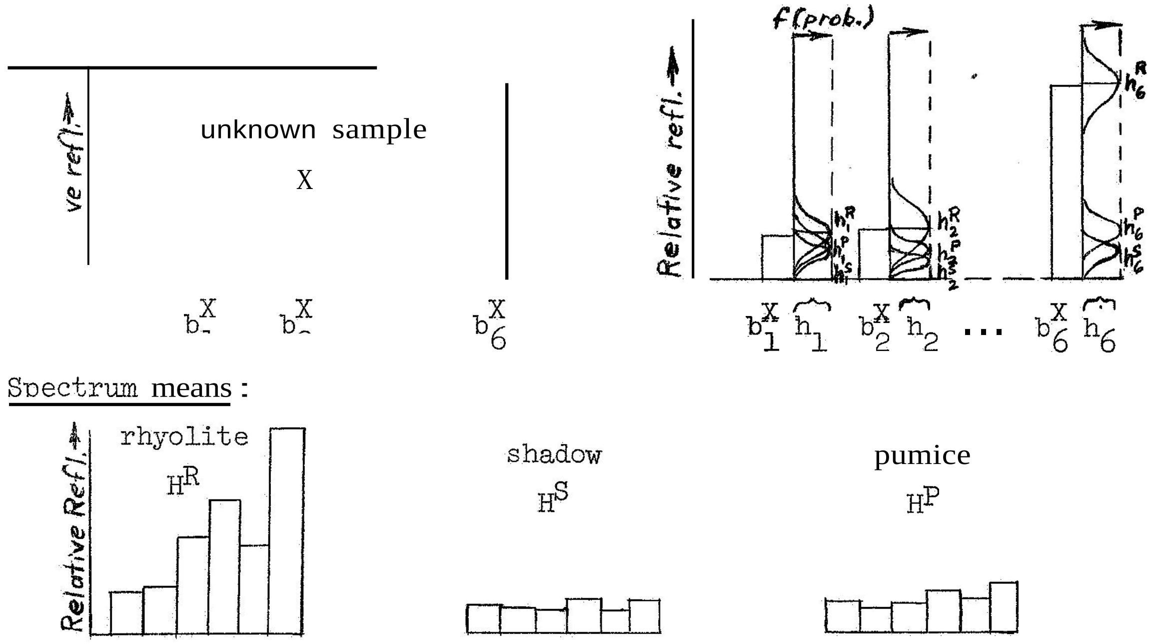

Figure 14

ideal spectra and the most probable group decided upon (Fig. 15).

We should be aware that the term "most probable" must be interpreted correctly. If, for instance, we have collected 18 rhyolite spectra, 15 shadow spectra and 46 pumice spectra we should realize that the probability of choosing any one and calling it rhyolite is $18/79^{ths}$ if no classification is used at all. By calling $p_R(s)$, $p_S(s)$, and $p_P(s)$ the estimated probabilities, and calling $P(s)$ the largest of these, then an estimate of the expected error rate for n spectra is equal to $1-1/n \sum_{i=1}^{n} P(s_i)$.

MULTIVARIATE CLASSIFICATION OF TERRAIN TYPES NEAR MONO LAKE, CALIFORNIA

DATA FROM SIX VISUAL BANDS OF MULTIBAND PHOTOGRAPHY

0615 SOUTH SHORE OF MOHO LAKE

PUMI50	BECH99	BECH99	BECH99	■
PUMI50	PUMI70	PUMI50	BECH99	■
PUMI50	PUMI70	PUMI50	PUHI70	BECH99
PUMI50	PUMI70	PUMI50	PUMI70	BECH05
PUMI50	PUMI70	PUMI50	PUMI70	PUMI70
PUMI50	PUMI70	PUMI50	PUMI70	PUHISO
PUMI50	PUMI70	PUMI50	PUMI70	PUMI50
PUMI50	PUMI70	PUMI50	PUMI70	PUMI50
PUMI50	PUMI70	PUMI50	PUMI70	PUMI50

C615 SOUTH SI-ORE OF MONO LAKE

PUMISG C.8256	PUMISG .8243	PUMICE C.7169	PUMISG 0.7020	■ 0.4250
PUHISG C.7681	PUUICE C.6896	SHADOW 0.7504	PUMICE 0.6265	■ 0.4554
PUMISG C.7991	PUMICE C.8595	PUMICE 0.7001	PUMICE 0.6982	■ 0.6066
PUHISG C.7646	PUUICE C.7725	SHADOW 0.7834	PUMICE 0.6286	PUMICE 0.7972
PUHISG C.6166	PUMICE .7405	PUMICE 0.7775	PUUICE C.7626	PUMISG 0.5704
PUMISG C.8138	PUUICE .7156	PUMICE 0.7844	PUUICE 0.7648	PUUISG 0.6664
PUMISG C.5934	■ .6465	PUUICE 0.7161	PUUICE 0.6859	PUUISG 0.6876
PUMISG 0.6752	SHADOW [illegible]	PUMICE 0.7176	SHADOW 0.8002	PUUISG 0.5989
PUHISG C.6884	PUUICE .8394	SHADOW 0.4382	PUMISG 0.5553	PURISG 0.4703

0616 NORTH CRATER

PUMI50	PUMI50	PUMI90	PUMI70	PUMI50
RDDT99	PUMI50	■	PUMI99	PUMI50
PUMI50	PUMI50	■	■	PUMI50
PUMI50	PUMI50	■	■	PUMI50
PUMI50	PUMI50	■	PUMI90	PUMI70
PUMI50	RDCT99	PUMI90	PUMI70	■
PUMI50	PUMI50	PUMI70	PUMI70	■
PUMI50	PUMI50	PUMI70	PUMI70	PUMI50
PUHISO	PUMI50	PUMI70	PUMI70	PUMI50

C616 NORTH CRATER

PUMISG C.5522	PUMISG .6497	■ C.6054	PUMISG 0.5784	PUMISG 0.5749
PUMISG C.4618	SHADOW .4754	■ 0.5730	SHADOW 0.4790	PUMISG 0.5986
PUMISG C.7208	SHADOW C.4265	■ 0.5611	■ C.4998	■ 0.5374
PUMISG C.8242	SHADOW C.5656	PUMISG 0.5995	■ 0.2272	PUMICE 0.6608
PUMISG C.8145	SHADOW .6670	■ 0.4806	■ 0.1338	■ 0.5807
PUMISG C.8740	PUMICE .7527	PUMICE 0.6890	PUMICE 0.8237	PUMISG 0.4535
PUMISG C.7337	PUMICE .7613	SHADOW 0.8363	SHADOW 0.4189	■ C.4718
PUHISG C.7263	PUMICE C.7107	PUMICE 0.6751	0.7535	■ 0.5544
PUMISG .7860	PUUISG .8107	PUUICE 0.7513	SHADOW 0.6390	PUUISG 0.3214

0617 AREA SOUTH OF NORTH CRATER

PUMI50	PUHISO	PUMI50	PUMI70	PUMI50
	PUMI50	PUMI50	PUMI50	PUMI50
PUMI50	PUMI50	PUMI50	RDCT99	PUMI50
PUMI50	PUMI50	PUMI50	PUMI30	PUMI50
PUMI50	PUMI50	PUMI50	PUMI30	PUMI50
PUMI50	PUHISO	RDCT99	PUMI30	RDDT99
PUMISO	PUMI50	PUMI70	PUMI30	PUMI50
PUMI50	PUMI50	PUMI70	PUMI30	PUMI50
RDDT99	PUMI50	PUMI70	PUMI30	PUMI50

C617 AREA SOLTH OF NORTH CRATER

PUMISG C.3572	PUMICE .6660	PUMICE 0.8501	PUMICE 0.7006	PUMISG 0.6846
PUMISG C.5792	PUMISG .6920	PUUICE 0.6781	PUMICE 0.7528	PUMISG 0.8749
PUMISG C.6678	PUMISG 0.6653	PUMISG 0.7159	■ 0.4821	PUUISG 0.7159
PUMISG C.6353	PUMISG .6632	PUMISG 0.5963	■ C.6772	■ 0.6042
PUMISG 0.6026	PUUISG .6200	PUMICE 0.6903	SHADOW 0.5255	■ 0.5775
PUMISG C.8066	PUMICE .6137	PUMISG 0.7534	PUMICE 0.6986	■ 0.4101
■ C.4469	PUUISG 0.5654	PUMICE 0.6459	PUMISG 0.6357	PUMISG 0.5545
PUHISG 0.4491	PUUISG .6658	PUMISG 0.6856	■ 0.4473	PUMISG 0.5279
■ C.3162	PUMISG .7279	PUMISG 0.7307	■ 0.5769	PUMISG 0.5668

1 Km

TERRAIN TYPES FOUND IN AREA:

RHY099 = RHYOLITE WITH LITTLE OR NO VEGETATION
PUMI99 = PUMICE WITH LITTLE OR NO VEGETATION
PUMI70 = PUMICE WITH SHALL PERCENTAGE OF VEGETATION
PUMI50 = PUMICE AND VEGETATION (SAGE) ABOUT EQUAL
PUMI30 = HEAVILY VEGETATED PUMICE
BECH99 = BEACH DEPOSITS WITH LITTLE OR NO VEGETATION
LAKE99 = LAKE WATER
RDDT99 = DIRT ROAD OF PUMICE MATERIAL

TERRAIN TYPES CONSIDERED IN ANALYSIS:

■ RHYOLT = RHYOLITE OBSIDIAN
PUMICE = PUMICE WITH LITTLE OR NO VEGETATION
PUMISG = PUMICE MODERATELY VEGETATED WITH SAGE
SHADOW = SHADED AREAS OF EITHER RHYOLITE OR PUMICE

If the six variables used here are reduced to two canonical variables and plotted in two dimensions, then the probabilities become smaller the further from an individual mean that a sample point is plotted. The locus of points along the perpendicular between means indicates areas of equal probability, and the intersection of these lines shows where all three terrain types are equally probable. The results of this particular classification example were: rhyolite 78% correctly classified, shadow 74% and pumice 85%, with the most favorable bands being (in order of reliability) 4, 1, 2, 6, 3 and 5--most unreliable. These bands correspond to the colors yellow, violet, blue, red, green, and orange; which suggests that for differentiating pumice, shadow and rhyolite the two best filters are yellow and violet. Although this appears to be a valid method for classifying rock and shadow areas near Mono Lake, it would be interesting to test the validity of Multiband data in other geologically similar areas.

This method was also applied to a field area near Mono Lake by comparing 135 spectra from areas 15 x 12 meters which were sampled on a 300 x 150m coordinate system. The eight terrain types present were compared to four general terrain types, the means and standard deviations of these being obtained from representative spectra in the area.

A significant geologic result was the ability to correctly identify the rhyolite areas within North Crater 83% of the time. Also, areas of rhyolite soil derived from craters located east of the region under study may account for the "rhyolite" classifications indicated by the program. As the photography was taken in the morning, all of the shadow areas near and in North Crater are correct classifications. In general, the accuracy of the resulting classifications is at least 80% for the four groups used..

Miller, R.L. and Kahn, Statistical Analysis in the Geological Sciences, Ch. 12 & 13, Wiley, 1961.

Sampson, Paul, BMD07M Stepwise Discriminant Analysis, Health Sci. Comp. Facility, UCLA, 1965.

Switzer, Paul, Statistical Analysis of Spectral Matching, Unpublished report, Stanford University, 1967. See Appendix A.

e. Analysis of Visual and Near Infrared Field Spectra from Mono Craters, California (Gary Ballew, Graduate Student)

Although much work has been done in the visible and near infrared region from 0.4 to 1.5 microns, there is very little data of a geological nature which can be used for field analysis. This situation is especially evident when analyzing the remote sensing data presently available in the form of multiband photography from Mono Craters, California. This is currently being studied in an attempt to perfect a method of multispectral geologic mapping.

The field spectra presented here were obtained at North Crater (sometimes known as Panum Crater), a rhyolite, obsidian and pumice explosion crater approximately one-half mile in diameter and rising 200 to 300 feet above a plain of moderately vegetated pumice. It is located about a mile south of Mono Lake and is a northern extension of the main arc of the Mono Craters.

Although the conditions for taking spectra on April 1, 1967 were not ideal, the methods employed were as consistent as possible.

An ISCO spectro-radiometer fitted with a fiber optics remote probe was used to obtain these spectra, which ranged in wavelength from 0.425 to 1.55μ. The reflectance at each wavelength was calculated by taking the ratio of reflected to total intensity, both intensities being measured over a 180° (2π steradian) field of view. As this is a completely portable instrument, spectra of samples were taken in place and the samples collected for further study. Of the twenty wavelengths used nine correspond to the filtered bands of the multiband camera.

When these reflectance values are plotted against wavelength we notice that most of the variation occurs in the visible region from 0.425 to 0.750μ and that, with the exception of black obsidian, the highest reflectance occurs in the near infrared. The two samples of gray obsidian are both from the Mono Craters area, but the one showing highest spectral reflectance is from a sample collected by the University of Nevada's NASA Project. Both of these spectra show surprisingly high values at 0.425μ (violet light) and minimum values at 0.475μ (blue light).

Assuming that this is not caused by instrumental errors, there appears to be a potential band in the violet which could discriminate between gray obsidian and other rocks. Note also the higher overall intensity of the one gray obsidian relative to the other. This may be caused by the rough surface of the first obsidian, which is more reflectant than the smooth surface of the other sample.

The spectrum of black obsidian is uniform and unexpectedly high over much of the visual region with reflectance reaching a minimum in the infrared. The smooth surface of this obsidian may help to explain its high reflectance, as the sun was at a very low angle and the obsidian was on a steep slope facing the sun.

The spectrum of red rhyolite shows that very low reflectance occurs in the shorter wavelength visible region, with an expected maximum in the 0.75μ (red) region. This high reflectance persists into the infrared and shows little variation except at very long wavelengths. In contrast, the pumice spectrum shows higher values in the violet and lower values in the red. regions of the visual, with a crossover near 0.60μ (Orange). The pumice spectrum does not extend into the infrared, as lighting conditions were poor when its spectrum was taken.

A characteristic of all the longer wavelength infrared spectra is their apparent convergence in the region near 1.55μ, with no crossovers occurring in the entire near infared region. Combining this information with that obtained in the visual portion, we note that there are a number of optimum wavelengths which could be used for rock spectra classification. In the visible these are 0.425 μ (violet), 0.475μ (blue), and 0.725μ (red), with 0.80μ in the photographic infrared and 0.90 to 1.35μ and 1.55μ in the region beyond photographic detection. Thus, by using these bands, the non-vegetated areas near Mono Craters could be classified as red rhyolite, black obsidian, gray obsidian or pumice. Hopefully, other areas of similar lithology and vegetation cover could be mapped using presently available data in the area around Mono Lake.

TABLE XIII

VISUAL AND NEAR INFRARED FIELD DATA

microns	rough obsidian*	smooth obsidian	smooth obsidian	smooth rhyolite	pumice soil
0.425	14.9	10.3	11.4	5.7	8.8
0.475	14.5	13.0	13.3	6.7	10.2
0.525	15.2	14.0	12.9	7.6	10.7
0.575	16.7	14.6	12.9	11.4	12.2
0.625	20.3	16.0	12.5	15.6	12.9
0.675	21.4	15.8	15.6	16.7	14.2
0.725	25.6	18.3	17.0	17.7	14.6
0.800	25.9	17.5	14.3	18.7	--
0,850	25.0	17.5	16.0	18.6	--
0.950	27.5	17.7	11.1	20.0	--
1.050	27.8	16.7	11.8	20.0	--
1.150	29.1	17.0	11.0	20.8	--
1.250	26.3	15.9	11.1	20.0	--
1.350	26.7	17.4	14.3	20.6	--
1.450	25.9	17.0	12.7	17.0	--
1.550	23.0	16.3	13.7	17.9	--

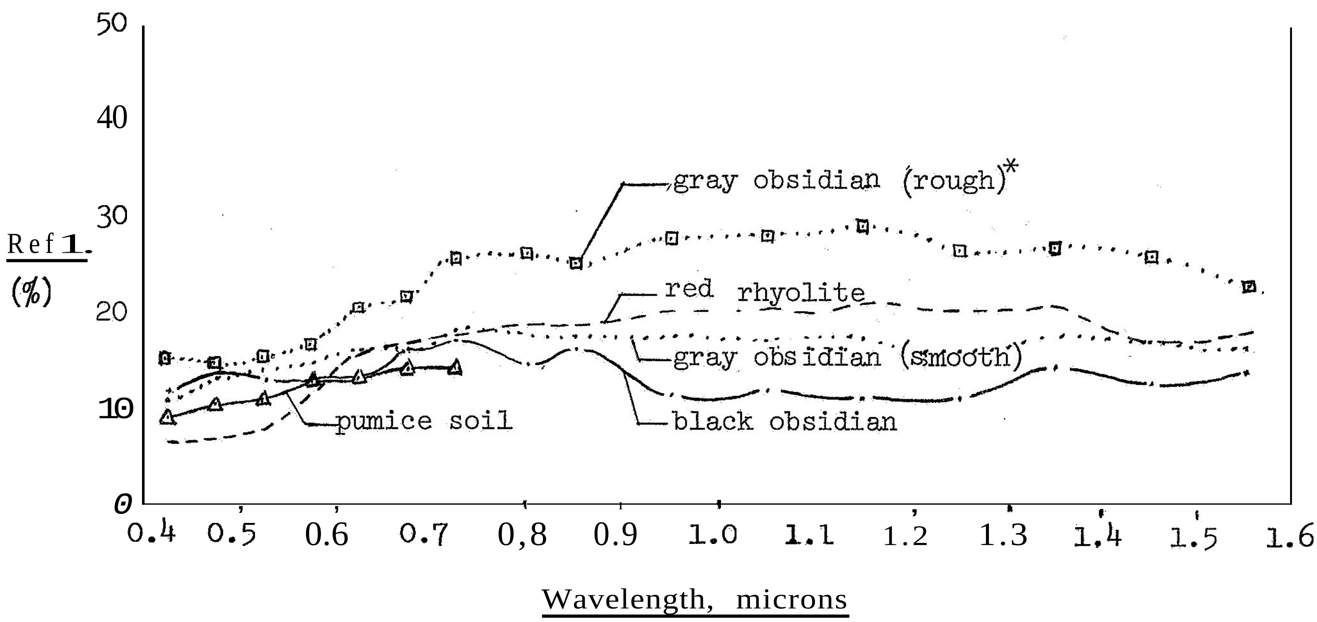

REFLECTANCE SPECTRA (5)

* Sample collected by Univ. of Nevada NASA Project.

IV. MAJOR EQUIPMENT STATUS

A. Field Equipment

The SG-4 spectrometer has had extensive testing and calibration work during this reporting period. It is now in a state where it can be taken in the field at any time, with a reasonably high level of confidence in its performance. The main problem left with this instrument is the difficulty and expense of reducing its analog data. This subject is dealt with separately in another section of this report.

Peripheral equipment such as vacuum pumps, helium gauges, tape recorder, etc. all are operational.

B. Laboratory Equipment

The construction of a test console for infrared detectors, radiometers and spectrometers has been completed, although some improvement in the final display system is planned. The console has already been used for evaluating the response time of a number of radiometers for field use.

The laboratory filter wheel spectrometer is partially dissembled awaiting the installation of a 4" Cassegrain telescope and a new immersed thermistor detector kindly furnished GFE by W. Hovis (GSFC). We have high hopes of this instrument becoming the'workhorse' for laboratory work in the not too distant future. Its compietion is also important to the development of new data reduction programs.

V. TRAVEL

In the six months covered by the report, fifteen man trips were made. These can be broken down as follows:

	Man Trips
Instrumentation oriented	2
Professional Meetings	2
Field Trip in support of NASA/MSC aircraft	2
Field trips to gather basic data	2
To NASA/MSC in support of aircraft and spacecraft programs	7

(The instrumentation trips were necessitated by the failure of our CuGe detector)

The visits to MSC were all at the request of MSC personnel. Although these requests were only occasionally in writing, they were more frequently made by telephone. As we feel supporting NASA personnel at MSC is an important part of an experimenter's responsibility, and is essential to the successful development of spacecraft experiments, no valid request for participation in MSC planning meetings has so far been turned down. The cost of these trips to MSC was $4962 (including salaries, overhead and expenses).

VI. FISCAL! DETAILS - NGR-05-020-115

17 MONTH COSTS

I. LABOR			
A. Stanford			
Payroll	$ 52,268		
Staff Benefits	5,130		
Overhead	24,043		
		81,441	
B. Outside Support			
Computer Programmer Support	6,690		
Lockheed Engineering* Support	6,467		
(*See IIC below)		13,157	
TOTAL LABOR			94,598
II CAPITAL EQUIPMENT (incl. major commitments)			
A. Laboratory & Field Equipment			
Lab. Equipment (Code 421)	6,195		
Field Equipment (Code 425)	10,583		
Optical Equipment (Code 425)	2,750		
Various Equipment	794		
		20,322	
B. ~~C.V.F. Spectrometer (Code 428)~~	7,148		
Commitment Santa Barbara Res. Center	3,865		
Commitment Develco	4,800		
	15,813		
C. New Optics for SG-4 (LMSC)	5,000		
D. Others (Office Equipment + Auto) (420/424)	1,119		
		21,932	
			42,254
III. TRAVEL	7,601		7,601
IV. EXPENDABLE MATERIALS			
Exp. Materials & Supplies (611)	4,328		
Cryogenics (681)	2,447		
Computer Center (641)	6,207		
Xerox and Photo (645)	2,581		
Telephone (650)	2,326		
Office Supplies (610)	1,398		
Books and Publications (612)	800		
Equipment Maintenance (Truck)(622/624)	814		
Report Costs (630)	604		
Postage and Freight (613)	433		
Minor Equipment (620)	228		
Insurance, Physical Plant (620)	484		
	22,650		22,650
TOTAL			167,103
V. LESS COST SHARING			- 4,755
TOTAL COST TO 3/31/67 (incl. major commitments)			162,348

TABLE XIV

DETAILED ALLOCATION OF RESEARCH EFFORT
(man months)

	PROFESSIONAL	SUBPROFESSIONAL	SECRETARIAL	GRAND TOTAL
Reports Publication Writing	3.17	.07	1.44	4.68
Meetings Travel				
MSC	1.52	-	.19	1.71
Elsewhere	.59	-	.20	.79
	2.11	-	.39	2.50
Field Data				
USDA (11)	.70	1.38	-	2.08
Field Spectra (1-10)	1.70	.55	-	2.25
New Field Data (17-20)	1.68	.28	.12	2.08
	4.08	2.21	.12	6.41
Laboratory Studies				
New Lab Data	.38	.09	-	.47
Rock Modes	.56	.05	-	.61
New Lab Spectra	.38	.09	-	.47
USGS Spectra	.06			.06
	1.38	.23	-	1.61
Equipment				
Repair	.72	-	-	.72
Manufacture	.72	-	-	.72
Calibration	.37	-	-	.37
Purchase	75	-	.75	.75
	1.81	-	.75	2.56
General Office Operation	-	-	3.80	3.80
Remote Sensing Course	2.15	.67	1.00	3.82
TOTALS	13.09	3.18	7.50	25.38

a

B. EXPENDITURES OVER $1000

The following new expenditures over $1000 were incurred during this reporting period.

1. I.S.C.O. $2277. Purchase of a visible/near I.R. spectroradiometer for laboratory studies.
2. Develco, Inc. $4800 for studying the feasibility of using upgraded thermistor detection systems (instead of cooled detectors) in field/aircraft/spacecraft spectrometers. Also, delivery of one detection system, associated amplifier and test data.
3. Santa Barbara Research Company ($3865 committed) for spare Cu:Ge detector for the SG-4 field spectrometer. The absence of such a spare caused nearly 12 months slippage in the program in the recent past.

DISTRIBUTION LIST

Adams, John	1
Alexander, R.	1
Alexiou, A.	2
Algranti J.	1
Badgley/Seitz	2
Barath, F.	1
Barringer, A.R.	1
Burke, Harlan	1
Casey, F.W. (MSC)	1
Childs, Leo	1
Christiansen, Bob	1
Cochran, C.D.	1
Colwell, R.	1
Conel J.	
Dickerson (MSC)	1
Eichmyer, Ike	1
Fary, Raymond	1
Fischer/Carter	2
Friedman, Jules	1
Gault, Don	1
George, Ted	1
Gerlach, A.	1
Grant, Chas. M. (MSC)	20
Hicks, E. (MSC)	1
Heller, G. (Huntsville)	1
Holmes, Roger	1
Hembree (Huntsville)	1
Hovis, Warren	1
Hemphill, Bill	1
IITRI/W. Vest	1
Kooyers, Gerald	1
Lintz, Joe	1
Lowe, Don	1
Marble, Duane	1
McDonald, Robert	1
Malloy, Martin	1
Marlatt, W.	1
Moxham	1
Myers, V.	1
Morgan, Winnie (NASA)	5
Moore, R.K.	1
Nordberg, Wm.	1
Orr, D.	1
Park, Arch	1
Patterson, Jere	1
Peake, W.H.	1
Quade, J.	1
Robinson, C.	1
Reeves, R.	1
Shay, R.	1
Shorthill, R.	1
Simonett, D.	1
Staelin, D.	1
Sabels, Bruno	1
Sabins, F.	1
Stanford Contracts Office	1
Scheps, B.B.	1
Snavely, Parke	1
Skibitze, H.	1
Toy, H.	1
Tiffany, Lyle	1
Whitten, E.H.	1
Watson, K. (USGS)	1
Wallace, Robert	1
Zeitler, Ed	1
Seibert, W. (USGS, W.D.C.)	1

APPENDIX A

STATISTICAL ANALYSIS OF SPECTRAL MATCHING

Suppose we wish to assign an object to one of several well-defined classes, e.g., we wish to say whether a particular rock is granite, basalt, or pumice. This is no problem if the known characteristics of the rock include those which are used to define the classes. However, if the known characteristics are not the defining ones then it may not be possible to make an assignment with certainty, for example, this would be the case if all we knew about the rock was its color index, or perhaps its mission spectrum over some wavelength band,

Let us look further at the case where our knowledge consists of an emission spectrum, (call it s), which is of particular interest here. Since the emission spectra are not what is used to define the three rock classes, our s may correspond to any kind of rock. However, if the emission spectrum is to have any value in making assignments, it will be more probable that our s corresponds to a granitic rock say than to either of the other two classes, and we therefore will make the assignment granite.

An interpretation of the word "probable" is in order. Loosely speaking, suppose we had taken spectra of every bit of rock in the region of interest, Some of these spectra (say 1000 of them) will be very nearly like the spectrum s. Of these 1000 s-spectra suppose 750 correspond to rocks in the granite class, 200 in the pumice class, and 50 in the basalt class. Hence, if we looked at a spectrum s and called it granite we would have a 75% chance of being right,

Now we introduce some convenient notation. Let $p_G(s)$ denote the probability that a given spectrum s corresponds to a rock in the granite class, Similarly, let $p_B(s)$ and $p_P(s)$ denote the probabilities that this s corresponds to a rock in the basalt and pumice classes, respectively. Then $p_G(s) + p_B(s) + p_P(s) = 1$. Finally, let $P(s)$ denote the probability that s will be correctly classified; then $P(s)$ is the largest of the numbers $p_G(s)$, $p_B(s)$ and $p_P(s)$. In the example of the last paragraph $p_G(s) = 0.75$, $p_B(s) = 0.05$, $p_P(s) = 0.20$ and $P(s) = 0.75$.

Suppose we knew the probabilities $p_G(s)$, $p_B(s)$, and $p_P(s)$ for every possible spectrum s. Then we would know how to make the best possible (most probable) assignments no matter what spectra we encounter, and we would know in each case the probability of a correct assignment. Note, that even in this state of "perfect" knowledge we would still be making assignment errors; however, our error rate would be the minimum possible for the particular wavelength band and the particular rock classes we had chosen. For example if we had n spectra to assign, say $s_1, s_2, \ldots s_n$, then the expected minimum error rate would be $1-1/n \sum_{i=1}^{n} P(s_i)$.

In general, our knowledge about the probabilities $p_G(s)$, $p_B(s)$, and $p_P(s)$ will not be precise. Instead, we will have good or not-so-good estimates of these probabilities based on an examination of a number of sample spectra; assignments to a rock class would then be based on the maximum of the estimated probabilities. This results in an assignment error rate higher than the minimum possible rate. For example, by using our estimates we assign the n spectra $s_1, s_2, \ldots s_n$ to the rock classes $c_1, c_2, \ldots c_n$ respectively (where each c_i is either G, B, or P), then the expected error rate is $1-1/n \sum_{i=1}^{n} p_{c_i}(s_i)$; this exceeds the minimum possible rate by the amount $1/n \sum_{i=1}^{n} P(s_i) - p_{c_i}(s_i)$. Let $\hat{p}_G(s)$, $\hat{p}_B(s)$, and $\hat{p}_P(s)$ be our estimated probabilities, and let $\hat{P}(s)$ be the largest of these; then an estimate of the expected error rate for the n spectra is given by $1-1/n \sum_{i=1}^{n} \hat{P}(s_i)$.

We now examine a method for obtaining the probability estimates $\hat{p}_G(s)$, $\hat{p}_B(s)$, $\hat{p}_P(s)$ for every possible spectrum. The first step is to cut the problem down to size in several ways by making assorted assumptions about the "true" probabilities. By doing so it will be possible to obtain relatively simple estimation methods which are reasonable for the restricted problem and which do not appear unreasonable if our assorted assumptions are not strictly valid.

The first assumption we make is that all the information in a spectrum is contained in a specified finite number of wavelengths, e.g. the wavelengths 7.8 microns to 13.0 microns at intervals of 0.1 microns. This says that if two spectra coincide exactly at those 53 wavelengths then the three class probabilities associated with the first spectrum are always the same as those for the second spectrum. This assumption makes our problem finite-dimensional and permits the use of ordinary multivariate statistical methods. The heights of a spectrum at the specified 53 wavelengths will be denoted by $h_1, h_2, \ldots h_{53}$ respectively.

Again, suppose we had spectra of every bit of rock in the region of interest, and let us confine attention to all those corresponding to granite, say. In general the values of h_i (fixing i) will bedifferent for different spectra even though they are all granite. In this way a joint frequency distribution of h_i values is created for the given rock class granite. Let $f_G(h_1, h_2, \ldots h_{53})$ denote this joint frequency distribution. Similarly, we can create the frequency distributions $f_B(h_1, h_2, \ldots h_{53})$ and $f_P(h_1, h_2, \ldots h_{53})$ for the other rock classes-basalt and pumice.

Of course we will never be able to know f_G, f_B, and f exactly, but if we did, then we could assign an arbitrary spectrum s to a rock class in an optimum way and know its misassignment probability. Suppose the spectrum s^o in question had heights $h_1^o, h_2^o, \ldots h_{53}^o$; the frequency function having the largest value at this configuration of heights is the one corresponding to the rock class to which the spectrum in question should be assigned - provided no particular class is favoured a priori, This follows because it can be shown that the probabilities $p_G(s^o)$, $p_B(s^o)$, and $p_P(s^o)$, as defined earlier are proportional to the values of $f_G(h_1^o, h_2^o, \ldots h_{53}^o)$, $f_B(h_1^o, h_2^o, \ldots h_{53}^o)$, and $f_P(h_1^o, h_2^o \ldots h_{53}^o)$. The proportionality constant is the reciprocal of $f_G + f_B + f_B$ evaluated at $(h_1^o, h_2^o, \ldots h_{53}^o)$.

Therefore, it would be reasonable to try to estimate the joint frequency distributions for the three rock types based on sample spectra taken from the region of interest. In general, this is a hopeless task unless we make some assumption about the shapes of the three frequency distributions f_G, f_B, f_P. For example, we might assume that f_G, f_B, f_P are each multivariate Gaussian distributions having a common covariance matrix, Roughly speaking this says that the three distributions have identical bell-shapes (in 53 dimensions) and differ only in that they are centered at different points.

The assignment rules derived from this assumption have given an indication of good performance in trial runs, but other assumptions may well lead to rules with better performance. For now we will stick with Gaussian distributions mainly because they afford us mathematical and presentational simplicity. The problem of estimating three multivariate distributions is thus reduced to the estimation of a covariance matrix (call it S) and three center locations or means (call them H^G, H^B, H^P). We will be able to estimate probabilities and make assignments once we have estimates of S, H^G, H^B, and H^P.

Now suppose we have a certain number of sample spectra known to be granites and chosen randomly from the region of interest. Let h_i^G denote the height at wavelength i <u>averaged</u> over all these known granite spectra, then $(h_1^G, h_2^G, \ldots h_{53}^G)$ is a reasonable estimate of H_G. Also let s_{ij}^G denote the covariance between the i-th and j-th wavelengths using the known sample granite spectra. Then the 53 x 53 matrix of all possible such covariances provides a reasonable estimate of S. Similarly a sample of spectra known to be basalts will provide us with an estimate of H^B and of S, and similarly for pumice. Notice we get three estimates of S, but these estimates should be pooled in the usual way.

Returning now to an unknown spectrum $s^o = (h_1^o, h_2^o, \ldots h_{53}^o)$, we can write down the density f_G of the granite distribution evaluatedat this configuration of heights - under the Gaussian assumption and using the estimates of the last paragraph. Similarly we can use our estimates to evaluate the basalt and pumice density functions at this configuration s^o. We will then approximate the optimum assignment by assigning s^o to that rock class having the largest estimated density at s^o.

The logarithms of the three density values are

$$\log f_G(s^o) = -\frac{1}{2} D_G^2(s^o) - \frac{1}{2} \log [\det S] - \frac{3}{2} \log 2\pi$$

$$\log f_B(s^o) = -\frac{1}{2} D_B^2(s^o) - \frac{1}{2} \log [\det S] - \frac{3}{2} \log 2\pi$$

$$\log f_P(s^o) = -\frac{1}{2} D_P^2(s^o) - \frac{1}{2} \log [\det S] - \frac{3}{2} \log 2\pi$$

where $D_G^2(s^0) = \sum_{j=1}^{53} \sum_{i=1}^{53} s^{ij} (h_i^o - h_i^G)(h_j^o - h_j^G)$, s^{ij} is the ijth element of the inverted covariance matrix S^{-1}, and $D_B^2(s^o)$ and $D_P^2(s^0)$ are the same as $D_G^2(s^o)$ above with the superscript G replaced by B and P respectively. The quantity $D_G(s^o)$ is sometimes called the Mahalanobis distance (M-distance) between the spectrum s^o and the center H^G of the distribution of granite spectra.

It follows that the rock type whose density value is largest at the configuration s^o is the one whose central value has the smallest M-distance to s^o. In the case that no rock type is favored a priori, the probability that the spectrum s^o is a granite can now be estimated by

$$(1)\quad p_G(s^o) = e^{-1/2\, D_G^2(s^o)} \Big/ \left[e^{-1/2\, D_G^2(s^o)} + e^{-1/2\, D_B^2(s^o)} + e^{-1/2\, D_P^2(s^o)} \right].$$

Similarly the probabilities $p_B(s^o)$ and $p_P(s^o)$ are estimated by replacing the subscript G in the numerator by B and P respectively.

Until this point the problem of assignment has been viewed as 53-dimensional, inasmuch as a spectrum was represented as a point with 53 eo-ordinates $(h_1, h_2, \ldots h_{53})$ - the heights of the spectrum at each of 53 chosen wavelengths. But regardless of the number of wavelengths chosen, the problem is really only two dimensional in the following sense: there exist pairs of pseudo-variables (let v_1 and v_2 be such a pair) which are linear combinations of $h_1, h_2, \ldots h_{53}$, say

$v_1 = \sum_{i=i}^{53} c_i h_i$ and $v_2 = \sum_{i=i}^{53} c_i h_i$, with the property that

$$(2) \qquad \begin{aligned} (v_1^o - v_1^G)^2 + (v_2^o - v_2^G)^2 &= D_G^2(s0) \\ (v_1^o - v_1^B)^2 + (v_2^o - v_2^B)^2 &= D_B^2(s0) \\ (v_1^o - v_1^P)^2 + (v_2^o - v_2^P)^2 &= D_P^2(s0) \end{aligned}$$

where v_1^G and v_2^G are the average values of v_1 and v_2 taken over all the sample granite spectra, v_1^B, v_2^B, v_1^P, v_2^P, are defined similarly, and v_1^o and v_2^o are the values of v_1 and v_2 computed for the spectrum so to be assigned.

In other words, if v_1 and v_2 are taken as the axes of a two-dimensional plot, then the-M-distance from s^o to the center of the granite distribution in 53-space is the–same as the ordinary Euclidean distance from (v_1^o, v_2^o) to (v_1^G, v_2^G) in ?-space. This is an especially useful fact for diagrammatic and representational purposes. For example, since probabilities and M-distances are related monotonically as in (1), it follows that the contours of equal probability in (v_1, v_2) - space are concentric circles radiating from each of the three rock-type means (v_1^G, v_2^G), (v_1^B, v_2^B) and (v_1^P, v_2^P), furthermore, the locus along which any two rock types are equally probable is the perpendicular bisector of the line joining the corresponding means, and the three such lines will therefore meet in a point at which all three rock types will be equally probable.

The variables v_1, and v_2 are sometimes called canonical variables. The fact that we could reduce the original 53 variables to two canonical variables depended on all our earlier distributional assumptions and the fact that we had three rock types. In general, if there are k rock types, then we can reduce to k-1 canonical variables, provided k is not larger than the number of original wavelengths used. Note that, regardless of our distributional assumptions, we can find a v_1 and v_2 such that the equivalence (2) holds, but formula (1) relating probabilities and M-distance holds only under the assumption of Gaussian distributions.

a

We havn't yet said how to find a pair of canonical variables other than that v_1 and v_2 are two linear combinations of the amplitudes of a spectrum at the 53 specified wavelengths. Sufficient to say here that to find the coeffieients of these linear combinations, we need the solution of an eigen-value problem, which can be routinely performed on a computer.

Even though the method of canonical variables allows us to represent the assignment problem and its results in two dimensions, we still need to measure any spectrum on all 53 of its wavelengths in order to compute the values of v_1 and v_2. The number of "participating" original variables is not reduced by this analysis. If we want to cut down the number of wavelengths used, say to pick the best 10 out of 53, then one would need to do the preceding analysis with all possible sets of 10 wavelengths and see which came out best. This can be quite laborious, even on a computer, but *ad hoc* approximate methods have been built into some computerized versions of the analysis, which seem to pick a good set of wavelengths (e.g. BMD07M) though not necessarily the best set. In any event, the reduction in the number of wavelengths looked at has nothing to do with the representational reduction afforded by using canonical variables.

Up to this point it has always been assumed that a spectrum s^o to be assigned must necessarily be one of the three rock types for which sample spectra were available. In this framework it is not possible to say that s^o is none of the three named types. This may or may not be disturbing. If the M-distances from s^o to the three rock type means are all quite large there is a temptation not to force an assignment, and this may indeed be sound practice. This may be formalized by saying that all of the three rock types will be rejected of the smallest M-distance to s^o is greater than 4.0, for example. Note, however, that such a decision is outside the conceptual model of our analysis; even if the M-distance to a particular rock type mean is large, the probability for that rock type may still be high if the other M-distances are even larger.

Finally, we look at the case where the three rock types are not equally likely a priori. This would be the case if we had information of the type: the proportion of the region covered by granite is π_G 'that covered by basalt is π_B, and that covered by pumice is π_P (where $\pi_G + \pi_B + \pi_P = 1$). Then, the assignment probabilities are no longer given by formula (1). The appropriate modification is

$$P_G(s^o) = \pi_G e^{-1/2\, D_G^2(s^o)} \Big/ \left[\pi_G\, e^{-1/2\, D_G^2(s^o)} + \pi_B\, e^{-1/2 D_B^2(s^o)} + \pi_P e^{-1/2 D_P^2(s^o)}\right].$$

REPRINT FROM: Stanford Today, Series I, No. 17, October 1966, Stanford University.

Remote Sensing: Vision Beyond Sight

The day is coming when intricate sensors aboard airplanes and satellites will explore for oil, minerals, and fish; spot forest fires and disease in crops; or map the geology of the moon and planets.

by RONALD J. P. LYON and ROGER S. VICKERS

MAN HAS ALWAYS used remote sensing in a primitive form. In ancient times he climbed a tree, or stood on a hill and looked and listened, or he sniffed for odors borne on the wind. In fact, taste and touch are the only ways man can live within his environment *without* remote sensing.

The extension of our natural remote sensing capabilities, such as we now do with complicated devices in aircraft and spacecraft, is really not a new concept, but is more correctly described as a refinement of the old art of reconnaissance. The first aerial photograph, for example, was taken in 1858 from a balloon hovering over Paris.

In the last few years our power of seeing—the sense that leads to most new knowledge—has been pushed far and fast by today's sophisticated research. One facet of this research involves the spectroscopic study of radiant energy. Again this is a modern development which relies on long-established concepts. The idea that radiant energy travels through space or matter in waves was put forward by a British physicist, James Clerk Maxwell, in 1864, and by **1900** the full spectrum of wavelengths—from the exceedingly short gamma rays on through X rays, ultraviolet, visible light, infrared, microwave, and the very long radio and audio frequencies—had been identified. Use of the spectrometer, one of the most powerful tools of the scientist, began in 1666 when Newton split a beam of sunlight with a prism into a band of spectral colors. The prism or the more modern diffraction grating, with telescopic and measuring attachments, is the basis of most spectrometers used today.

The last few years have seen advances in remote sensing, particularly in spectral analysis, such that they have been used first in telescopes, then in airplanes, and now in orbiting satellites. In addition, powerful computers can now be applied to the analysis of the data received. Remote sensing has advanced greatly since Galileo and now identifies a whole new regime of modern geoscience, in this and many related fields.

The technological advances in this field were made to a large extent by and for the armed services, and it is only in the last two or three years that much of this equipment has been released from security and the new data made available to the general body of scientific users. Side-looking radars, for example, which are probably the most exciting development for the geoscientist, for years were a closely guarded project. Imagery of a resolution suitable for geological use is now available in an unclassified form.

A BASIC **PROBLEM** still remains for the civilian geoscientist. For years the military-sponsored development has aimed at the discrimination of a *target* (persons, tanks, vehicles, buildings, armament, etc.) against the unwanted clutter of *"background."* The geoscientist now

a

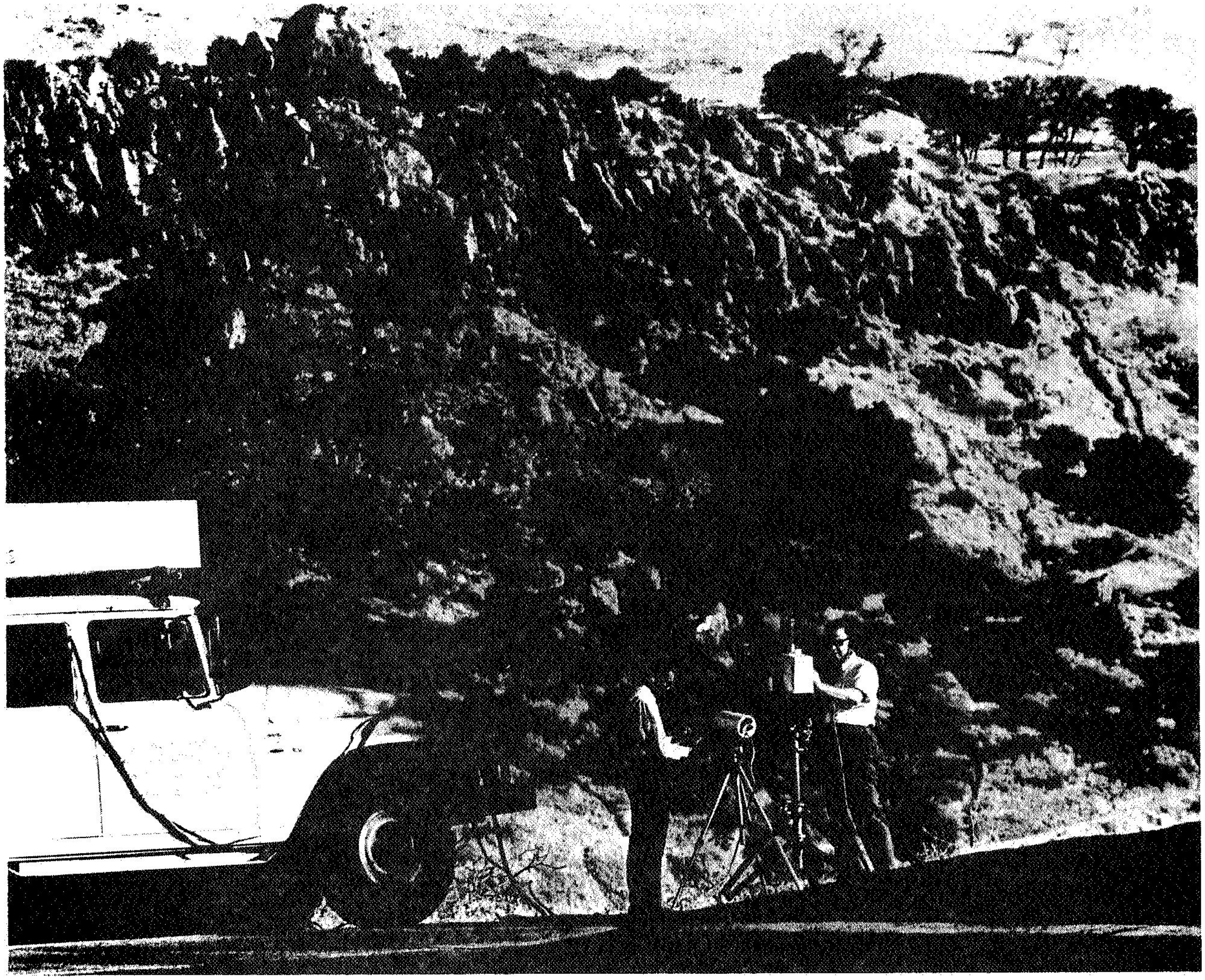

COMPOSITION OF THE ROCKS in the distance will be measured by the remote sensing equipment being set up by the authors, Ronald J. P. Lyon (right) and Roger S. Vickers. The tubular instrument is an infrared radiometer for measuring broad band intensity of the heat emitted by the rocks. The boxy one is an infrared spectrometer for determining narrow band intensity. Equipment in the truck records the two readings on tapes which, back in the laboratory, will be matched with "library spectra" of known rocks. The equipment is being adapted for use in airplanes and later in spacecraft for orbiting the earth, moon, and other planets.

seeks discrimination *within* this clutter. He really wants to understand the background. He needs rock and soil classifications, tree types and lumber volumes, and moisture content as well as areal coverage of snow. The key to this lies in the fact that no two types of rocks, vegetation, or material of any kind have identical spectral distribution of radiation, because of differences in their chemical composition, surface irregularity, degree of consolidation, and moisture content. These spectral differences can be recorded by electromagnetic remote-sensing devices and then matched by computer with taped "libraries" of the known spectra of various materials, a process similar to fingerprint identification.

Imagine the questions one could now ask of a remote sensing system mounted in a spacecraft in polar orbit, scanning from horizon to horizon and covering the entire globe every several days. For the first time one could arrive at a shipping count by location, an agricultural census with crop forecasts, traffic flow studies, air pollution monitoring, perhaps a count of tlie whale population of tlie world, or a monthly assessment of the water content of the world's snowfall during winter. Satellite observers could significantly reduce the loss in forest fires. Due to atmospheric haze and inversions, most forest fires burn an estimated 12 to 18 hours before they are located. It has been calculated that an "early warning" system could save some $32 million in the forestry system of the United States alone. These are but a few of the possible applications of the data.

GLOBAL COVERAGE in a significantly short period of time and on a repetitive schedule is one of the more exciting aspects of a satellite-borne remote sensing system. But there are many other aspects. In April this year the Department of Agriculture announced a satellite observational program of its own to determine the yield of crops, the distribution of various timbers, and the general state and vigor of farming throughout the world. In mid-September the Department of the Interior announced Project EROS (Earth Resources Observation Satellite) for 1969. EROS would be a polar-orbiting satellite gathering geologic, geographic, and hydrologic data.

The extension of remote sensing by spacecraft, from the earth to the moon and then to other planets, is a natural step. Radiometers to measure the apparent temperatures of Venus have already been flown on the Mariner II spacecraft. Surveyor I and the several Rangers did a sensational job of sending back moon photographs, although, being data from the visible wavelength range of the electromagnetic spectrum, these photographs did not tell us anything about the composition of the rocks of the moon. As part of the forthcoming Apollo program, infrared spectrometers in satellites orbiting close to the moon are expected to relay back extensive chemical information on terrain as part of the manned landings now projected for 1968. After man has been on the moon, the orbiting spectrometers will continue this work, applying in widening circles the information which the astronauts found within their limited radius around the spaceship.

One problem will be to find enough people to interpret the data which will come flowing out of these satellite programs. It is not widely known that between 1960 and 1963 over 210,660 photographs were transmitted by TIROS I–IV, that Nimbus **1** and **2** have transmitted 42,000 photographs in only 52 days of operation, or that Surveyor I transmitted over 11,000 photographs of the lunar surface. And this is only the photographic data! It is easy to see that we are liable to be engulfed in data, tapes, and telemetered photographic images. The **U.S.** Geological Survey estimates that 300 more geoscientists are needed by 1969 to interpret the lunar pictures alone. Probably 700 would be needed in the five years after the EROS launch in 1969. Several universities, Stanford among them, are now offering courses in these new fields of geoscience. One must remember, however, that by 1969, when remote sensing will have moved from the experimental to the operational phase, today's freshman will be only a junior. He would not have his Ph.D. until 1973 or 1974. Clearly the understanding of remote sensing must be extended by exposing greater numbers of students to the subject as early as possible. To this end we are now teaching "Remote Geologic Sensing" as a new course in geophysics at Stanford.

REMOTE SENSORS have been built to operate in all regions of the electromagnetic spectrum. (See Figure 1.) To the geoscientist they have one common capability, that of being able to discriminate between differing characteristics of the terrain. Some wavelength bands enable certain identifications to be made better than others, while other bands contain specific information (e.g., chlorophyll in new leaf and plant growth is readily apparent at 0.7 microns).

Most important of these are variations in the penetration below surfaces. (See Figure 1.) At the short wavelength end of the spectrum, gamma ray detectors can estimate the abundance of natural (and man-made) radioactive elements to some depth. At the other extreme bursts of radio frequency energy are being used to determine subsurface layering in parts of the earth's surface, and the conductivity of buried ore deposits. Between these two extremes, however,

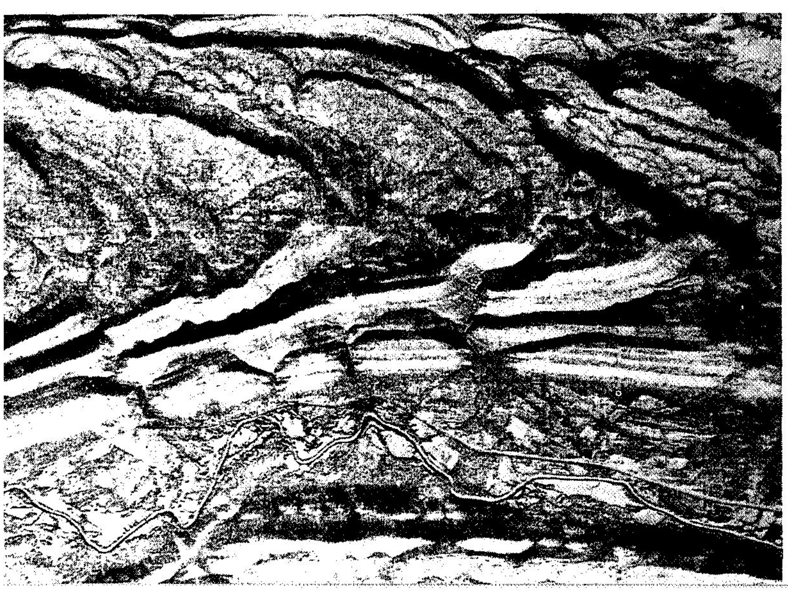

THE **STRUCTURE AND FOLDING** of the earth's surface is strikingly revealed by a side-looking radar image taken from a **NASA** plane flying at medium altitude. Remote sensing equipment operating in the radar wavelength cuts through clouds, rain, smog, superficial ground cover, and other obstructions to give essentially an image of the bare ground. It provides an ideal all-weather mapping system. Side-looking radar, recently released from security by the military, looks from the plane toward the horizon rather than straight down. This image is typical of the sophisticated signaling process systems in use today.

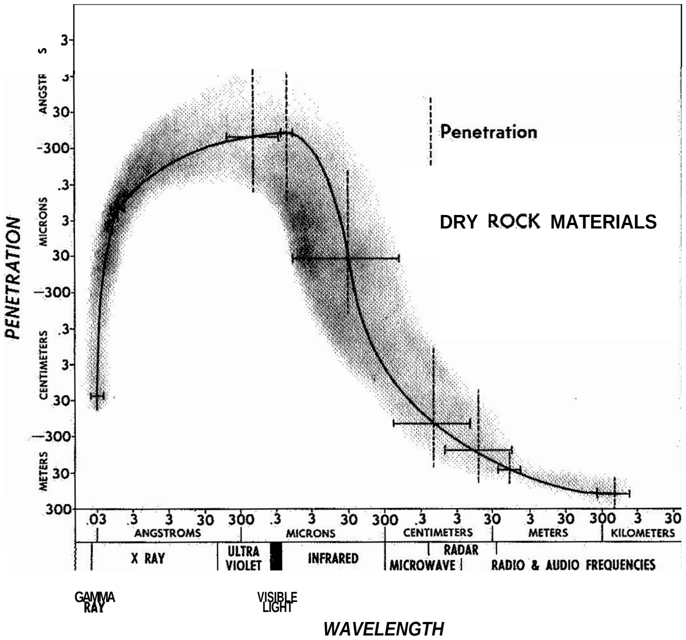

FIGURE 1. The penetration below a surface which a remote sensing detector can achieve varies greatly with the wavelength being used. As this curve for "dry rock materials" indicates, the penetration decreases with wavelength until a point is reached where the wave is so short it is able to slip between the atoms of the material. The range in scale here is tremendous, from the familiar kilometer to the not-so-familiar Angstrom, 1/10,000,000,000th of a meter. The atomic nucleus is 1/100th of an Angstrom in diameter.

until one reaches at least the longer microwave region, remote sensing can only provide information from the top few microns of surface, and a micron is only one-thousandth of a millimeter. A study of Figure 1 quickly identifies this problem. If one relies upon only one instrument, the choice must be made between the ability to determine chemical and mineralogical compositions of the infrared wavelength or the deeper penetrability of radar without such specificity.

The visible region of the spectrum is probably the most developed for remote sensing. Even *so,* complete coverage of the earth's *land masses* (58 million square miles) at a scale of 1:60,000 still requires 800,000 frames of film, and the continental United States 41,500 frames. Local photographic coverage at high resolution and low altitudes has been possible for **20** years or more. The trend is now toward high-resolution, high-altitude systems taking imagery in several spectral bands. Several other types of imaging devices have been flown in the last twelve months which simultaneously scan in as many as 20 different bands, from ultraviolet out into the middle infrared wavelengths, producing simultaneous images in each. When these images are compared it is possible to select those bands which provide maximum differentiation between the terrain types of interest. The photogeologist now has to be a spectroscopist as well. The same principle **is** being studied by agriculturists and foresters, and is being investigated as a method of detecting life on other planets.

The middle infrared region is, at present, probably the most useful band available to the geoscientist because it can be used for producing thermal images of terrain, for deducing apparent temperatures, and for discriminating between different terrain types (see accompanying text, The Stanford Program). It differs from conventional photography in that instead of using ***reflected*** solar energy as the source of the image, it uses the thermal energy ***emitted*** by the terrain; that is, it produces an image which differentiates between bodies of different temperatures or emissivities. The same technique is now being used in hospitals for detecting breast cancer, blood clots, and other internal disturbances which give rise to anomalous surface temperatures.

An airborne combination of infrared spectrometers, imagers, and the longer microwave equipment should be used increasingly for exploration by petroleum and mining industries. However, even these sets of apparatus are not going to be the magic black boxes to solve the prospector's task of finding El Dorado. These techniques help select the best places for the prospector to look, to decrease his cost of covering vast areas. For example, if the airborne instruments identify serpentine rocks, this would

THE AUTHORS, both of whom conduct research in remote sensing in the School of Earth Sciences at Stanford. Professor Lyon (left) came from his native Australia to obtain the Ph.D. in structural geology at UC-Berkeley in 1954. He was with the Kennecott Research Center in Salt Lake City, Stanford Research Institute, and the NASA Research Center at Moffett Field before joining the faculty in 1965. Dr. Vickers worked for three years in the NASA remote sensing program at the research institute of the Illinois Institute of Technology before coming to Stanford last July. He was educated through the doctorate in physics at University of Southampton in England.

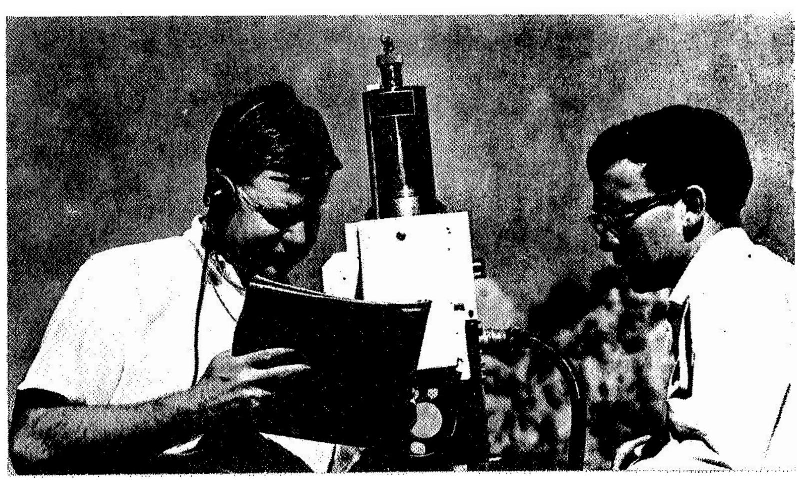

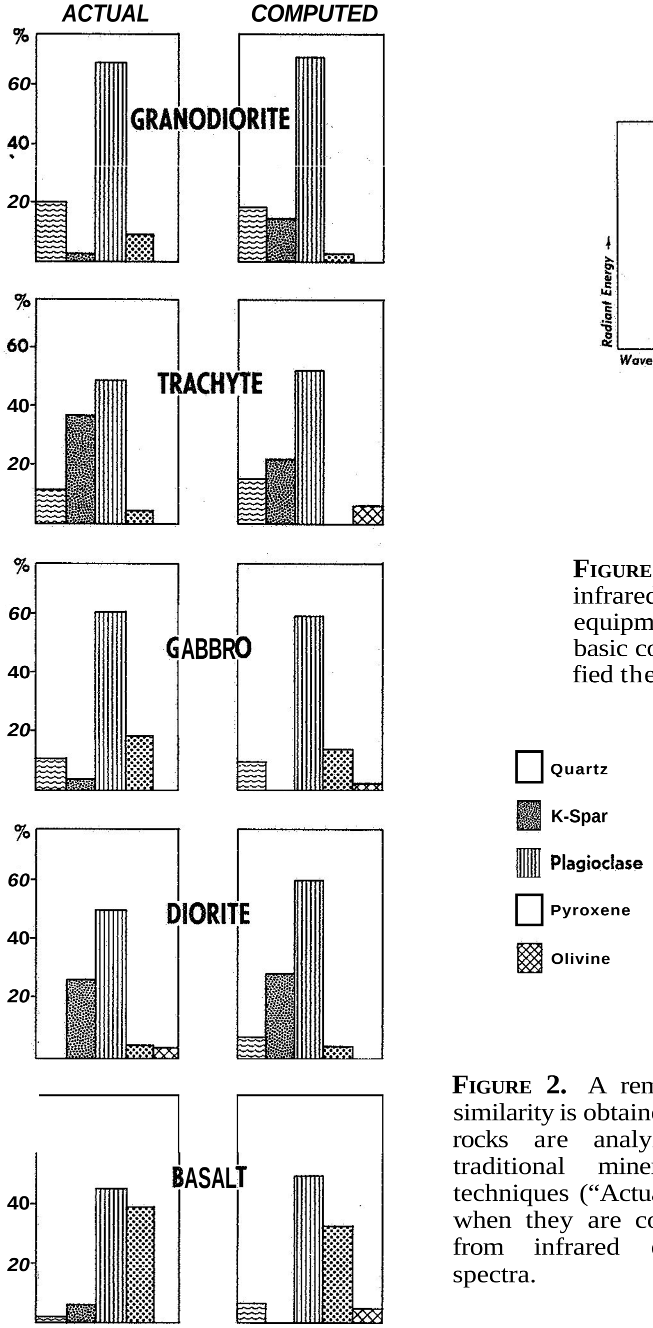

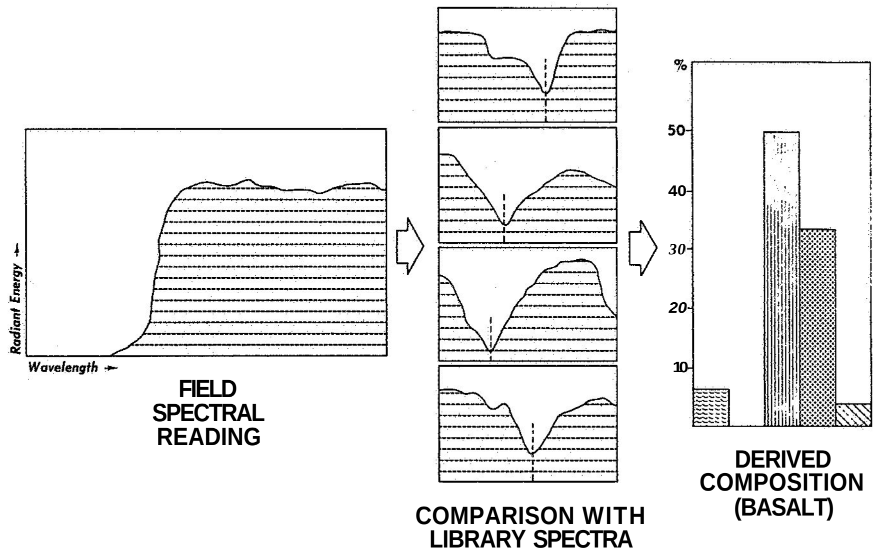

FIGURE 3. A diagrammatic representation of the steps in compositional analysis by infrared remote sensing. Data obtained by the Stanford RSL in the field with mobile equipment are fed into the computer for comparison with the library profiles of five basic components of dry rock materials. In this example the quantities of each identified the material as basalt.

FIGURE 2. A remarkable similarity is obtained when rocks are analyzed by traditional mineralogical techniques ("Actual") and when they are computed from infrared emission spectra.

be a good clue to look for the presence of chrome or nickel; certain granite host-rocks would indicate copper deposits; etc.

A technique in the radio frequency region has been developed to measure the conductivity of terrestrial surface and subsurface materials from aircraft altitudes. It was used recently in a survey for magnetite ore in the Gulf of Bothnia in the Baltic Sea. The remote sensing package (radio frequency, magnetics, and gamma ray) predicted commercially valuable ore in a given location, and gave its probable depth as 290 feet. Subsequent drilling revealed a large tonnage of medium grade iron ore lying beneath 75 feet of salt water and 170 feet of soil.

ADVANTAGES which remote sensing can have over field geology in certain situations become obvious. One is that greater areas and inaccessible places can be covered. A more subtle one is that the field man must infer from surface indications what lies below. Although much developmental work remains to be done, remote sensing can in many cases truly "see" material underground by reading its electromagnetic signature. In the case of the moon, this is especially pertinent where the surface rocks have a demonstrably low electrical conductivity.

Remote sensing can be used in many ways for mapping the earth—its land and water outlines, topography, vegetation, transportation systems, population, economies—and realistically we think it will have its maximum utilization in this area. Agriculture also stands to benefit. In shorter wavelengths we can determine the difference between healthy and diseased plants. In the "near infrared wavelengths we can even tell the types of crops by their spectra. Reconnaissance planes could watch over large plantations in tropical areas, telling the growth status of the produce or giving early warning of disease so that an epidemic could be controlled. Fishing nations could be aided by "maps" of plankton in the sea and upwelling ocean currents that would guide their boats to the most productive areas.

Prospective benefits from remote sensing such as these—the replenishment and conservation of natural resources, increases in the world's food supply, help for underdeveloped nations—are as exciting and important in their way as the race to the moon and other missions in space.

The Stanford Program

SCIENTISTS in the Remote Sensing Laboratory of the School of Earth Sciences at Stanford are developing infrared techniques for analyzing the composition of terrestrial and lunar soils. Their current objective is to be ready for the second generation of Apollo capsules which will soon be orbiting the earth and the moon, probably in **1969–70.** Dr. Ronald **J. P.** Lyon, the director of this study, is associate professor of geophysics, and has been the recipient of NASA funding for this work since **1961.** The work, which he originated at Stanford Research Institute, was further advanced as a field project while Dr. Lyon was at NASA Ames Research Center at Moffett Field.

The Remote Sensing Laboratory's basic approach is one developed by Dr. Lyon over the past ten years in infrared mineralogical research for mining companies — measuring the spectrum of *emitted* heat directly radiated from rocks rather than measuring the sun's radiation *reflected* off the rocks. The chemistry of any one type of rock will cause it to emit heat energy in a different way from any other type. For silicate rock minerals — by far the most common of all on the earth's surface — the fundamental vibration of the silicon-oxygen bond at **9–10** microns modifies the spectrum of emitted energy in a unique and predictable manner. An infrared spectrometer is used to record the spread of heat radiation as a wavelength pattern which can be identified by comparing it with "library spectra" stored in a computer.

In the Remote Sensing Laboratory, scores of rock samples were analyzed first by traditional mineralogical means and then by computation from their infrared emission spectra. The similarity of results was remarkable. (See Figures 2 and **3.)**

Laboratory studies were followed by outdoor tests, using a self-contained infrared system mounted in a truck. The spectrometer can be operated up to **100** feet from the truck, either on the ground or in the air from a "cherry-picker" high-rising platform. Targets as far away as **1,000** to 2,000 feet from the spectrometer were "sensed and their infrared spectra recorded on magnetic tapes in the truck, at the rate of one spectrum every **30** seconds. Test sites in desert and Sierra locations were chosen because of their similarity to what is known or guessed about the surfaces of the moon and other planets. (For crop studies being conducted by Stanford for the Department of Agriculture, the mobile unit also recorded the infrared spectral responses of over 60 types of vegetables, fruit trees, vines, etc., at the UC-Davis campus.)

THE REMOTE SENSING LABORATORY group in the Stanford Department of Geophysics has a variety of talents. Left to right: Mel **A.** Kuntz, graduate student, mineralogist; Ronald J. P. Lyon, associate professor, geophysicist; Gary Ballew, graduate student, geologist; Roger S. Vickers, research physicist; and Paul Switzer, assistant professor, statistician. Gerald Kooyers (absent), consultant, is the computer programmer.

The Remote Sensing Laboratory group members are now working on application of the technique to aircraft operation. A new spectrometer is being built which will sweep the appropriate section of the infrared spectrum every sixth of a second, or once every 40 feet of forward motion of the aircraft flying at **175** miles per hour at 2,000 feet.

After the airplane tests will come adaptation of the equipment to the Apollo capsule. A considerable body of research is needed both in hardware and in pattern analysis techniques for spectral identification before this step can be taken. For a lunar-orbiting experiment the lack of an obstructive lunar atmosphere and the closeness of the Apollo orbit to the lunar surface are in the project's favor. Provided the "window" in the atmosphere (at the 8 to 13-micron wavelength) proves to be "clean" enough, the system developed for lunar study can also be used in spacecraft orbiting the earth. Regardless of its ultimate role in spaceflight, use of the spectral technique in aircraft for mapping the earth's geology is clearly in view.

s

No. 67-284

INFRARED SENSING FROM SPACECRAFT – A GEOLOGICAL INTERPRETATION

by

ROGER S. VICKERS and R. J. P. LYON
Stanford University
Stanford, California

AIAA Paper
No. 67-284

AIAA Thermophysics Specialist Conference

NEW ORLEANS, LOUISIANA / APRIL 17-20, 1967

1.06, 1.11, 11.20

INFRARED SENSING FROM SPACECRAFT - A GEOLOGICAL INTERPRETATION*

Roger S. Vickers and R.J.P. Lyon
Geophysics Department
Stanford University
Stanford, California

ABSTRACT

Most measurements of thermal radiation are based on an assumption that the body radiates as a blackbody, or at least that it has emissive efficiency which is invariant with wavelength. In other studies, spectral emissivities are found to depart significantly from even a graybody concept, in regions of marked interactions between the radiation and the molecular or crystalline structure. Plane parallel slabs of silicate glass and polished quartz show the "reststrahlen" effect to a high degree, as seen in the early work of McMahon. Recently, Stierwalt has shown a temperature dependence on emittance of some longer wavelength bands. Both of these regions have important relationships to geological studies. Using the 9-11 (and 18-25) micron "reststrahlen" band common to all solid crystalline or glassy silicate material, it can be shown that these are fundamental vibrations of the Si-0 bond when in tetrahedral coordination. It is germane to geological studies that silicates form most earth (and planetary) materials, and most significantly, that the exact wavelength of this vibration is modified by the metal at the secondary coordinating position. Iron silicate can thus be distinguished from alumino-silicate and, hence, "basic" rocks (basalts) from "acid" rocks (granite).

I. INTRODUCTION

In the last few years orbital experiments have provided an abundance of scientific data on the earth's surface, atmosphere and environment, and even on the nature of the lunar surface. Orbiting platforms can now maintain a world-wide coverage on a continuous basis, and have been used for experiments operating in all regions of the spectrum from gamma rays down to radio frequencies. In particular a large number of experiments have been flown in orbit operating in portions of the infrared spectrum. These experiments have mostly examined the earth's atmosphere, and to a lesser extent, the emission from its surface.

II. RADIOMETRY FROM ORBITAL ALTITUDES

Excellent examples of what can be achieved with infrared radiometers are provided by the successful Tiros and Nimbus programs. Data from satellite borne radiometers has to be interpreted with an appreciation for what is really being measured however. Planck's law states that the radiated intensity in a given wavelength interval from a blackbody is a function of its temperature only. In the real world, surface materials do not obey this law, even approximately, over many regions of the spectrum, and in addition, the atmosphere contributes absorption and emission characteristics of its own to any surface measurement.

The Nimbus' high resolution system operated from 3.4 to 4.2 microns, a region in which the atmosphere is relatively clear (See Fig. 1).

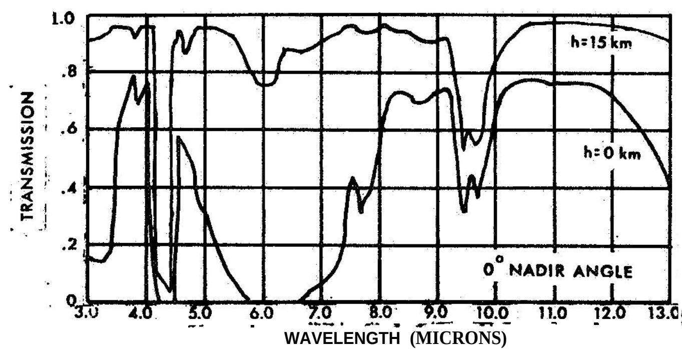

FIG. 1.

TRANSMISSION FROM OUTSIDE ATMOSPHERE
TO ALTITUDE h ABOVE SEA LEVEL
(After S. B. R. C.)

However, as demonstrated by Hovis[1], many surface materials have average emissivities significantly less than unity (0.7 - 0.9) and measurements from these materials may therefore be in serious error, if blackbody emission is assumed. This spectral region appears to be sufficiently accurate for surfaces such as water and heavy vegetation which form the majority of the Earth's surface cover. The errors in temperature data from Nimbus due to variatio n emissivity are discussed by variation i, and a similar analysis of errors in Nordberg[2] temperatures is performed by Burns[3].

* The research at Stanford University discussed in this paper was supported by NASA Grant NGR-05-020-115.

Other wavelengths may be chosen for specific atmospheric studies, as is illustrated by the Nimbus measurements in the H_2O band (6.4 - 6.9μ) and CO_2 band (14 - 16μ).

Since those types of measurement have been widely published, this paper will concentrate on infrared spectral techniques rather than wide-band radiometry.

III. SPECTRAL EMITTANCE EXPERIMENTS

The use of infrared radiation as a diagnostic tool in the analysis of minerals and mineral bearing rocks has not received much attention until recent years. Coblentz in 1910 performed some of the earliest work in this field using polished samples and Pfund in 1945 extended the technique to the identification of gems.[4-6] Any extensive work on samples in the real world, which is neither polished nor of gem-like purity, did not occur until recently. It has been known for some time that the analysis of transmission or reflection spectra from polished samples has provided a potential laboratory method for mineral identification.[7] The diagnostic value of emission spectra, andmoreover, spectra of materials which are rough or even powdered, was not so clear. It has been recently demonstrated, however, that even emission spectra, with their essentially broader spectral characteristics, can lead to the identification of the material under examination, and even to mineralogical analysis of that material.[8]

In a logical program to adapt this laboratory technique to eventual spacecraft use, naturally occurring surfaces had to be examined, in the field, to see if they could be identified or analyzed from a distance, by measurement of their emission spectrum. Considerable work in this area has been performed by Lyon with the result that such identification and analysis has become possible from spectra taken in the field at ranges of a few thousand feet.[9] The immediate extension of this work is to go to aircraft altitudes and subsequently to spacecraft altitudes and to determine whether the same compositional data can be obtained.

IV. FUNDAMENTAL CONCEPTS

It is perhaps germane at this point to examine some of the fundamental concepts involved in this analytical technique. Figure 2 shows the relative emittance of quartz and a blackbody as a function of wavelength and temperature, from 250°K to 500°K. It can be seen that there are several distinctive characteristics of quartz in the spectrum. These are due to the well-known "reststrahlen" effect discovered originally by Rubens in 1890 and are precisely located at specific wavelenths for different minerals. By examining the shape and position of the minima it is possible to identify the sample from which the spectra were taken. Figure 3 shows the spectral emission of a number of samples and it will be noticed that the wavelengths of the minima change from sample to sample. The samples shown display a total shift of 2.5 microns, a very significant amount. Looking at the spectra generally, it can be seen that sufficient differences exist to make identification by some kind of pattern matching technique a possibility.

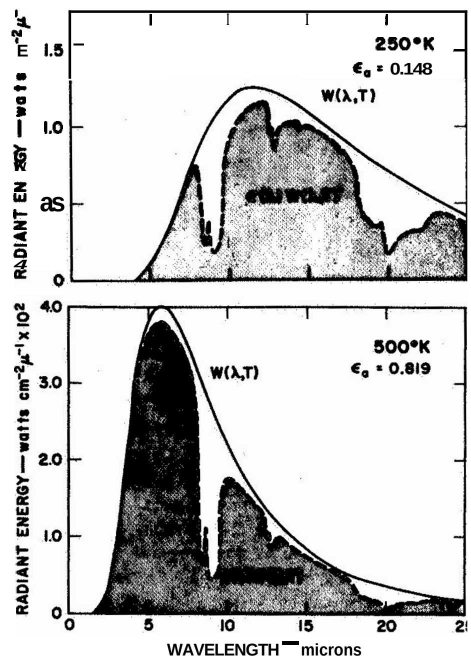

EMITTANCE OF QUARTZ AND BLACKBODY AT 250° K AND 500° K

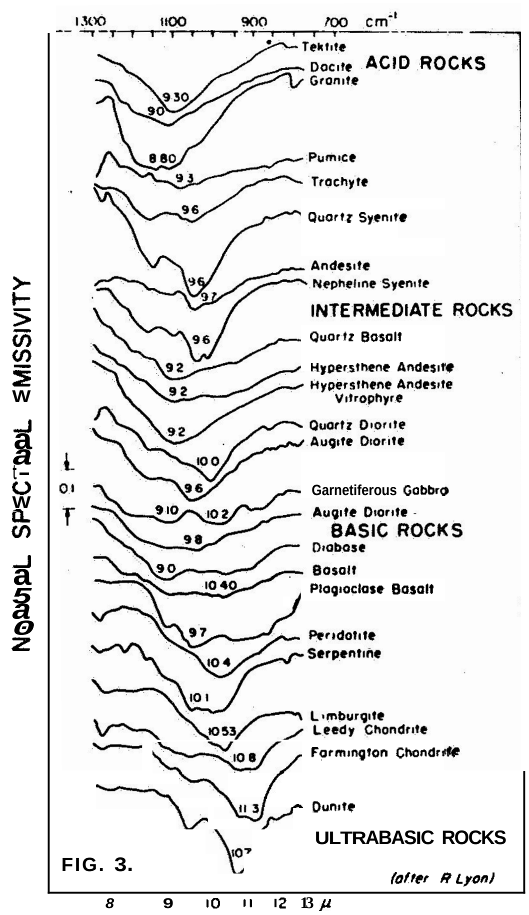

EMISSION SPECTRA OF VARIOUS ROCK TYPES SHOWING RESTSTRAHLEN MINIMA

One question which has been raised frequently in the past is what effect a covering of dust-like material would have on the emission spectra and the ability to analyze these spectra and produce computational data.

The problem has been studied extensively, and there is general agreement that while the spectra do indeed lose some of their uniqueness as the sample becomes more powdered, they nevertheless retain some of their diagnostic characteristics. It should be noted in addition that the spectral signatures used in calculations reported later in this paper were all taken in the field and were all of natural, rough and weathered surfaces. Figure 4 shows the spectra of quartz in polished and powdered forms. The differences in the position of the 20μ minimum are primarily due to the fact that the sand sample, being randomly oriented, presents all possible faces to the spectrometer, including the Z cut face which has a minimum at 20.6μ.

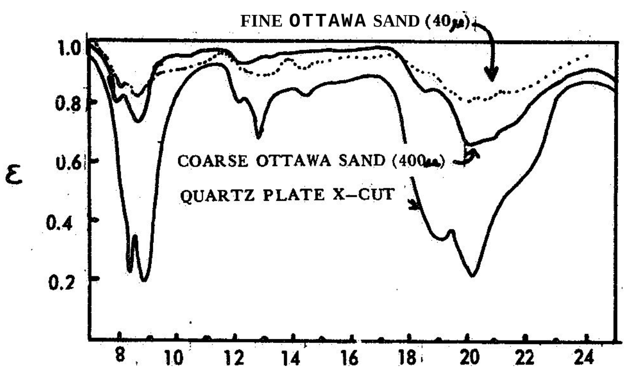

FIG. 4

EFFECT OF PARTICLE SIZE ON QUARTZ EMISSION SPECTRA

The problem of deciding which spectral region is most appropriate for surface compositional analysis has been attacked by several authors(10-12). For geological analysis, the most important contribution to infrared emission spectra is the Si-O bonding since most terrestrial (and probably most planetary) materials are composed of silicates. When included in mineral structures the bond gives rise to reststrahlen bands at 9 - 11μ and 18 - 25μ. The exact wavelength of this vibration is determined by the metal at the second coordinating position and by the bond angles and bond strengths i.e. by the composition of the mineral in question. Iron silicates can thus be distinguished from alumino-silicates and hence "basic" rocks from "acid" rocks, also whether they be coarsely crystalline (granite) or glass-rich (basalt).

Aronson argues for an extended (2.5 - 85.0μ) spectral range, for spacecraft compositional mapping.(11) The increase in possibly diagnostic range is undeniably impressive, but in order to examine the low energy end of this range one pays the price of considerably larger field of view than is desirable even from a geological standpoint (8" or 17 miles square from 125 n. mile orbit). The energy reaching the detector of this type of terrain viewing spectrometer, increases with the field of view, and of course with the energy/micron being emitted from the target. Thus, for a given instrument one can increase the spatial resolution (i.e. decrease the field of view) by operating in a higher energy region of the spectrum. For planetary bodies between 300-400°K the emission peak occurs between 7 and 10μ, which suggests the use of the 9-11μ reststrahlen region.

Figure 5 shows the relative dominance of the 9-14. and 18-25μ reststrahlen regions as the target temperature is reduced from 400°K to 150°K. From these and similar data it could be argued that the 9-14. region would give the maximum diagnostic contribution during the lunar day, and the 18-25μ region during the night.

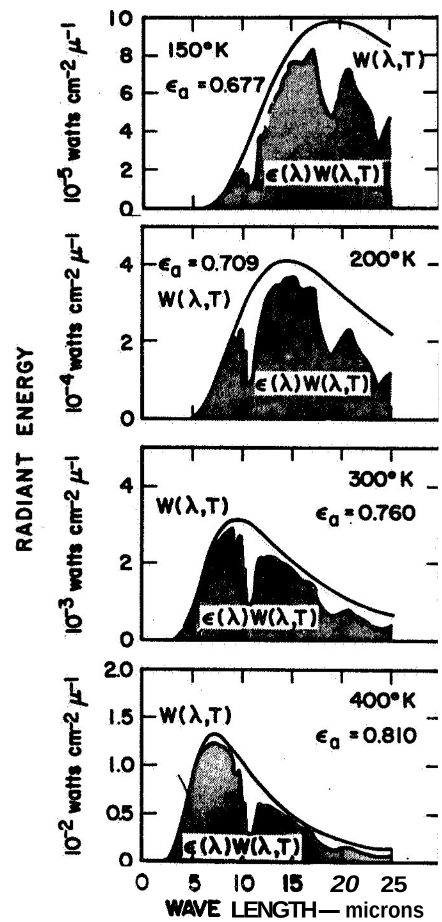

FIG. 5

EMITTANCE SPECTRA OF DUNITE FROM 150° K TO 400° K

a

In earth orbit, the only region available is the so-called 8-14 μ "window", and to use this successfully, a radiometer monitoring the H_2O, O_3 and CO_2 absorption of the atmosphere would be an advisable (if not essential) part of the experiment.

V. SPECTRAL MATCHING TECHNIQUES

Having demonstrated that the types of rock present on the terrestrial surface do have differences in their spectra, the question arises as to what is the most accurate and sensitive method for discriminating between them. All such methods rely on performing some form of spectral matching or correlation with a library of reference spectra. In one system described by Hunt, Salisbury and Reed[13] the matching is performed by reflecting the target radiation from a polished plate of the reference material. The reflection process multiplies the incident spectrumby the reference spectrum, and subsequent integration by a Golay cell detector over the desired spectral range gives a measure of the correlation between a target and reference spectra. This use of reststrahlen plates (Ruben's filters) is interesting but has limited application due to its apparent low sensitivity in discriminating between targets even when the spectral signatures are substantially different. The necessarily slow nature of the matching process when a library of more than a few samples is required is also a disadvantage for spacecraft use. For rapid analysis of multiple spectra, computerized data reduction appears to be essential.

An example of the output of a program wherein the target spectrum was correlated with 50 reference spectra, using an IBM 7094, is shown in Fig.6. In this case the target was a naturally occurring granite surface near Tioga Pass, 2000 feet away from the spectrometer. The differentiation between the target and materials of different gross mineralogical composition is very striking. The spectrum in this case was taken from approximately 8.3-13.5 microns and the instrument used was a conventional grating spectrometer. Other programs have been developed at Stanford for reducing the data taken with this instrument.

One such program performs analysis in terms of individual mineral spectra and calculates the percentage of minerals needed to produce the closest fit to the sample spectrum. Hence, in output one obtains the mineralogical composition (modal analysis) of the target rock. An example of this output is given in Fig. 7 where in this case the spectra of the five commonly occurring minerals shown were computed from a test set and produce the compositional analyses of the unknown rocks shown. There is nothing to stop the program being extended to include other less abundant minerals, although it is doubtful that the output from such an extended program would be any more meaningful.

FIG. 6.

STATISTICAL INFORMATION TPOP01
706 TPOP01 CX GRANITE ACROSS VALLEY (2000') #6

LIBRARY SPECTRA	CORRELATION COEFFICIENT
Q.M.P. ROUGH (NTS)	0.97369256E 00
GRANITE ROUGH	0.96835477E SO
WELDEO TUFF (NTS-RAINIER)	0.96345377E 00
DACITE SAWN	0.96286719E 00
QUARTZ BEACH SAND	0.95227173E 00
GRANITE APLITE VEIN (SHOAL)	0.94865768E 00
PYROX APLITE	0.94755526E 03
CHERT (WITTENCOM) ROUGH	0.92913143E 00
QUARTZ X-CUT ROUGH	0.92904866E 00
QUARTZ X-CUT PUL- ISHED	0.92317742E 00
TRACHYTE (ROUGH)	0.90155987E 03
TEKTITE	0.89015909E 00
GRANITE GNEISS ROUGH	0.88848187E 03
RHYOLITE PUMICE (V FROTHY)	0.88566212E 00
GRAPHIC GRANITE ACROSS GR.	0.87556277E 00
OBSIDIAN - 3424	0.87094110E 00
OBSIDIAN - 3365	0.85309923E 00
PLAG. BASALT ROUGH	0.82723571E 00
H. ANDES VITRO	0.81436798E C0
RHYULITE PUMICE SAWN	0.81296425E 00
AUGITE DIORITE	0.81254726E 00
NEPHELINE SYENITE	0.76693591E 03
QUARTZ BASALT SAWNPORUUS	0.71423221E 00
AUG. OIORITE ROUGH	0.70797863E C0
QUARTZ SVENITE SMOOTH	0.70707814E 0D
GARNET	0.70574555E 00
M.Q.S. SCHIST ALOYG GR.	0.68671916E 0b
MONCHIQUITE	0.67896153E 0C
ANDESITE	0.61261045E 00
HYP. ANDES	0.58448285E CC
ANHYDRITE SANO	0.56380793E 0C
DIABASE	0.52234443E 03
QUARTZ DIORITE	0.48271875E 00
NEPH. RASALT ROUGHPITTED	0.47840763E 00
K-FELDSPAR ROUGH CLEAVAGE	0.46489677E 00
BASALT	0.38807067E 00
OLIV INE GABBRO	0.35144284E 00
POLYSTYRENE STD.	0.29290722E 00
CALCITE	·0.13670082E 00
SERPENTINE	0.12522651E 00
LEEOEV METEORITE	0.72103220E-01
HORN. GABBRO GNEISS SAWN	-0.33469796E-06
METEORITE LAOCER CREEK	
PERIDOTITE SAWN	-0.34036493E 00
WNITE GRIT (+850 MIC.)	-0.42435645E 00
LIMBURGITE	-0.43254008E 00
OUNITE ROUGH WITH SANO	-0.46359276E 00
DUNITE POLISHED	-0.50918773E C0
WNITE ROUCH	-0.53647120E 00
FARMINGTON METEOR-ITE	-0.55509164E 00

TYPICAL PAGE OF COMPUTER OUTPUT SHOWING ANALYSIS OF FIELD SPECTRA OF QUARTZ MONZONITE TAKEN AT A HORIZONTAL RANGE OF 2,000 FT.

A third program was generated to separate out all the target spectra into a number of categories. The computer was given a mixture of granite, basalt and pumice spectra, and was programmed to find some combination of variables that would best separate the given spectra. The preliminary output is plotted in Fig. 8 and it can be seen that in many examples the differentiation is clear. There is, however, a region of indecision between the boundary of granite and pumice, both acid rocks of the same compositions but differing in crystal structure. The boundaries are not constrained to follow any particular shape by the program, and are picked after the fact. The next step in such a program is to input a large number of additional spectra using the presently established criteria and see if the same separation is successfully accomplished. These are field spectra taken from natural surfaces, not the spectra prepared or polished samples taken in the laboratory.

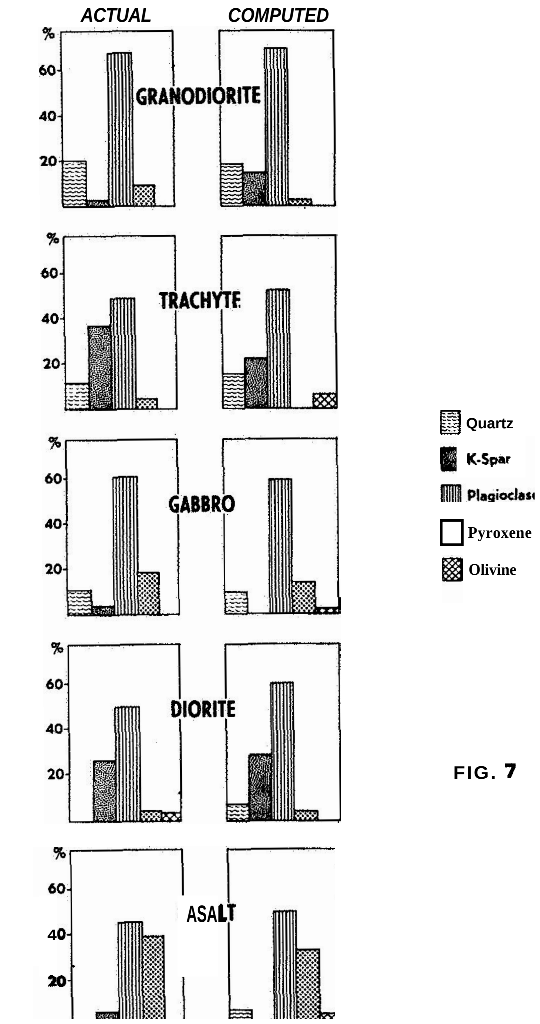

FIG. 7

COMPARISON OF ACTUAL AND COMPUTED COMPOSITIONS OF FIVE TYPICAL SAMPLES

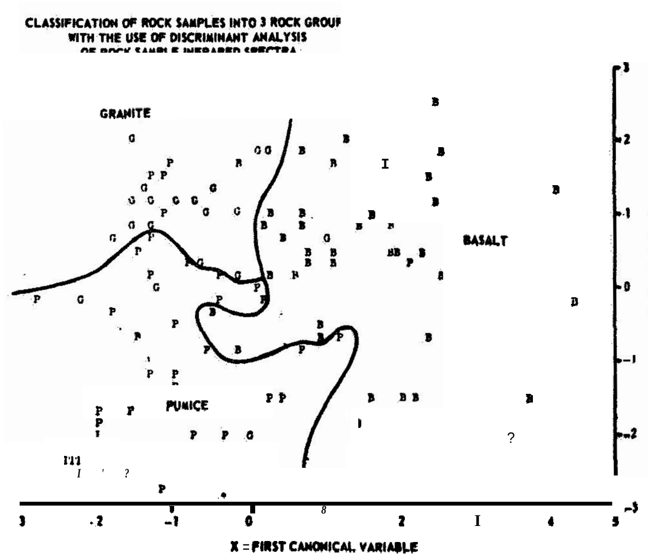

FIG. 8.

VI. INSTRUMENTATION

There are several schools of thought on what is the best type of equipment for infrared spectral remote sensing. M.J.D. Lowe has published a considerable quantity of data obtained with a Michleson interferometer.[14] The resolution (40 cm^{-1}), in this case was typical of the state of the art, although for Martian experiments Aronson suggests that a similar instrument could be built with 10 cm^{-1} resolution.[11] The advantage of this type of interferometer for space use lies primarily in the small size and weight of the optical head, and the use of uncooled detectors. The instrument, however, has several drawbacks, and of these the chief offender is the time taken to produce sufficient data to compute a satisfactory spectrum in the thermal regime. Most published spectra of targets at room temperature from this type of instrument are composites of between 100 and 200 scans, each scan taking of the order one second. Since the ground speed of earth orbital s acecraft is usually between 1 (Lunar) and 5 (Earthy miles per second, it is of great importance to complete each spectral scan as rapidly as possible in order to avoid smearing of the ground resolution patch.

The development of the circular variable filter (C.V.F.) makes the design of a rapid scanning spectrometer for orbital use comparatively simple. Present suggested designs for earth orbital equipment show that scan times of 0.1 sec for the 6.3-13μ range axe feasible with a field of view of about 0.2°. The resolution of these filter wheels is presently between 1% and 1.5%.

An alternative approach to the problem is presently being pursued by the University of Michigan.[15] In this program an optical-mechanical scanner is used in conjunction with a dispersive system in order to produce imagery in a large number of spectral channels. Using this technique it should be possible to produce a matrix in which both an image, and the spectrum of each point on that image are known. Presently the system operates with twelve of its channels in the visible, and it is not clear whether sufficient sensitivity is available to split the thermal band into small enough spectral slices to be of use in any type of compositional analysis program. If the problem can be overcome, however, the potential output of the system is a terrain map showing areas of similar or dissimilar gross composition. For such a system to be operational in the foreseeable future, however, some mechanism for reducing the volume of transmitted data must be found, since the data rate of a 20 channel system would be of the order of 10 Megabits/second (including a *gray* scale).

VII. GEOLOGICAL RATIONALE FOR SPECTRAL EMISSIVITY EXPERIMENTS FROM ORBITING SPACECRAFT

It is a very valid question to ask what is the use of such a mineralogical compositional, or geological analysis. The following are pertinent facts.

1. True, Rather Than Inferred Rock and Soil

In each orbit spectroscopy in the 6.5 - 13.0μ region yields the only remote sensing data from which the chemical and mineralogical nature of the rocks and soil beneath the spacecraft can be derived. Within a resolution cell a true composition can be read from earth orbit in a unique manner. The rock doesn't merely "look" like a granite-- it is a granite With quantifiable constituent minerals. The sandy or silty nature of the surface soils can be determined. Carbonates can be differentiated from sandy rocks, lavas basalt from andesites and from rhyolite lavas.

2 Sedimentary Basins and Igneous Rocks

In most sedimentary basins the correct identification of the rock types and structure is essential to the exploration for hidden oil reservoirs or artesian water. Igneous rocks are the genetic parents of most metal-bearing ore bodies and their correct location and classification can open up areas for prospecting or even close others for certain metals.

3. Detection of Mining Districts

Most large mining districts of the world have surface extents measurable in one to tens of square miles. These are often bleached and altered areas capped with reddish outcrops, invariably richer in quartz minerals than the surrounding barren ground. Such a target is clearly identifiable by its "anomolous mineralogy" with this technique.

The following concepts describe a typical and orbital experiment.

a. Well-resolved infrared spectra yield precise identifications of the surface layer of rocks and soil. With a ground velocity of 5 miles/sec a spectral rate of 11 spectra/second, a field of view of 0.2 degrees square at 125 n. miles yield one spectrum per 2600 x 2600 plus ground smear of 2300 feet. A total field of view of 2600 x 4930 feet (800 m. x 1500 m.) per spectrum is obtained from earth orbit (roughly one every 1/2 square mile). Gimballed units could avoid the ground smear effects and give a spectrum every 1/4 square mile.

b. The wavelengths to be used for this experiment (6.5 - 13μ) would be chosen specifically to cover the water vapor bands at 6.5μ, nitrous oxide bands around 7.5μ, and the ozone bands at 9.6 and 9.8μ (16) (See Fig. 9). Accordingly, their content in the total atmospheric pile can be examined with the experiment. Lakes or oceanic water bodies ($\epsilon_{8-13\mu}$ = 0.98) are to be examined immediately before or after the rock targets to calibrate the atmosphere column for the geological experiment.

c. Earth orbital checkout of a lunar orbital instrument is a vital step before a lunar mission.

d. Used concurrently With microwave radiometers the infrared unit should give the surface gradient temperature and composition to aid the interpretation of the deeper penetrations (1-5 cm) of the microwaves.

e. When used with the infrared imager the infrared spectrometer gives its most significant assistance in identifying *many* of the spurious (i.e. non-geologic) causes of gray scale variation e.g. water vapor and ozone variations.

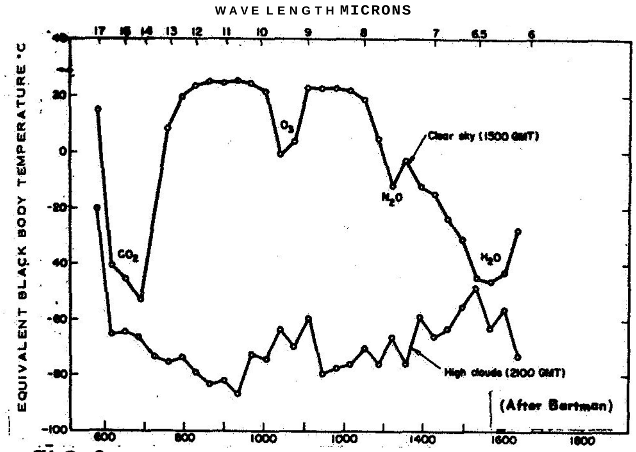

FIG. 9.

ABSORPTION BANDS OF H_2O O_3 AND CO_2 TAKEN FROM HIGH ALTITUDE BALLOON

In Lunar or Martian orbit the benefit of such an analysis capability by remote infrared sensing would be extreme. The presently planned Apollo Lunar surface missions will only cover approximately 1 percent of the Lunar surface in the first 5-10 years (to envisage this remember the moon has a surface area greater than that of Africa). One percent should provide a significant amount of ground control, which could then be used (in a "leap frog" fashion) to calibrate orbital devices which are performing remote surface analysis. It should, therefore, be possible to provide complete lunar coverage and establish a lunar geological map, purely from orbital data, with the help of a limited number of ground stations. The importance of a complete map of this sort to geologists and those concerned with the origin and history of the moon cannot be overemphasized.

VIII. CONCLUSIONS

The infrared region of the spectrum can be made to divulge a considerable quantity of data with geological and physical significance by the use of orbital experiment platforms. By studying Wide-band thermal emission over a period of time, information can be deduced about the thermal inertia and emissivity of the surface materials. In estimating surface temperatures from radiometric methods, the errors due to graybody emission must be taken into account. It must be remembered that infrared sensing alone only gives direct information on the uppermost 100μ or so of the surface.

The real potential of all remote sensing experiments, however, infrared included, lies in the correlation of data from a number of wavelengths. The combination of radar imagery, infrared imagery and infrared and microwave spectrometry for example promises to be an extraordinarily powerful tool for geological analysis of planetary surfaces. In order to remove the ambiguities from the interpretation of such data, it is imperative that existing data collection programs, using combined instrumentation in medium and high altitude aircraft, be accelerated.

Compositional data can be deduced from the analysis of infrared emission spectra, and particularly from the 9-11μ and 18-25μ regions. In earth orbit, the effects of H_2O, O_3 and CO_2 must be measured and removed from surface data. In the rare event that the surface of a particular planet is covered with solid material of a completely unknown (i.e. non-terrestrial or meteoritic) type, it appears highly likely that the techniques presently being evolved will be able to resolve the terrain into regions of 'like' and 'unlike' materials. Subsequent sample analysis from a limited surface exploration program will then provide the control points necessary for a complete interpretation of the orbital data.

REFERENCES

1. Hovis, W.A. Jr., Infrared Spectral Reflectance of Some Common Minerals, Applied Optics, Vol. 5, No. 2, February 1966.

2. Nordberg, William, Geophysical Observations from Nimbus 1, Science, Vol. 150, No. 3696 October 1965.

3. Burns, Eugene A., and Lyon, R.J.P., Errors in the Measurement of the Lunar Temperature, Jour. of Geophysical Research, Vol. 69, No. 18, September 1964.

4. Coblentz, W.W., Investigation of Infrared Spectra, Pub. 65, Carnegie Institute of Washington, 1906.

5. Coblentz, W.W., Selected Radiation from Various Solids, II, Nat. Bur. Standards (US) Bull, 6, 301 (1901).

6. Pfund, A.H., The Identification of Gems, J. Opt. Soc. Amer., 35, 611-614 (1945).

7. Hunt, J.M. and Turner, D.S., Determination of Mineral Constituents of Rocks by Infrared Spectroscopy, Anal. Chem. 25, 1169-1174 (1953).

8. Lyon, R.J.P., Field Infrared Analysis of Terrain, 1st Annual Report on Grant NGR-05-020-115, October 1966.

9. Lyon, R.J.P., and Patterson, J.W., Infrared Spectral Signatures - A Field Geological Tool, in 4th Symposium on Remote Sensing of Environment, University of Michigan, pp. 215-230, 1966.

10. Lyon, R. J.P., Evaluation of Infrared Spectrophotometry for Compositional Analysis of Lunar and Planetary Soils (Part II) NASA Contractor Report, NASA-CR-100, November 1964.

11. Aronson, J.R., et.al., Studies of the Middle and Far-Infrared Spectra of Mineral Surfaces for Application in Remote Compositional Mapping of the Moon and Planets, Jour. of Geophysical Research, Vol. 72, No. 2, January 1967.

12. Hovis, W.A. Jr., Optimum Wavelength Intervals for Surface Temperature Radiometry Applied Optics, Vol. 5, NO. 5, May 1966.

13. Hunt, G.R., Salisbury, J.W., and Reed J.W., Rapid Remote Sensing by Spectrum Matching Technique, Jour. Geophysical Research, Vol. 72, No. 2, January 1967.

14. Lowe, M J.D., and Coleman I., The Measurement of Infrared Emission Spectra Using Multiple-Scan Interferometry, Spectrochemica Acta Vol. 22, pp. 369-376, 1966.

15. Lave, D.S., University of Michigan, private communication.

16. Bartman, F.L. et. al., Infrared and Visible Radiation Measurements by Radiometer and Interferometer on High Altitude Balloon Flights at 34-KM Altitude, Presented at the International Symposium on Radiation Processes at Leningrad, U.S.S.R, Aug. 5-12, 1964

BIBLIOGRAPHY

McMahon, H.O., Thermal Radiation Chaxacteristics of some Glasses, Jour. Am. Ceram. Soc. 34, 91-6 (1950).

Proc. of The Third Symposium on Remote Sensing of Environment, Institute of Science and Technology, The University of Michigan, February 1965

Proc. of the Fourth Symposium on Remote Sensing of Environment, Institute of Science and Technology, The University of Michigan, June 1966

APPENDIX

COMPARISON BETWEEN REFLECTANCE AND EMITTANCE FOR A SERIES OF ROCK AND POWDER SURFACES

A. ACID ROCKS (HIGH SILICA, > 65% SiO_2)

Sample	Polished reflectance $1-\rho_\lambda$ min	Polished reflectance $1-\rho_\lambda$ avg (a)	Emittance ϵ_λ min	Emittance ϵ_λ avg (b)	Spectral minima emittance stronger underlined) (microns)	Roughness
Quartz						
Polished Z-cut	-	-	0.20	0.72	9.0	polished
Polished X-cut	0.18*	0.72*	.28	.76	8.6 9.0 12.4	polished
Rough X-cut	-	-	.62	.83	8.5 9.2 12.7	rough
Fused plate	-	-	.45	.75	8.3 9.0	polished
Powders						
25 to 45μ	.77*	.92*	.81	.90	9.0	F.C.
10 to 20μ	-	-	.85	.92	9.0	F.C.
1 to 10μ	-	-	.91	.94	9.1 11.1	F.C.
Sand (beach)	.67*	.91*	.67	.80	9.1	loose
Opal	.62	.92	-	-	9.09(reflectance)	polished
Chert	-	-	.59	.84	9.2	uneven, smooth
Obsidian						
No. 3424	-	-	.64	.72	8.7 9.4	smooth
No. 3365	-	-	.72	.80	9.2 11.6	smooth
No. 3581	.63	.87	-	-	-	polished
Rhyolite pumice	-	-	.79/.80	.88/.86	9.2/9.3	pitted
Rhyolite	.80	.94	-	-	-	-
Welded tuff	-	-	.69	.76	8.9	v. rough
Tektite	-	-	.64	.74	9.3	uneven
Q.Monz.Porphyry	.73	.88	.70	.81	8.9	rough
Dacite	.85	.94	.83/.85	.92/.95	8.8/9.0	sawed
Granite						
No. 158	.60	.85	.73/.76	.88/.90	8.8/8.9 9.1	broken
No. 3382	.64*	.81(*)	-	-		polished
Graphic granite	.60	.92	.70/71	.87/.88	9.30	broken
Granite aplite	-	-	.60	.77	8.8	broken
Pyroxene aplite	.70	.86	.76	.85	8.8	broken
Granite gneiss	.64	.87	.78/.71	.88/.82	9.3/9.6	broken
Trachyte	.85	.94	.75/.79	.84/.86	8.7 9.6	sawed

Slash (/) repeat run
* Hemispherical reflectance
F.C. "Fairy Castle" structures

(a) averaged over 7 to 2[?] microns
(b) averaged over 7.8 to [?]3 microns
(*) averaged over 8 to 1[?] microns

B. INTERMEDIATE ROCKS (53% to 65% SiO_2)

Sample	Polished reflectance $1-\rho_\lambda$ min	Polished reflectance $1-\rho_\lambda$ avg (a)	Emittance ϵ_λ min	Emittance ϵ_λ avg (b)	Spectral minima emittance (stronger underlined) (microns)	Roughness
Quartz syenite	0.47	0.85	0.71	0.86	9.6	rough
Andesite	.63	.86	.70	.77	<u>9.6</u> 10.1	rough
Nepheline syenite	.67	.92	.74/.76	.81/.91	9.6/9.7 <u>9.9</u>	broken
Quartz basalt	.83	.92	.67/.65	.73/.72	9.2/9.15	eawed
Hypersthene andesite	.75	.87	.72/.73	.78/.78	9.2/9.2	sawed
Hyp. Andesite vitrophyre	.73	.91	.74	.83	9.2	broken
Quartz diorite	.70	.85	.81/.82	.91/.92	10.0/10.1	broken
Augite diorite	.79	.88	.75	.85	9.6	sawed

C. BASIC (AND ULTRABASIC) ROCKS, < 53% SiO_2

Sample	Polished reflectance $1-\rho_\lambda$ min	Polished reflectance $1-\rho_\lambda$ avg (a)	Emittance ϵ_λ min	Emittance ϵ_λ avg (b)	Spectral minima emittance stronger underlined (microns)	Roughness
Garnet gabbro	).76	0.84	).77	0.81	<u>9.1</u> 10.2	sawed
Augite diorite gabbro	.63	.88	.78	.84	9.8	sawed
Schist	.80	.88	.70/.74	.84/.86	9.6/9.6	broken
Diabase	.80	.89	.78	.83	9.0	sawed
Basalt	.76/.78	.86/.88	.65	.69	10.4 10.1	broken
Plagioclase basalt	.80	.90	.79/.81	.86/.89	9/1 <u>9.4</u>/9.7	sawed
Monchiquite	.77	.90	.77	.84	9.2	broken
Hornblende gabbro gneiss	.67	.84	.69/.72	.79/.82	10.1/10.0	sawed
Peridotite	.73	.84	.79	.88	10.4	sawed
Olivine gabbro	.80	.87	.78	.83	m.3	sawed
Nepheline basalt	.68	.85	.84	.90	9.7	broken
Serpentine	.75	.83	.76	.87	<u>10.1</u> 10.4	broken
Limburgite	.82	.96	.72	.82	10.5	broken
<u>Dunite</u>						
Polished (Solid-specular)	.31	.76				
(Hemispherical)	.29*	.69(*)	.44	.71	9.5 <u>10.7</u> (10.8*)	polished
Rough	-	-	.66	.80	9.6 <u>10.7</u>	rough
Grit(> 850µ)	-	-	.73	.78	9.6 <u>10.7</u>	loose
Sand(300 to 150µ	-	-	.74	.79	10.6	sifted
Dust(80 to 40µ)	.79*	.91(*)	.79	.86	10.7	F.C.
Powder(10 to 25µ	-	-	.86	.89	10.7	F.C.
Rough + sand	-	-	.69	.76	9.6 <u>10.6</u>	loose
Rough + dust	-	-	.82	.84	9.6 <u>10.6</u> 11.1	F.C.

Slash (/) repeat run
* Hemispherical reflectance
F.C. "Fairy Castle" structures

(a) averaged over 7 to 25 microns
(b) averaged over 7.8 to 13 microns
(*) averaged over 8 to 13 microns

D. METEORITIC COMPOSITION - CHONDRITES

Sample	Polished reflectance $1-\rho_\lambda$ min	$1-\rho_\lambda$ avg (a)	Emittance ϵ_λ min	ϵ_λ avg (b)	Spectral minima emittance (stronger underlined) (microns)	Roughness
Haven	0.68	0.81	-	-	10.75 (reflectance)	polished
Leedey - 1	-	-	0.70	0.77	10.7	sawed
- 2	-	-	.73	.77	10.8	sawed
Ladder Creek	-	-	.72	.76	~~10.8~~ 11.1	rough
Farmington - 1	.69	.87	.76	.87	11.2	sawed
- 2	.73	.88	.76	.88	11.3	sawed
E. SPECIAL MATERIALS						
K-Feldspar	-	-	.61	.81	9.6	rough
Silicon Carbide						
12μ powder	-	-	.80	.93	12.5	F.C.
1711 powder	-	-	.83	.93	12.5	F.C.
75 to 150μ powder	-	-	.56	.81	12.3	rough
Crystals	-	-	.27	.54	12.2	smooth
Alumina						
0.02μ powder	.86*	.92*	.88/.90	.91/.96	10.9	F.C.
Fine grain tubing	-	-	.58	.71	11.8 (broad)	smooth
Coarse grain tubing	.84*	.91*	-	-	26.5	rough
Poly.crystal. platelets	.31*	.63*	.36	.54	11.8 16.5 22.0	smooth
Sapphire rods	-	-	.61	.77	11.85	frosted
Sapphire plate	.08*	.41*	.53	.68	11.5 15.0 22.0	frosted
Al Foil	-	-	.08	.09	13.0	metallic
Sulfate						
Anhydrite ($CaSO_4$) sand	-	-	.76	.84	8.3 8.6	loose
Carbonate						
Calcite	-	-	.32	.76(c)	6.7 11.3	cleavage
Dolomite	-	-	.72	.90(c)	6.45 11.2	rough
Aragonite	-	-	.47	.76(c)	6.7 11.5	rough

Slash (/) repeat run
* Hemispherical reflectance
F.C. "Fairy Castle" structures

(a) averaged over 7 to 25 microns
(b) averaged over 7.8 to 13 microns
(c) minimum lies outside 7.8 to 13 microns band forming average limits